

**Oxford Brookes University**  
**Faculty of Health and Life Sciences**  
**Department of Biological and Medical Sciences**

# The role of subunit interfaces in the function of nicotinic acetylcholine receptor

Silvia García del Villar

*A thesis submitted in partial fulfilment of the  
requirement of Oxford Brookes University for  
the degree of Doctor of Philosophy*

PhD Thesis  
January 2018



For my parents



## Contents

Publications	8
List of figures	10
List of tables	11
List of abbreviations	12
Abstract	14
Chapter 1. Introduction	16
1.1 Chemical communication in the Nervous System	18
1.2 nAChRs	20
1.2.1 nAChR subunits	21
1.2.2 The membrane topology of of nAChRs	23
1.2.3 The ECD and the agonist binding site	26
1.2.4 The TMD and the ion channel	29
1.2.5 The activation of nAChRs	33
1.2.6 nAChR distribution in the brain	36
1.3 $\alpha 4\beta 2$ nAChRs	37
1.3.1 Native ( $\alpha 4\beta 2$ ) <sub>2</sub> $\beta 2$ and ( $\alpha 4\beta 2$ ) <sub>2</sub> $\alpha 4$ nAChRs	37
1.3.2 $\alpha 4\beta 2^*$ nAChRs in brain pathologies	38
1.3.2.a Nicotine addiction	38
1.3.2.b Depression	41
1.3.2.c Analgesia	42
1.3.2.d Alzheimer's disease	43
1.3.2.e Parkinson's disease	44
1.3.2.f Schizophrenia	45
1.3.2.g Autosomal dominant nocturnal frontal lobe epilepsy	45
1.3.3 The Pharmacology of $\alpha 4\beta 2$ nAChRs	46
1.3.3.1 Agonists	46
1.3.3.2 Antagonist	48
1.3.3.3 Allosteric modulators	48
1.3.4 Alternate forms of the $\alpha 4\beta 2$ nAChR	53
1.3.5 Concatenated $\alpha 4\beta 2$ receptors	54
1.4 Thesis rationale	56
1.5 Aims of the thesis	58

Chapter 2. Materials and methods	60
2.1 Reagents	62
2.2 Animals	62
2.3 Molecular Biology	62
2.3.1 Single Point Mutations	63
2.3.2 Concatameric $\alpha 4\beta 2$ receptors	64
2.3.3 Engineering mutant concatenated $\alpha 4\beta 2$ receptors	65
2.4 Microinjection of cRNA	65
2.5 Electrophysiological Recordings	67
2.6 Agonist concentration response curves	68
2.7 Substituted cysteine accessibility method	69
2.7.1 Maximal effects of MTSET- modification of substituted cysteines	70
2.7.2 Rates of MTSET reaction	72
2.7.3 Protection assays	75
2.8 Double mutant cycle analysis	76
2.9 Comparative modeling	77
2.10 Statistical analysis	77
Chapter 3. The fifth subunit in $(\alpha 4\beta 2)_2\alpha 4$ receptors modulates the function of canonical agonist sites	78
3.1 Introduction	80
3.2 Results	83
3.2.1 Agonist sites and subunit interfaces in $\alpha 4\beta 2$ nAChRs	83
3.2.2 Functional asymmetry of agonist binding sites	84
3.2.3 Effects of MTSET on cysteine substituted $\beta 2_{-}\alpha 4_{-}\beta 2_{-}\alpha 4_{-}\alpha 4$ nAChRs	87
3.2.3.a Maximal effects of MTSET	87
3.2.3.b Rate of MTSET Reaction and Protection Assays	89
3.2.4 Do $\beta 2(+)/\alpha 4(-)$ interfaces contain elements of intersubunit communication?	91
3.2.5 $Zn^{2+}$ potentiating pathway	95
3.3 Discussion	99
Chapter 4. The $\beta 2(+)/\beta 2(-)$ subunit interface of $(\alpha 4\beta 2)_2\beta 2$ receptors is a key element of an allosteric system that modulates maximal agonist responses	102
4.1 Introduction	104
4.2 Results	106

4.2.1 Identification of residues in $\beta 2(+)/\beta 2(-)$ that may modulate agonist responses in $(\alpha 4\beta 2)_2\beta 2$ nAChRs _____	106
4.2.2 The allosteric unit in $\beta 2(+)/\beta 2(-)$ is coupled to gating _____	115
4.2.3 F144 from loop E also contributes to the modulatory ensemble in $\beta 2(+)/\beta 2(-)$ ____	118
4.2.4 $\beta 2(+)/\alpha 4(-)$ interfaces do not affect TC2559 responses in $\alpha 4\beta 2$ nAChRs _____	121
4.2.5. The modulatory unit $\beta 2W176-\beta 2F144-\beta 2L146$ is transferable _____	123
4.3 Discussion _____	126
Chapter 5. Final discussion _____	130
Acknowledgments _____	138
Bibliography _____	140





## **PUBLICATIONS**

- New K, Del Villar SG, Mazzaferro S, Alcaino, C and Bermudez I (2017). The fifth subunit of the  $(\alpha 4\beta 2)_2\beta 2$  nicotinic ACh receptor modulates maximal ACh responses. *Br. J. Pharmacol. In Press*.
- Gallagher T, Campello HR, Honraedt A, Sessions R, Shoemark D, Ranaghan K, Oliveira S, Del Villar SG, Bermudez I, Minguez T, Mulholland A, Wonnacott S and Gotti C (2017). Unlocking Nicotinic Selectivity via Direct C–H Functionalisation of (–)-Cytisine. *Chem. Submitted*.
- Del Villar SG, Minguez T, Mazzaferro S, New K, Bermudez I (2017). Mapping the allosteric link between agonist binding sites and the accessory subunit in the  $(\alpha 4\beta 2)_2\beta 2$  nicotinic receptor. Submitted to *J Neurosci*

## **AWARDS**

- Nigel Groome PhD grant.
- Travel grant sponsored by the British Journal of Pharmacology to attend the Nicotinic Acetylcholine Receptors 2017 International Conference in Crete

## **CONFERENCE ATTENDANCE**

- OXION day. Ion Channels and Diseases of Electrically Excitable Cells. Oxford, UK (2014). Poster presentation
- Frontiers in Integral Membrane Protein Structural Biology (October, 2015), Oxford. Poster presentation.
- Nicotinic Acetylcholine Receptors 2017 International Conference. Crete, Greece. (May 2017). Two minutes lightning talk and poster presentation.
- 37<sup>th</sup> Spanish Society of Pharmacology (SEF) National Meeting with guest Society: The British Pharmacological Society. Barcelona, Spain (June, 2017). Poster presentation
- OXION Symposium “Ion Channels and Diseases of Electrically Excitable Cells”. Oxford, UK (2017). Poster presentation
- XXXIX Annual Congress of Pharmacology Society, Chile (November 2017). Workshop.



## **LIST OF FIGURES**

### **CHAPTER 1. Introduction**

<b>Figure 1.1</b> Neuronal communication through chemical synaptic transmission.....	19
<b>Figure 1.2</b> Neuronal nAChR Structure.....	21
<b>Figure 1.3</b> Architecture and fold of the $(\alpha 4\beta 2)_2\beta 2$ and $(\alpha 4\beta 2)_2\alpha 4$ nAChRs.....	25
<b>Figure 1.4</b> Structure of the $(\alpha 4\beta 2)_2\beta 2$ and $(\alpha 4\beta 2)_2\alpha 4$ nAChRs.....	28
<b>Figure 1.5</b> Cys-loop receptor ion channel conformations.....	31
<b>Figure 1.6</b> Cartoon representation of GluCl active with L-Glutamate and ivermectin.....	32
<b>Figure 1.7</b> The activation of pLGICs.....	35
<b>Figure 1.8</b> Regional distribution of the nAChRs subunits in the rodent brain.....	36
<b>Figure 1.9</b> The mesocorticolimbic “reward” circuitry.....	41
<b>Figure 1.10</b> Alternate forms of the $\alpha 4\beta 2$ nAChR.....	54

### **CHAPTER 2. Materials and methods**

<b>Figure 2.1</b> Diagram showing $\alpha 4\beta 2$ cRNA injection into <i>Xenopus</i> oocytes.....	66
<b>Figure 2.2</b> Covalent MTS modification of substituted cysteine.....	71
<b>Figure 2.3</b> Decay and Protection assay.....	75

### **CHAPTER 3. The fifth subunit in $(\alpha 4\beta 2)_2\alpha 4$ receptors modulates the function of canonical agonist sites**

<b>Figure 3.1</b> Subunit position and orientation in concatenated $\alpha 4\beta 2$ nAChRs.....	82
<b>Figure 3.2</b> Effects of ACh on wild type and mutant $(\alpha 4\beta 2)_2\alpha 4$ receptors.....	85
<b>Figure 3.3</b> Amplitude of ACh responses after maximum MTSET application.....	88
<b>Figure 3.4</b> Rates of covalent modification of cysteine substituted concatenated $(\alpha 4\beta 2)_2\alpha 4$ nAChRs.....	90
<b>Figure 3.5</b> Effect on the ACh sensitivity on concatenated $(\alpha 4\beta 2)_2\alpha 4$ nAChRs.....	93
<b>Figure 3.6</b> $Zn^{2+}$ pathway in $(\alpha 4\beta 2)_2\alpha 4$ nAChR.....	96
<b>Figure 3.7</b> Maximal potentiation of $Zn^{2+}$ .....	97

### **CHAPTER 4. The $\beta 2(+)/\beta 2(-)$ subunit interface of $(\alpha 4\beta 2)_2\beta 2$ receptors is a key element of an allosteric system that modulates maximal agonist responses**

<b>Figure 4.1</b> Effects of maximal MTSET in wild type and cysteine substituted concatenated $(\alpha 4\beta 2)_2\beta 2$ nAChRs.....	107
<b>Figure 4.2</b> Effect of ACh on the rate of MTSET modification of substituted concatenated $(\alpha 4\beta 2)_2\beta 2$ nAChRs.....	112

<b>Figure 4.3</b> Effect of impaired agonist binding sites on the rates of MTSET reaction with $^{W176C}\beta2\_ \alpha4\_ \beta2\_ \alpha4\_ \beta2^{L146C}$ .....	114
<b>Figure 4.4</b> The elucidating long-range functional coupling.....	117
<b>Figure 4.5</b> Alanine substitution of conserved residues in $\beta2 (+)/\beta2(-)$ interfaces.....	120
<b>Figure 4.6</b> Structure of the $\beta2(+)/\beta2(-)$ and $\beta2(+)/\alpha4(-)$ in $\alpha4\beta2$ nAChRs.....	121
<b>Figure 4.7</b> Effect on the ACh and TC2559 sensitivity of concatenated $\alpha4\beta2$ nAChRs.....	124

## **LIST OF TABLES**

### **CHAPTER 1. Introduction**

<b>Table 1.1</b> nAChR family subunits.....	21
<b>Table 1.2</b> Classical $\alpha4\beta2$ nAChRs ligands.....	51
<b>Table 1.3</b> Allosteric modulators of $\alpha4\beta2$ nAChRs.....	52

### **CHAPTER 2. Materials and methods**

### **CHAPTER 3. The fifth subunit in $(\alpha4\beta2)_2\alpha4$ receptors modulates the function of canonical agonist sites**

<b>Table 3.1</b> Agonist potency ( $EC_{50}$ ) and efficacy ( $I/I_{AChmax}$ ) on wild type and mutant concatenated $(\alpha4\beta2)_2\alpha4$ nAChRs.....	86
<b>Table 3.2</b> Rates of MTSET-covalent modification of cysteine substituted concatenated $(\alpha4\beta2)_2\alpha4$ nAChRs.....	91
<b>Table 3.3</b> Relative potency and efficacy of ligands on concatenated $(\alpha4\beta2)_2\alpha4$ nAChRs.....	94
<b>Table 3.4</b> $Zn^{2+}$ potentiation of ACh responses of concatenated $(\alpha4\beta2)_2\alpha4$ nAChRs.....	98

### **CHAPTER 4. The $\beta2(+)/\beta2(-)$ subunit interface of $(\alpha4\beta2)_2\beta2$ receptors is a key element of an allosteric system that modulates maximal agonist responses**

<b>Table 4.1</b> Concentration effects of ACh and TC2559 on concatenated $(\alpha4\beta2)_2\beta2$ nAChRs.....	108
<b>Table 4.2</b> Effects of MTSET on the ACh responses of wild type and cysteine substituted concatenated $(\alpha4\beta2)_2\beta2$ nAChRs.....	111
<b>Table 4.3</b> Second order rate constants for MTSET-modification of residues within the $\beta2(+)/\beta2(-)$ interface of concatenated $(\alpha4\beta2)_2\beta2$ nAChRs.....	111
<b>Table 4.4</b> ELFCAR analysis of E loop and L9' in concatenated $(\alpha4\beta2)_2\beta2$ .....	117
<b>Table 4.5</b> PISA analysis of the $(\alpha4\beta2)_2\beta2$ isoform crystal structure.....	119
<b>Table 4.6</b> Effects of ACh and TC2559 on concatenated $(\alpha4\beta2)_2\alpha4$ nAChRs.....	122
<b>Table 4.7</b> Maximal effect of Saz-A responses of concatenated $(\alpha4\beta2)_2\alpha4$ receptors.....	125

<b><u>LIST OF ABBREVIATIONS</u></b>	
<b>ACh</b>	Acetylcholine
<b>ANOVA</b>	Analysis of variance
<b>C-terminus</b>	Carboxy-terminus
<b>cDNA</b>	Complementary deoxyribose nucleic acid
<b>CI</b>	Confidence interval
<b>CRC</b>	Concentration response curve
<b>cRNA</b>	Complementary ribonucleic acid
<b>Cyt</b>	Cytisine
<b>DA</b>	Dopamine
<b>dNTP</b>	Deoxyribonucleotide triphosphate
<b>dFBr</b>	Desformylflustrabromide
<b>DH<math>\beta</math>E</b>	Dihydro- $\beta$ -erythroidine
<b>DMSO</b>	Dimethylsulphoxide
<b>EC<sub>50</sub></b>	Concentration producing half maximal effect
<b>EC<sub>50-1</sub></b>	Concentration producing half maximal high sensitivity stimulatory effect in a biphasic CRC
<b>EC<sub>50-2</sub></b>	Concentration producing half maximal low sensitivity stimulatory effect in a biphasic CRC
<b>ECD</b>	Extracellular domain
<b>ELFCAR</b>	Elucidating long-range functional coupling of allosteric receptors
<b>GABA</b>	$\gamma$ -aminobutyric acid
<b>HEPES</b>	N-2-hydroxyethylpiperazine-N'-2-ethansulphonic acid
<b>HS</b>	High sensitivity
<b>IC<sub>50</sub></b>	Concentration producing half maximal inhibition
<b>LS</b>	Low sensitivity
<b>MTS</b>	Methenosulphate reagents
<b>MTSET</b>	[2-(Trimethylammonium)ethyl]methanethiosulfonate
<b>N-terminus</b>	Amino-terminus
<b>NAcc</b>	Nucleus accumbens
<b>nAChR</b>	Nicotinic acetylcholine receptors
<b>nH</b>	Hill coefficient
<b>NAMs</b>	Negative allosteric modulators
<b>Nic</b>	Nicotine
<b>PAMs</b>	Positive allosteric modulators
<b>PCR</b>	Polymerase chain reaction
<b>pLGIC</b>	Pentameric ligand-gated ion channel
<b>Saz-A</b>	Sazetidine-A
<b>SCAM</b>	Substituted Cysteine Accessibility Method
<b>SEM</b>	Standard error of the mean
<b>TC-2559</b>	4-(5-ethoxy-3-pyridinyl)-N-methyl-(3E)-3-buten-1-amine difumarate
<b>TMD</b>	Transmembrane domain
<b>Var</b>	Varenicline
<b>VTA</b>	Ventral tegmental area



## Abstract

Nicotinic acetylcholine receptors (nAChR) containing  $\alpha 4$  and  $\beta 2$  nAChR subunits are the most prevalent type of nAChR in the brain, where they modulate an assortment of physiological functions such as cognition, mood, reward and analgesia.  $\alpha 4\beta 2$  nAChRs have been implicated in a wide range of diseases such as depression, Alzheimer's, Parkinson's, Schizophrenia and a type of familial epilepsy. Also,  $\alpha 4\beta 2$  nAChRs are necessary and sufficient for the rewarding and reinforcing effects of nicotine.

The  $\alpha 4\beta 2$  receptors assemble in two functional forms,  $(\alpha 4\beta 2)_2\alpha 4$  and  $(\alpha 4\beta 2)_2\beta 2$ . These two receptors have different pharmacological properties, which is partly accounted for by the presence of an additional agonist site at the signature  $\alpha 4/\alpha 4$  interface of the  $(\alpha 4\beta 2)_2\alpha 4$  nAChR. The canonical agonist sites of these receptors function asymmetrically, even though they are structurally equivalent. These findings suggested that the fifth subunit ( $\alpha 4$  in the  $(\alpha 4\beta 2)_2\alpha 4$  and a  $\beta 2$  in the  $(\alpha 4\beta 2)_2\beta 2$  may asymmetrically modulate the agonist sites.

The impact of the fifth subunit on receptor function was investigated by using concatenated  $(\alpha 4\beta 2)_2\alpha 4$  and  $(\alpha 4\beta 2)_2\beta 2$  nAChRs expressed heterologously in *Xenopus* oocytes in combination with mutagenesis and functional analysis. Concatenated receptors permit the expression of only one type of receptor stoichiometry and the mutations can be introduced in defined subunits of the pentamer.

The overall aim of this PhD study was to advance our understanding of how the signature  $\beta 2/\beta 2$  and  $\alpha 4/\alpha 4$  interfaces of  $(\alpha 4\beta 2)_2\beta 2$  and  $(\alpha 4\beta 2)_2\alpha 4$  nAChRs respectively affect the function of neighbouring  $\alpha 4\beta 2$  nAChRs.

In  $(\alpha 4\beta 2)_2\alpha 4$  receptors, the presence of an additional site at the  $\alpha 4(+)/\alpha 4(-)$  interface underlies differences in sensitivity to ACh but the interface flanking agonist sites also modulate the function of this site. For the  $(\alpha 4\beta 2)_2\alpha 4$  receptors, this thesis examined the effects of mutations introduced in the fifth subunit or flanking subunits on  $Zn^{2+}$  potentiation of  $(\alpha 4\beta 2)_2\alpha 4$  receptors.  $Zn^{2+}$  potentiation of the agonist responses of the  $(\alpha 4\beta 2)_2\alpha 4$  receptors is mediated by a site located on the fifth subunit ( $\alpha 4$ ). It was found that  $Zn^{2+}$  potentiation is inhibited by alanine substitutions of amino acids linking the fifth subunit to neighbouring agonist sites.

For the  $(\alpha 4\beta 2)_2\beta 2$  receptors, the findings suggest that residues in loop B (W176, T177) and loop E (L146 and F144) of  $\beta 2(+)/\beta 2(-)$  interface link to the canonical agonist site anticlockwise to  $\beta 2(+)/\beta 2(-)$  to modulate maximal agonist responses. Long-range coupling analysis with the modulator  $\beta 2(+)/\beta 2(-)$  residues and a reported mutation in the ion channel,  $\beta 2L9'T$ , showed these residues functionally couples, thus suggesting that the modulation of maximal agonist currents likely occur at the gating domain.

Overall, it is proposed that the fifth subunit allosterically communicates with adjacent subunits to modulate agonist binding site function. These findings may lead to the development of stoichiometry- or interface-specific  $\alpha 4\beta 2$ -selective drugs.





# **Chapter 1**

## **Introduction**



## 1.1 Chemical communication in the Nervous System

Neuronal chemical signalling requires the depolarisation of the presynaptic terminal to initiate the release of neurotransmitter, a small organic molecule or a peptide that communicates the presynaptic terminal with the post-synaptic cell (**Fig 1.1, A**). Depolarisation of the presynaptic terminal is primarily achieved through the arrival of action potentials at the terminal. The action potential propagates from the axon hillock of the presynaptic neuron to its axon terminal and, once it reaches it, the terminal depolarises allowing  $\text{Ca}^{2+}$  entry through voltage-gated  $\text{Ca}^{2+}$  channels.  $\text{Ca}^{2+}$  entry initiates the fusion of neurotransmitter-containing synaptic vesicles with the presynaptic membrane facing the synaptic gap. Fusion then leads to neurotransmitter release into the synaptic gap (space between the pre- and postsynaptic cells). Neurotransmitters diffuse across the gap towards the post-synaptic cell to bind integral membrane proteins (neurotransmitter receptors) located on the membrane of the post-synaptic cell. Binding of these molecules triggers conformational changes in the receptors that are transduced into signals (**Figure 1.1, B**). If the receptors are ligand-gated ion channels (LGICs), the signals are ionic currents that depolarise or hyperpolarise the post-synaptic neuron, depending on the ionic permeability of the LGIC activated. The function of the nervous system is primarily driven by this type of synaptic signalling, and when it is impaired, debilitating disorders, such as mood disorders (e.g., depression), cognitive impairment (e.g., dementia, attention deficit disorder), neurological diseases (e.g., epilepsy) or psychiatric diseases (e.g., schizophrenia) develop (Lepeta *et al.*, 2016).

A key component of chemical signalling is the post-synaptic receptor that binds the neurotransmitters. These receptors may be metabotropic, which typically alter transiently the basal status of second messengers, or LGICs, which as stated in the previous paragraph, generate transient ionic currents. The ion channel element of LGICs opens in response to the binding of endogenous ligands (neurotransmitters) or exogenous agonists to allow the flow of ions (**Fig. 1.1, B**). If the ion channel is permeable to cations (e.g.,  $\text{Na}^+$ ,  $\text{Ca}^{2+}$ ), the current generated is depolarising. In contrast, if the channel is permeable to anions (e.g.,  $\text{Cl}^-$ ), the current is hyperpolarising. LGICs are also present in pre-synaptic terminals or the cell body of presynaptic neurones, from where they regulate the balance between excitation and inhibition of the cell, an essential mechanism to modulate chemical signalling in neurones (Wonnacott, 1997). A receptor family that plays a key role neuronal signalling is the neuronal

nicotinic acetylcholine receptor (nAChR) family (Wonnaccott, 1997). This thesis focuses on the function and structure of a brain nAChR, the  $\alpha 4\beta 2$  nAChR.

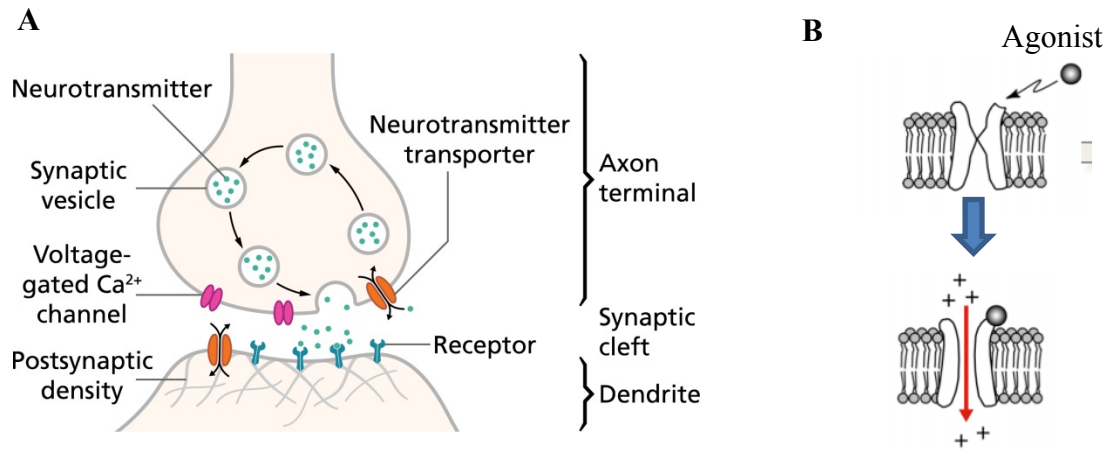


**Figure 1.1 Neuronal communication through chemical synaptic transmission. A)** Chemical synapses comprise a pre-synaptic terminal that contain neurotransmitter-containing vesicle and the post-synaptic terminal that contains the receptors for the neurotransmitter released during signalling. **B)** Post-synaptic ligand-gated ion channels undergo conformational rearrangement upon neurotransmitter binding to allow ions to traverse the membrane.

## 1.2 nAChRs

nAChRs were first suggested by Langley in 1905 (Langley, 1905). Langley showed that nicotine (Nic) could stimulate denervated muscle cells, which led him to propose the concept of receptor and signal transduction. Almost 70 years later, the nAChR from the electric fish organ was biochemically isolated, a breakthrough that led to a new molecular and structural approach to the characterisation of LGICs (Changeux *et al.*, 1970).

nAChRs belong to the pentameric ligand gated ion channel (pLGIC) family that includes prokaryotic (GLIC and ELIC) and eukaryotic (Cys loop receptors) LGICs (Lester *et al.*, 2004). Within the pLGICs, nAChRs belong to the Cys-loop LGIC family, which comprises excitatory (e.g., nAChR, 5HT<sub>3</sub>) and inhibitory (e.g., GABA<sub>A</sub>, Glycine receptors, and the invertebrate glutamate-gated chloride channel (GluCL) receptor). The name Cys-loop is because the receptor subunits of this family possess a conserved 13 residue loop (the  $\beta$ 6- $\beta$ 7 loop) in the extracellular portion that is flanked by two di-sulfide bond forming cysteine residues. All pLGICs comprise five subunits arranged around a central ion-conducting pore (the ion channel) (Corringer *et al.*, 2012).

Cys-loop LGICs exist in at least four distinct, interconvertible states: resting (agonist unbound, closed), flipped (agonist-bound, closed), open (agonist-bound, open) and desensitised (agonist-bound, closed) conformations or states, and the binding of agonists, antagonist and allosteric compounds alters the equilibrium between these states. Agonists such as neurotransmitters bind the agonist site, which is located in the extracellular domain (ECD) of the receptors, and this triggers rapid opening of an intrinsic ion channel. Prolonged exposure to the agonist induces the non-conducting (desensitised) state of the ion pore.

nAChRs are divided into two groups: muscle receptors, which mediate skeletal muscle contraction at the neuromuscular junction, and neuronal receptors which are present in the peripheral and central nervous system, where they are involved in both fast synaptic transmission and presynaptic modulation of neurotransmitter release (Wonnacott, 1997; Albuquerque *et al.*, 2009). nAChRs have also been found in diverse type of non-neuronal cells, including cells of the immune system (leukocytes and macrophages), skin cells and small cell lung cancer cells (Zoli *et al.*, 2017). They have also been found in mitochondria (Gergalova *et al.*, 2012).

### 1.2.1 nAChR subunits

To date, seventeen nAChR subunits have been identified. The nAChR subunits include multiple  $\alpha$  ( $\alpha 1$ – $\alpha 10$ ) and  $\beta$  subunits ( $\beta 1$ – $\beta 4$ ) as well as  $\delta$ ,  $\gamma$ , and  $\epsilon$  subunits. These subunits have been highly conserved through evolution and each single subunit has more than 80% amino acid identity across vertebrate species (Albuquerque *et al.*, 2009). The nAChR subunits can be divided into four subfamilies (I–IV) based on similarities in protein sequence (Table 1.1) (Millar, 2003).

**Table 1.1. nAChR family subunits**

nAChR Subunits					
Neuronal-Type Subunits					Muscle-Type Subunits
I	II	III			IV
$\alpha 9, \alpha 10$	$\alpha 7, \alpha 8$	$\alpha 2, \alpha 3, \alpha 4, \alpha 6$	$\beta 2, \beta 4$	$\beta 3, \alpha 5$	$\alpha 1, \beta 1, \delta, \gamma, \epsilon$

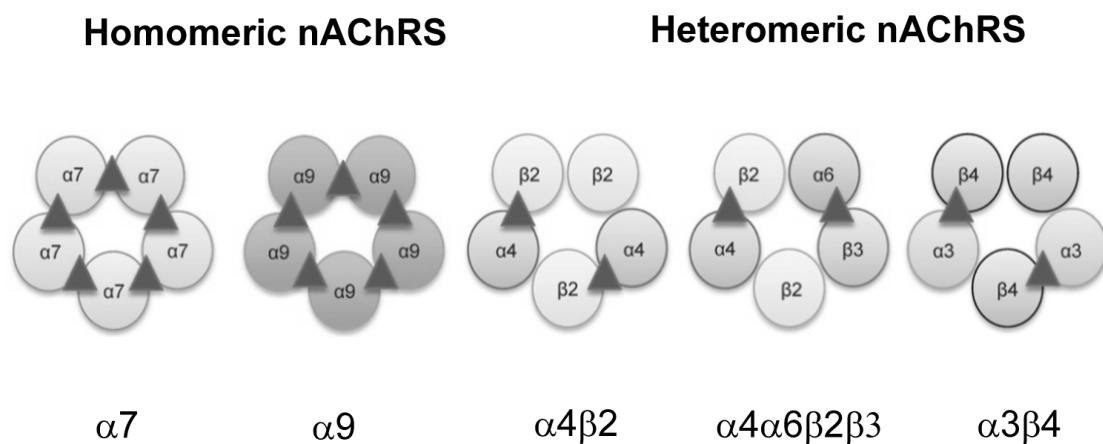


**Figure 1.2. Neuronal nAChR Structure.** Cartoon of the nAChR subunits arranged as pentamers around the pore. ACh binding sites are depicted as red triangles (Figure adapted from Hendrickson *et al.*, 2013).

Subunit composition determines the functional characteristics of nAChRs, including number of agonist sites present and ligand sensitivity (Harpsoe *et al.*, 2011; Mazzaferro *et al.*, 2011; 2014), channel kinetics (Mazzaferro *et al.*, 2017),  $\text{Ca}^{2+}$  permeability (Fucile, 2004), assembly (Gotti *et al.*, 2009), interactions with chaperones (Jeanclous *et al.*, 2001), trafficking and cell localisation (Colombo *et al.*, 2013) (Fig. 1.2). Foetal muscle-type nAChRs are composed of

$\alpha 1$ ,  $\beta 1$ ,  $\gamma$ , and  $\delta$  subunits in a 2:1:1:1 ratio, whereas in the adult the receptor is made up of  $\alpha 1$ ,  $\beta 1$ ,  $\delta$  and  $\epsilon$  subunits in a 2:1:1:1 ratio. Neuronal nAChRs are homomeric (e.g.,  $(\alpha 7)_5$ ) or heteromeric (e.g.,  $\alpha 4\beta 2$ ,  $\alpha 5\alpha 4\beta 2$ ;  $\alpha 6\beta 2\beta 3$ ) from combinations of twelve different nicotinic receptor subunits,  $\alpha 2$ – $\alpha 10$  and  $\beta 2$ – $\beta 4$  (Zoli *et al.*, 2017). The  $\alpha 7$  subunit was considered to be the homomeric member of the nAChR family. However, recent evidence has demonstrated the presence of heteromeric  $\alpha 7\beta 2$  nAChRs in rodent and human brain (Liu *et al.*, 2009; Moretti *et al.*, 2014; Thomsen *et al.*, 2015).

In nAChRs,  $\alpha$  subunits contribute to the principal side (+) of the agonist binding, although due to the conservation of complementary residues involved in agonist binding in nAChRs, they can also contribute the complementary side (-) of the agonist sites (e.g., agonist sites in the homomeric  $\alpha 7$  nAChR) (**Fig. 1.2**) or the additional agonist site on the  $\alpha 4(+)/\alpha 4(-)$  interface of the  $(\alpha 4\beta 2)_2\alpha 4$  nAChR. In heteromeric neuronal nAChRs,  $\beta 2$  and  $\beta 4$  subunits contribute to the complementary side of agonist sites on  $\alpha/\beta$  interfaces; these subunits lack the cysteine doublet of loop C, a key agonist-binding transduction element present in all  $\alpha$  subunits, except the  $\alpha 5$  subunit. In heteromeric LGIC consisting of three  $\beta$  subunits [e.g.  $(\alpha 4\beta 2)_2\beta 2$ ], there are two agonist sites, one at each of its  $\alpha/\beta$  interfaces; the fifth subunit does not contribute to agonist binding. The non-agonist binding subunit is termed as accessory subunit. However, in heteromeric receptors containing three  $\alpha$  subunits [e.g.,  $(\alpha 4\beta 2)_2\alpha 4$ ], there are three agonist sites: one at each  $\alpha/\beta$  interface and one at the  $\alpha/\alpha$  interface between the “accessory subunit” and an  $\alpha$  subunit that is also part of a  $\alpha/\beta$  interface (**Fig 1.3**).  $\beta 3$  and  $\alpha 5$  are considered accessory subunits but recent studies that have used tethered nAChR receptors have shown they can contribute to operational agonist sites (Jain *et al.*, 2016). Therefore, for clarity purposes, the accessory subunit, whether an agonist binding or non-agonist binding subunit will be referred to as the fifth subunit throughout this thesis.  $\alpha 10$  subunits cannot form operational pLGICs on their own but assembled with  $\alpha 9$  forms  $\alpha 9\alpha 10$  receptors, where it contributes the complementary side of  $\alpha 9(+)/\alpha 10(-)$  agonists sites (Zoli *et al.*, 2017). In muscle nAChRs,  $\delta$ ,  $\gamma$  and  $\epsilon$  contribute the complementary side of the agonist sites, whilst  $\alpha 1$  subunit is the principal subunit and  $\beta 1$  the fifth subunit (Unwin, 2005).

### 1.2.2 The membrane topology of nAChRs

Since the resolution of the atomic structure of the acetylcholine binding protein (AChBP) (Brejc K *et al.*, 2001), structural studies of pLGICs have been progressing steadily, providing insights into the three-dimensional structure and function of prokaryotic and eukaryotic pLGICs. The first high resolution structure of a pLGIC that became available was that of the *Torpedo* nAChR ion pore (Miyazawa *et al.*, 2003). Cryo-electronmicrographs of the closed/resting *Torpedo* nAChR pore of the receptor were obtained at 4 Å and these were subsequently refined by incorporating the crystal structure of the snail homologue of the nAChR, the AChBP (Brejc *et al.*, 2001), in 2005 (Unwin, 2005). The 4 Å model provided the first direct insight into the structure of the extracellular domain (ECD) of the nAChR and critically of the transmembrane domain (TMD), confirming the existence of four membrane-spanning  $\alpha$  helices in each subunit, as initially predicted by hydrophathy plots (Schofield *et al.*, 1987). In 2008 and 2009, the full-length crystal structure of two prokaryotic pLGICs, ELIC (Hilf and Dutzler 2008) and GLIC (Hilf and Dutzler, 2009), was resolved, which opened the gates to the determination of full length atomic structures of a number of eukaryotic pLGICs confirming the basic structure of these proteins and adding further insights into their structure-function relationship. Both ELIC and GLIC are cation-selective ion channels that show high sequence and structure similarity to the nAChRs and the 5HT3 receptor. In 2011, the first X-ray structure of a eukaryotic pLGIC, the GluCl pLGIC from *Caenorhabditis elegans*, was resolved (PDB ID 3RIA) (Hibbs and Gouaux, 2011). The crystal structure of the GluCl protein revealed an open conformation of the pLGIC. Subsequently, the atomic structures of homopentameric GABA<sub>A</sub>  $\beta$ 3 receptor (Miller and Aricescu, 2014), serotonin type 3 (5HT3) receptor (Hassaine *et al.*, 2014), glycine  $\alpha$ 3 subunit bound to antagonists (Huang *et al.*, 2015) and human  $(\alpha$ 4 $\beta$ 2)<sub>2</sub> $\beta$ 2 nAChR (Morales-Pérez *et al.*, 2016) were determined. In addition to the *Torpedo* nAChR (Unwin, 2005; Unwin and Fujiyoshi, 2012; Unwin 2013), high-resolution cryo-electronmicrographs for the Glycine receptor are also available (Du *et al.*, 2015). All of these structures, with the exception of the cryo-micrographs of the Glycine receptor (Du *et al.*, 2015) correspond to the desensitized or closed (bound to antagonist) conformation of these proteins.

Comparison of the prokaryotic and eukaryotic aforementioned structures confirmed that the overall structure is conserved among the pLGICs, in which five homologue subunits assemble around the ion channel (**Fig. 1.3 A, B**). The different eukaryotic Cys loop LGICs



subunits share a basic scaffold composed of an extracellular domain (ECD), the TMD, an intracellular domain (ICD) between the third and fourth transmembrane helix and a short extracellular C-terminus. The receptors are therefore built from modular units with an ECD containing the agonist/antagonist binding site, a TMD containing the ion pore and allosteric modulatory sites and a large cytoplasmic domain involved in receptor trafficking and regulation (Colombo *et al.*, 2013) (**Fig. 1.3, C**). Comparison of available structures revealed that the overall structure of cation-selective pLGICs (nAChRs and 5-HT<sub>3</sub>R) is different from anion-selective pLGICs (GABA<sub>A</sub>Rs and GlyRs) in that the former contains a relatively large ICD that may play an important role in cation conduction (Lambert *et al.*, 1989).

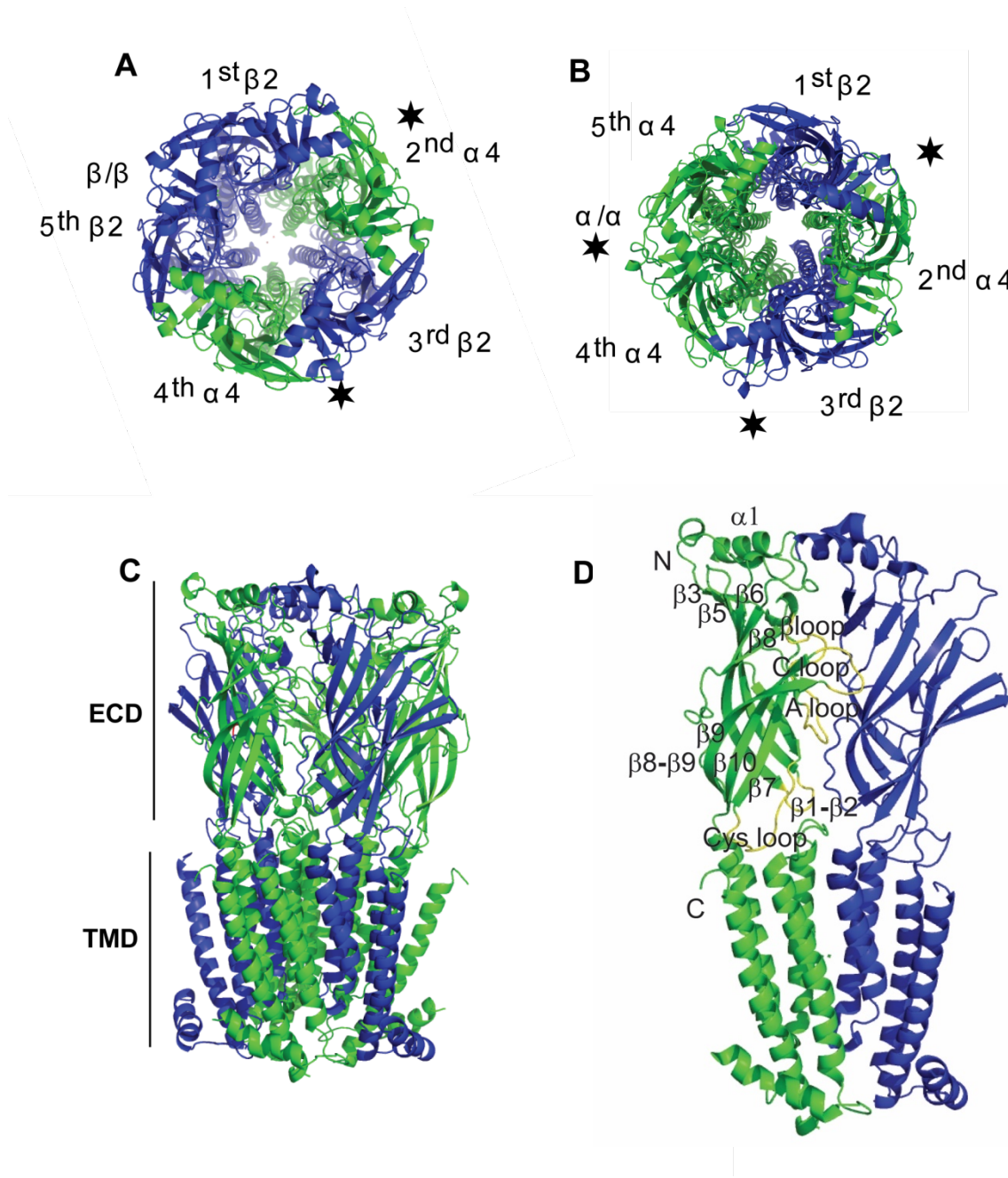


**Figure 1.3. Overall structure and fold of the  $(\alpha 4\beta 2)_2\beta 2$  and  $(\alpha 4\beta 2)_2\alpha 4$  nAChRs.** **A, B)** Top view of the  $(\alpha 4\beta 2)_2\beta 2$  and  $(\alpha 4\beta 2)_2\alpha 4$ , as viewed from the extracellular side. **C)** Whole assembly, lateral side view, showing the ECD and TMD domains of the receptor. **D)** Close up of the ECD showing the  $\beta$ -sandwich structure of this domain. The receptors are represented as ribbon structures. The  $(\alpha 4\beta 2)_2\beta 2$  receptor was generated from the published structure of this receptor. PDB ID 5kxi(Morales-Pérez *et al.*, 2016) using PYMOL (<http://www.pymol.org>). A homology model of the  $(\alpha 4\beta 2)_2\alpha 4$  receptor based on the structure of  $(\alpha 4\beta 2)_2\beta 2$  was used to generate the images for this receptor. The individual subunits are distinguished by colour (green,  $\alpha 4$  and blue,  $\beta 2$ ).

### 1.2.3 The ECD and the Agonist Binding Site

The atomic structure of the ECD was first solved for the AChBP from invertebrate snails (Brejc *et al.*, 2001; Celie *et al.*, 2005; Hansen *et al.*, 2005). In agreement with the structure of the AChBP (Brejc *et al.*, 2001), the ECD domain of nAChRs is folded into a highly conserved immunoglobulin-like  $\beta$  sandwich stabilised by inner hydrophobic residues (Unwin, 2005; Delissanti *et al.*, 2007; Unwin and Fujiyoshi, 2012; Morales- Pérez *et al.*, 2016). The inner  $\beta$ -sheet is formed by  $\beta$ 1,  $\beta$ 2,  $\beta$ 3,  $\beta$ 5,  $\beta$ 6 and  $\beta$ 8 and the outer  $\beta$ -sheet by  $\beta$ 4,  $\beta$ 7,  $\beta$ 9 and  $\beta$ 10. The N- and C-termini are located at the top and bottom of the pentamer fold, respectively. The C-terminus of  $\beta$ 10 is connected to the N-terminus of TM1. The linker between strands  $\beta$ 6 and  $\beta$ 7 forms the signature Cys-loop found in all members of the Cys-loop LGIC family (**Fig. 1.3, D**). This Cys-loop is close to the TMD and plays a role in the propagation of conformational changes from the ECD to the TMD (Lee and Sine, 2005).

Each AChBP molecule has five identical binding sites for ACh and nicotine (Nic), located at the interface between subunits (Brejc *et al.*, 2001; Celie *et al.*, 2005; Hansen *et al.*, 2005). In Cys loop LGICs, agonist binding sites are also located at the interface between neighbouring subunits. The agonist binding site is asymmetrical, comprising a principal side contributed by the principal subunit and the complementary side, contributed by the complementary subunit. In non-muscle heteromeric nAChRs, the agonist sites are located at  $\alpha/\beta$  interfaces, where, as mentioned previously,  $\alpha$  subunit is the principal subunit and  $\beta$  the complementary subunit (**Fig 1.3 A, B**).  $\alpha$  subunits that contribute the principal side to  $\alpha/\beta$  agonist sites include  $\alpha$ 2,  $\alpha$ 3,  $\alpha$ 4 and  $\alpha$ 6. The complementary subunit in  $\alpha/\beta$  agonist sites is contributed by  $\beta$ 2 or  $\beta$ 4 subunits. Because there are two of these interfaces, the heteromeric nAChRs contain two  $\alpha/\beta$  agonist sites. In the muscle receptor, the agonist sites are at  $\alpha$ 1/ $\delta$  and  $\alpha$ 1/ $\gamma$  or  $\epsilon$  interfaces. Recent studies have shown that heteromeric nAChRs may contain additional agonist sites at interfaces not thought to bind agonists. Thus, for example,  $\alpha$ 4 $\beta$ 2 nAChRs made of three  $\alpha$ 4 and two  $\beta$ 2 subunits contain an additional site at its signature  $\alpha$ 4/ $\alpha$ 4 interface (Harpsøe *et al.*, 2011; Mazzaferro *et al.*, 2011). Additional agonist sites have more recently been identified on  $\alpha$ 5/ $\alpha$ 4,  $\beta$ 3/ $\alpha$ 4, and  $\alpha$ 4/ $\alpha$ 5 subunit interfaces (Jain *et al.*, 2016; Jin *et al.*, 2014; Wang *et al.*, 2015). In homopentamers, the same type of subunit provides both principal and complementary faces of the agonist binding site (Taly *et al.*, 2009) resulting in five putative binding sites per homomeric receptor, although not all of them need to be bound to activate the receptor (Rayes *et al.*, 2009).

Early mutagenesis and photoaffinity studies (Corringer *et al.*, 2000) and the more recent high resolution crystal structures of AChBPs and nAChRs in complex with several nicotinic receptor ligands revealed the agonist binding sites for agonists and antagonists in detail (Unwin, 2005; Delissanti *et al.*, 2007; Unwin and Fujiyoshi 2012; Morales-Pérez *et al.*, 2016). As stated above, the agonist binding sites are situated at the interface between two neighboring subunits with the contribution of three regions from the principal subunit named loops A, B and C, and from 4 regions from the complementary subunit,  $\beta$ -strands D/E and loops F and G. Agonist binding residues within these loops are highly conserved in the Cys loop receptors. Loops A (Tyr), B (Trp), C (two Tyr), and D (Trp) form an aromatic “box” chelating the quaternary ammonium moiety of ACh (**Fig. 1.4**). Among these residues, Trp from loop B elicits a direct cation- $\pi$  interaction with the quaternary amine group of ACh (Zhong *et al.*, 1998; Xiu *et al.*, 2009). Unnatural amino acid mutagenesis further shows that the extent of cation- $\pi$  interaction critically contributes to the ligand binding affinity and, notably, is responsible for the high affinity of nicotine for the neuronal  $\alpha 4\beta 2$  nAChR (Xiu *et al.*, 2009). The acetyl portion of ACh interacts with loops E and F that are highly variable in sequence among nAChRs.

At present, several structures of AChBP with various bound ligands (Rucktooa *et al.*, 2009) including agonists such as nicotine (Celie *et al.*, 2004), partial agonists such as anabasein (Hibbs *et al.*, 2009), and antagonists such as d-tubocurarine and  $\alpha$ -cobratoxin (Bourne *et al.*, 2005; Brams *et al.*, 2011) have been determined. All AChBP structures display the same conformation, with the notable exception of the extension of loop C capping because its shape adapts to the size of the ligands. Binding of small molecules such as nicotine fits with a capped loop C, which lead to a contraction of the binding site (**Fig. 1.4, D**). In agreement with this finding, crystal structures of the  $(\alpha 4\beta 2)_2\beta 2$  nAChR bound to nicotine show loop C capping (Morales- Pérez *et al.*, 2016). Larger compounds, typically antagonists such as  $\alpha$  toxins from snakes, are associated with an uncapped loop C conformation, which is characterized by its outward motion, allowing sufficient space for ligand binding. These findings have suggested that loop C capping may be the first event of the agonist binding-gating transduction pathway (Billen *et al.*, 2012). However, Loop C capping has also been observed for nAChR antagonists such as dihydro- $\beta$ -erythroidine (DH $\beta$ E) (**Fig. 1.4, D**) (Shahsavari *et al.*, 2012) so not all agonists induce capping (for a review, see Nys *et al.*, 2013).

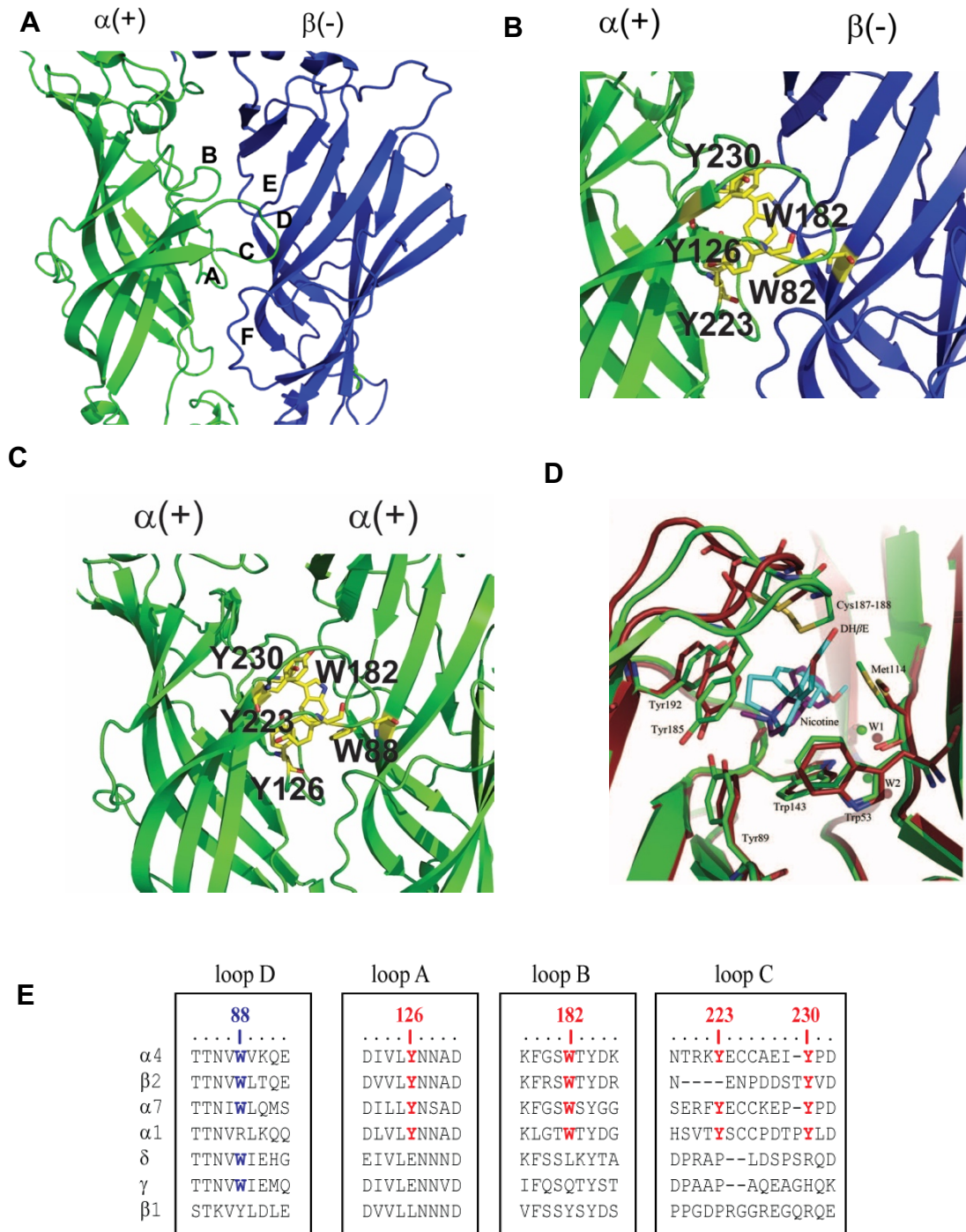


**Figure 1.4. Structure of the  $(\alpha 4\beta 2)_2\beta 2$  and  $(\alpha 4\beta 2)_2\alpha 4$  nAChRs.** **A)** Conserved loops at  $\alpha 4/\beta 2$  subunit interfaces in  $\alpha 4\beta 2$  nAChRs (agonist binding site). **B, C)** Agonist binding residues in the agonist site, at  $\alpha 4/\beta 2$  and  $\alpha 4/\alpha 4$  interfaces respectively, showing conserved agonist binding aromatic amino acids. Images were generated using PYMOL from the X-ray structure of the  $(\alpha 4\beta 2)_2\beta 2$  nAChR. PDB ID 5kxi. (Morales-Pérez *et al.*, 2016). **D)** Conformational change of the C-loop due to DHbE binding to Ls-AChBP. The DHbE-bound structure (red) has been superimposed onto the nicotine-bound LS-AChBP structure (green). (Figure adapted from Shahsavari *et al.*, 2012). **E)** Alignment of conserved aromatic residues contributing to agonist binding in human  $\alpha 4\beta 2$ ,  $\alpha 7$  and muscle nAChRs.

### 1.2.4 The TMD and the Ion Channel

The 4 Å model of the *Torpedo* nAChR provided the first direct insight into the structure of the TMD (Miyazawa *et al.*, 2003; Unwin, 2005), confirming the existence of four membrane-spanning  $\alpha$  helices in each subunit, as initially predicted by hydrophathy plots (Schofield *et al.*, 1987). The  $\alpha$ -helical nature of the TMD was subsequently confirmed by nuclear magnetic resonance (NMR) structures of the TMD of the neuronal  $\alpha 4\beta 2$  nAChR (Bondarenko *et al.*, 2012, 2013) and by crystal structures of full-length prokaryotic and eukaryotic pLGICs (Lee and Sine, 2005; Hilf and Dutzler, 2008; 2009). Recent X-ray structures of the 5HT<sub>3</sub> (Hassaine *et al.*, 2014), GABA<sub>A</sub>  $\beta 3$  (Miller and Aricescu, 2014) and  $(\alpha 4\beta 2)_2\beta 2$  receptors (Moralez- Pérez *et al.*, 2016) have confirmed the overall topology of the TMD and they have provided a more refined view of this domain. The four transmembrane regions fold into  $\alpha$ -helices forming a single ion channel along the pseudo-symmetry axis of the protein (Miyazawa *et al.*, 2003; Unwin, 2005). The TMD is covalently linked to the ECD. The M2  $\alpha$ -helices from each subunit lines the ion pore walls (Imoto *et al.*, 1986, 1988) and are surrounded by a ring of  $\alpha$  helices made of M1, M3 and M4. The latter helices are located on the periphery of each subunit and highly exposed to the lipid bilayer with which it appears to interact extensively (Henault *et al.*, 2015).

The assembly of the five M2 helices forms the ion channel pore, which is an important segment of the ion conduction pathway. This pathway is composed of an extracellular vestibule, an inner pore-forming domain and an  $\alpha$ -helix from the intracellular M3-M4 loop (Unwin, 2005; Hilf and Dutzler, 2008; 2009). The M2 helices are highly homologous within pLGIC families. The helices align vertically within the membrane, making the lining of the pore consist of concentric rings of similar or identical residues (**Fig. 1.5, A**) For comparison reasons, a prime number notation is used starting with the highly conserved positively-charged residues on the cytoplasmic end of M2, defined as 0', increasing to another ring of charged residues at the extracellular end denoted by 20' (Miyazawa *et al.*, 2003). The rings are hydrophobic in the nAChR (9' and 16' leucines; 13' valine). Ring residues are polar at position 2' (threonine) and 6' (serine) and at the intracellular and extracellular ends of M2, they are charged (-1 and 20', glutamate) (**Fig. 1.5, B**) (Unwin, 2005).

The ion pore changes its overall conformation, depending on the functional state of the receptor (i.e., closed, open, desensitised). As seen in the *Torpedo* nAChR (Miyazawa *et al.*,

2003; Unwin, 2005), M2 is constricted mid-way between position 9'-14', strongly suggesting that this position is the main gate. Here, two rings, 9' leucine and 13' valine face into the lumen and constrict the channel by forming a hydrophobic girdle of about 6 Å in diameter (Miyazawa *et al.*, 2003; Unwin, 2005). This constriction is sufficient to block the passage of hydrated Na<sup>+</sup> and K<sup>+</sup> ions, which are about 8 Å in diameter, whereas permeation by smaller dehydrated ions is prevented because the hydrophobicity of the girdle cannot compensate for the lost hydration shell (Unwin, 2005; Hilf and Dutzler, 2008). In the  $\alpha 4\beta 2$  nAChR, which was crystallised in the desensitised, non-conducting conformation, the diameter of the pore increases in the constricting hydrophobic region near the middle of the membrane, and the narrowest region shifts near to the intracellular membrane surface where the pore is lined by polar residues (glutamate -1' position of the M2  $\alpha$ -helices) (Morales-Pérez *et al.*, 2016). This position of the constriction is also observed in crystals of the GABA<sub>A</sub>  $\beta 3$  receptor bound to the agonist benzamidine (Miller and Aricescu, 2014) and in cryo electron micrographs of the Glycine receptor bound to Glycine (Du *et al.*, 2015), suggesting that desensitisation constricts the intracellular portion of TM2 (**Fig. 1.5, C**). In the open pore conformation, according to cryoelectron micrographs of the Glycine receptor (Du *et al.*, 2015), the TMD of each subunit rotates outwardly and anti-clockwise, pulling the side chains of 9' leucine and -2 proline away from the channel axis, thus enlarging the pore size.

The TMD of the nAChRs and, indeed of all pLGICs (Taly *et al.*, 2014) contain binding sites for various allosteric modulators. General anesthetics are small hydrophobic compounds that allosterically inhibit the receptors by binding to a small cavity formed by specific residues located between M3 and M4. Crystal structures of the GluCl in complex with a hydrophobic ligand enabled visualisation of this allosteric binding site (**Fig 1.6**) (Martin *et al.*, 2017).

These allosteric modulators act by binding to regions called allosteric sites, which are separate from the agonist binding sites. Ivermectin, PNU-120596, volatile and intravenous anaesthetics are examples of compounds that bind the TMD of pLGICs to allosterically modulate the function of pLGICs (Corringer *et al.*, 2012; Pandya and Yakel, 2013).

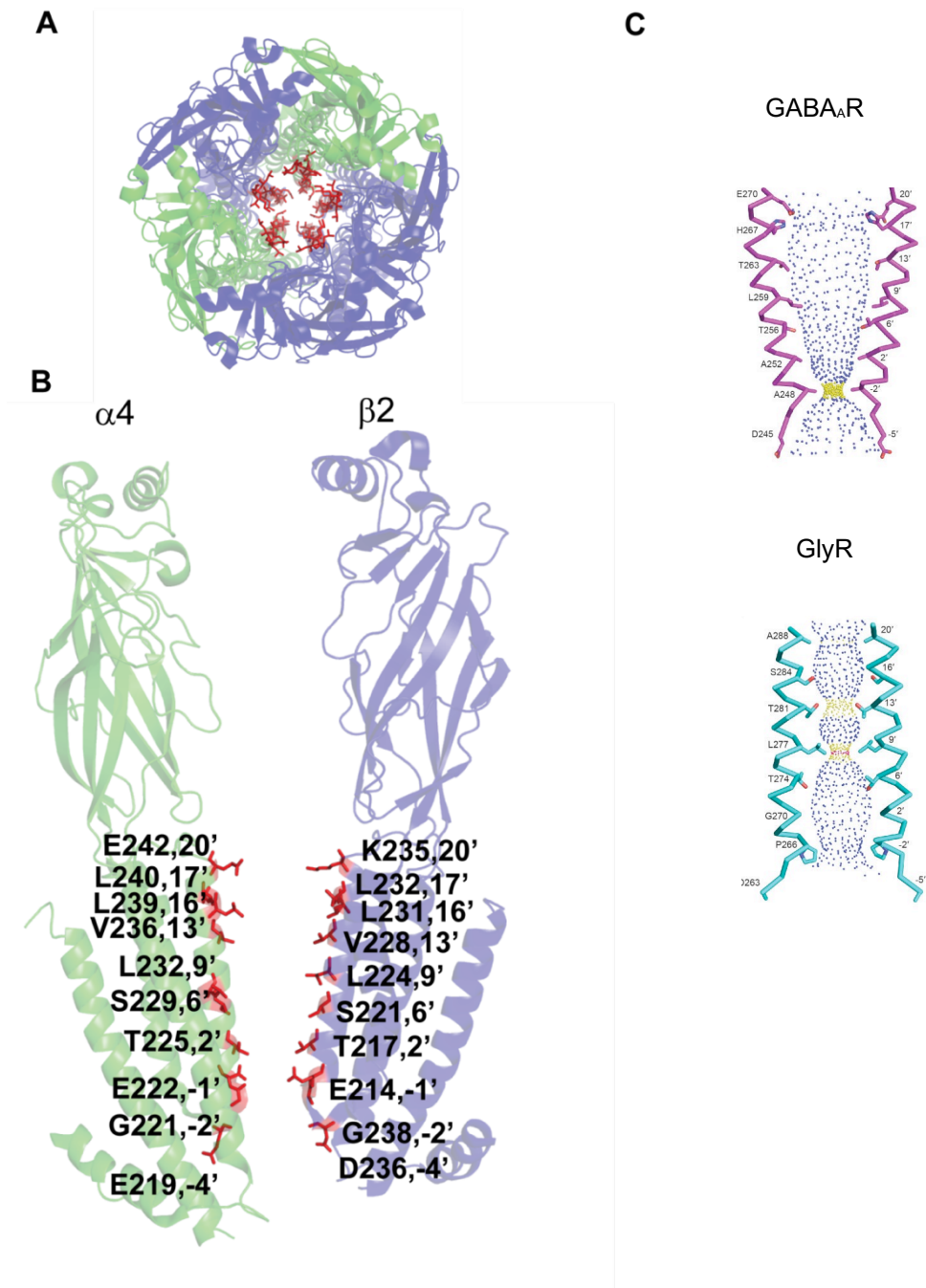


**Figure 1.5. Cys-loop receptor ion channel conformations.** **A)** Whole assembly of  $(\alpha 4\beta 2)_2\beta 2$  (lateral view) with individual subunits distinguished by colour (green,  $\alpha 4$  and blue,  $\beta 2$ ). M2 residues are in red. **B)** X-ray crystallographic structure of the human  $\alpha 4\beta 2$  nicotinic receptor (Morales-Pérez *et al.*, 2016). M2  $\alpha$ -helices (residues in red) from opposing  $\alpha 4$  and  $\beta 2$  subunits with side chains shown for pore-lining residues. **C)** M2  $\alpha$ -helices of GABA<sub>A</sub>R and GlyR with side chains shown for pore-lining residues (Morales-Pérez *et al.*, 2016).



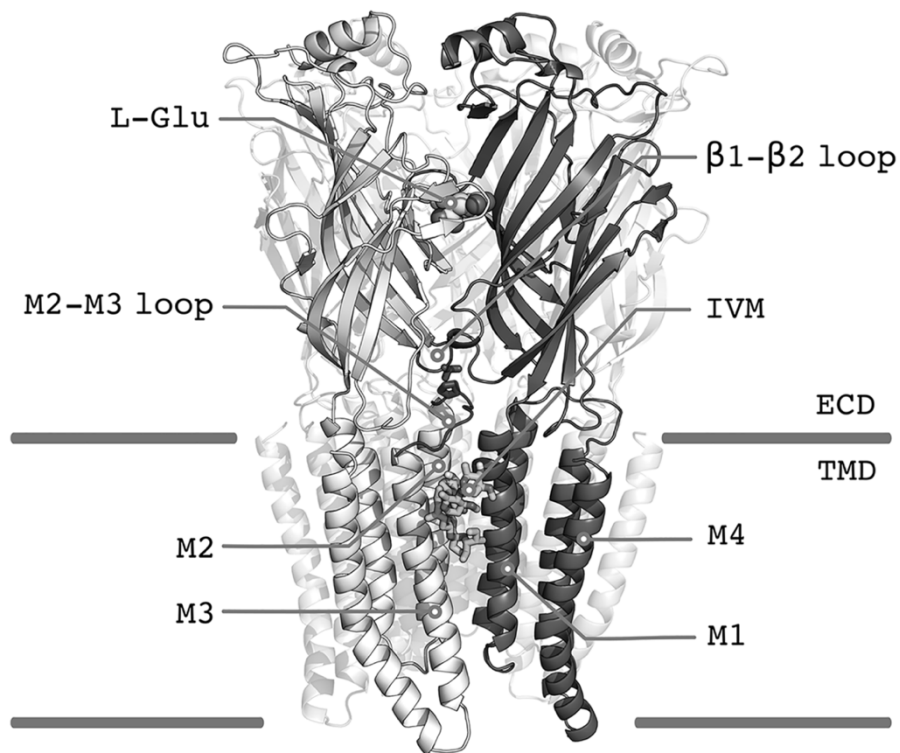


**Figure 1.6. Cartoon representation of GluCl active with L-Glutamate (L-Glu) and ivermectin (IVM) bound. PDB ID 3RIF. The structural regions corresponding to the extracellular (ECD) and the transmembrane (TMD) domains are shown. (Figure adapted from Martin *et al.*, 2017).**

### 1.2.5 The activation of nAChRs

pLGICS are prototypical allosteric proteins, in that the gating of the ion channel in the TMD is allosterically regulated by the binding of the neurotransmitter to the agonist site in the ECD (Changeux and Edelstein, 1998; Corringer *et al.*, 2012; Taly *et al.*, 2005). Agonist binding in these proteins triggers rigid body motions, which are transduced into transient movements of the pore lining M2  $\alpha$  helices of the TMD that is 50 Å away from the agonist site by a primary coupling pathway that runs along the long axis of the protein involving a series of loops of the subunit contributing the principal side of the agonist site ( $\beta$ 1- $\beta$ 2 loop, the Cys loop and M2-M3 linker) at the ECD/TMD interface (Lee and Sine 2005; Jha *et al.*, 2007; Lee *et al.*, 2009; Althoff *et al.*, 2014; Sauguet *et al.*, 2014). In the Cys loop receptors, binding to two agonist binding sites causes efficacious activation. Binding to a single site fails to induce the overall conformational change needed for efficacious gating (Wang *et al.*, 2015). For heteromeric receptors with three agonist sites, such as the  $(\alpha$ 4 $\beta$ 2) $\alpha$ 4 nAChR (Harpsoe *et al.*, 2011; Mazzaferro *et al.*, 2011), the additional  $\alpha$ 4(+)/ $\alpha$ 4(-) site increases the maximal activation driven by the  $\alpha$ 4/ $\beta$ 2 sites by five fold (Harpsoe *et al.*, 2011; Wang *et al.*, 2015), although it also increases acute and long-term high affinity desensitisation (Benallegue *et al.*, 2013). Similarly, in the  $\alpha$ 7 receptors, which contains five agonist sites, the receptor is gated more efficaciously by three bound agonist sites than by two. Higher occupancy than two or three binding sites promotes desensitisation (Rayes *et al.*, 2009).

The structural changes associated with activation have been inferred from the X-ray high resolution crystal structures of pLGICs as well as from molecular dynamic simulation studies of these proteins (Calimet *et al.*, 2013; for a review see, Cecchinni and Changeux, 2014). Currently, it is thought that the process of gating is a progressive stepwise isomerization. The mechanistic event involves twisting (closed) and blooming (open) phases (**Fig 1.6, A**). The receptor twisting contribute to the activation process by “locking” the ion channel in the open-pore form. This event starts from the agonist binding site (loops A, B and C). The side chains of conserved amino acid residues from the primary and complementary subunits bind the agonist in a non-covalent manner. Despite some contradictory data (see Nys *et al.*, 2013), it is generally thought that movement of loop C following agonist binding is a critical event in receptor activation. Loop C moves about 11 Å towards the receptor core, capping the agonist site and thus trapping the agonist within the binding site (Celie *et al.*, 2004; Hansen *et al.*, 2005; Billen *et al.*, 2012; Rucktooa *et al.*, 2012). Then it propagates to the ECD/TMD

interface via a rigid-body rearrangement of the extracellular  $\beta$ -sandwiches (**Fig. 1.6, B**) and moves down to the transmembrane helices (M2, M4, M3) to ultimately open the gate (blooming) (Calimet *et al.*, 2013; Sauguet *et al.*, 2014). Agonist binding-induced movements are also seen in subunits adjacent to the agonist site (Unwin and Fujiyoshi *et al.*, 2012; Du *et al.*, 2015), reiterating that receptor activation involves the whole receptor rather than just the agonist site and the ion channel.

Recent studies have shown that there are intermediate closed states between agonist binding and channel opening termed priming (Mukhtasimova *et al.*, 2009) or flipping states (Lape *et al.*, 2009). Interestingly, the efficacy of agonist is determined by their ability to reach the flipping states (Lape *et al.*, 2009). Partial agonists are as good as full agonists at opening the channel but they are less effective in reaching the flipping states (Lape *et al.*, 2009; see also, Sivilotti, 2010). Structures associated with priming have not been resolved, as yet. However, since it has been proposed that the extent of loop C contraction induced by agonist binding could reflect agonist efficacy (e.g., Billen *et al.*, 2012), loop C capping may be the structural determinant of the priming state.

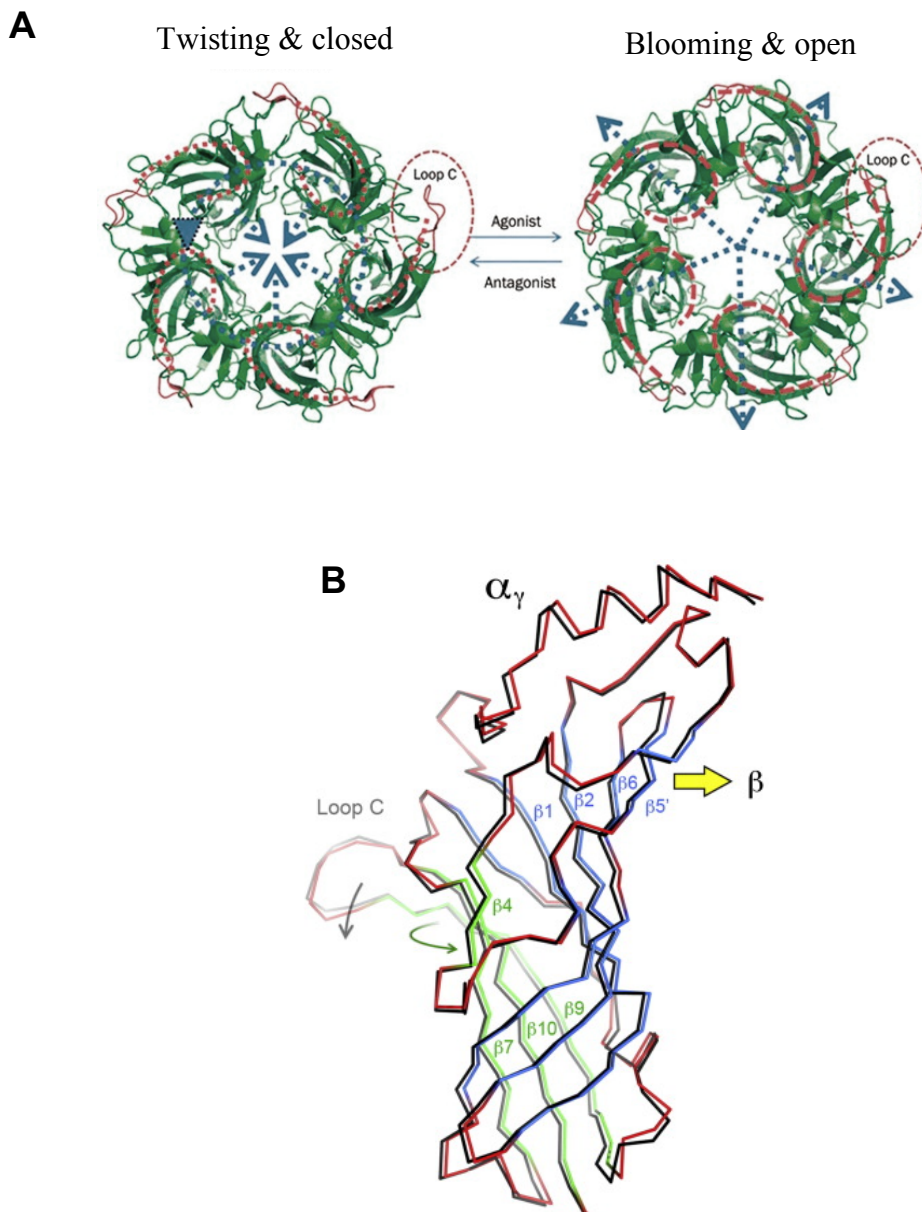


**Figure 1.7. The activation of pLGICs.** **A)** pLGICs activate through a process termed twisting (closing) and blooming (opening). Loop C caps during blooming. The blue dashed arrows illustrate the direction of the twisting and blooming. (Figure adapted from Wu *et al.*, 2015). **B)** The ECD of the  $\alpha 1$  subunit interfacing with the  $\gamma$  subunit viewed from the lumen of the channel. ACh binding to the agonist site on the  $\alpha 1/\gamma$  interface triggers a rearrangement of the inner and outer  $\beta$ -sheets of the  $\alpha 1$  subunit as shown by superposing the carbon backbone of the  $\alpha 1$  subunit in the open (red) and close (black) conformation. The inner and outer sheets of the open channel are coloured blue and green, respectively. Arrow denotes ACh-induced displacements (Adapted from Unwin and Fujiyoshi, 2012).

## 1.2.6 nAChR distribution in the brain

nAChRs are widely distributed in the central nervous system (CNS) as well as in the peripheral nervous system (PNS), where they are involved in a variety of functions such as cognition, reward, nociception, motor functions and mood (Gotti *et al.*, 2005; 2009).

In the mammalian brain, the most abundant nAChRs are the heteromeric  $\alpha 4\beta 2^*$  nAChR (the asterisk indicates that another subunit may also be present, e.g.,  $\alpha 5$ ,  $\alpha 6$ ) and the homomeric  $\alpha 7$  nAChR (Lindstrom *et al.*, 1996) (Fig. 1.7). This thesis focuses on the  $\alpha 4\beta 2$  nAChR, with particular emphasis on the structural mechanisms underlying the function of this receptor subtype.

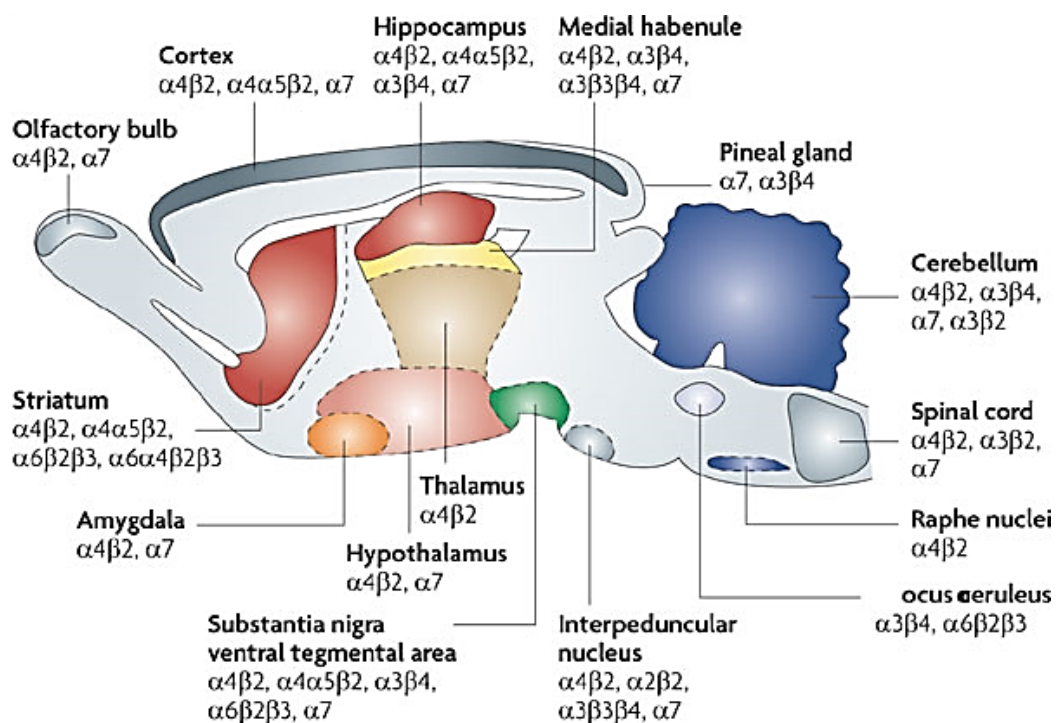


**Figure 1.8. Regional distribution of the nAChRs subunits in the rodent brain.** The nAChRs are predominantly expressed in CNS regions (Adapted from Gotti *et al.*, 2006).

### 1.3 $\alpha 4\beta 2$ nAChRs

In the brain,  $\alpha 4\beta 2$  nAChRs appear to be predominantly modulatory receptors rather than synaptic (Wonnacott *et al.*, 1989; Wonnacott, 1997; Dickinson *et al.*, 2008). As non-synaptic receptors, they modulate the synaptic release of diverse neurotransmitters, including ACh, dopamine, serotonin, GABA and ATP (Exley *et al.*, 2008; Galindo-Charles *et al.*, 2008; Marchi and Crilli, 2010). However, anatomical studies of rats and humans have identified cholinergic synapses in the neocortex and anterior temporal lobe (Turrini *et al.*, 2001) suggesting  $\alpha 4\beta 2$  nAChRs are post-synaptic. In addition, nicotine (Nic) directly applied to neurons induces inward currents, mediated by  $\beta 2$  subunit containing nAChRs (Picciotto *et al.*, 1995, 1998; Léna and Changeaux 1999).

This thesis focuses on the function of  $\alpha 4\beta 2$  nAChRs, particularly the role of  $\beta/\alpha$  interfaces in agonist responses.  $\alpha 4\beta 2$  nAChRs exist in two alternate stoichiometries,  $(\alpha 4\beta 2)_2\beta 2$  and  $(\alpha 4\beta 2)_2\alpha 4$  nAChRs. These receptors are termed HS (high sensitivity) and LS (low sensitivity), respectively, due to their markedly different sensitivity to activation by ACh (HS  $EC_{50}$  5-8  $\mu M$ ; LS  $EC_{50}$  80-100  $\mu M$ ; Nelson *et al.*, 2003; Moroni *et al.*, 2006; Carbone *et al.*, 2009; Mazzaferro *et al.*, 2011).

#### 1.3.1 Native $(\alpha 4\beta 2)_2\beta 2$ and $(\alpha 4\beta 2)_2\alpha 4$ nAChRs

$\alpha 4\beta 2$  nAChR function with alternate stoichiometries has been inferred in a number of brain regions such as the thalamus and the cortex by using a combination of mice lacking the  $\alpha 4$  or  $\beta 2$  subunits (Marks *et al.*, 1999; Gotti *et al.*, 2008; Marks *et al.*, 2010). The presence of alternate  $\alpha 4\beta 2$  nAChRs in thalamic and cortical neurones was subsequently confirmed by studies that used a novel  $(\alpha 4\beta 2)_2\alpha 4$  selective allosteric modulator showing that thalamo-cortical neurones express both  $(\alpha 4\beta 2)_2\beta 2$  and  $(\alpha 4\beta 2)_2\alpha 4$  nAChRs (Rode *et al.*, 2012; Timmermann *et al.*, 2012). Interestingly, the latter study also found that striatal neurones express solely the high-sensitivity  $(\alpha 4\beta 2)_2\beta 2$  isoform, suggesting that nAChR-modulation of dopamine release in the striatum is driven by this isoform and not by the two isoforms, or the  $(\alpha 4\beta 2)_2\alpha 4$  type. There is also evidence that both  $\alpha 4\beta 2$  receptors are present in motoneuron-Renshaw cell synapses, where the  $(\alpha 4\beta 2)_2\alpha 4$  receptor may act post-synaptically and the  $(\alpha 4\beta 2)_2\beta 2$  presynaptically (d'Incamps and Ascher, 2014).

### 1.3.2 $\alpha 4\beta 2^*$ nAChRs in Brain Pathologies

$\alpha 4\beta 2^*$  nAChRs are involved in many physiological functions, such as cognition, mood, reward and nociception (Picciotto *et al.*, 2001). Likely, this wide range of functional effects stems from the modulatory effect of presynaptic  $\alpha 4\beta 2$  nAChR on the release of synaptic neurotransmitters. Diseases in which  $\alpha 4\beta 2^*$  nAChRs seem to be involved are addiction to tobacco smoking, depression, cognitive impairment in ageing and neurodegenerative diseases such as Alzheimer's diseases, a rare familial epilepsy (autosomal dominant nocturnal frontal lobe epilepsy, ADNFE), impaired pain sensation and Parkinson's disease (Corringer *et al.*, 2000; Picciotto *et al.* 2000; Gotti *et al.*, 2009; Picciotto *et al.* 2012). Despite numerous attempts at developing  $\alpha 4\beta 2$  nAChR-drugs for the treatment of these diseases, there has been little. This lack of success is likely to be multifactorial. For example, limited knowledge on which  $\alpha 4\beta 2^*$  nAChRs contribute to function or disease or the high level of homology between the nAChR family is an unsurmountable obstacle to receptor specific drugs. As more crystal structures become available, we will have more knowledge and may allow the therapeutical potential of this receptor type to be realised. The discussion that follows focuses on the functions or diseases that have been targeted for drug development.

#### 1.3.2.a Nicotine addiction

Nicotine addiction is a serious public health issue. Tobacco use is the most important preventable cause of early morbidity and mortality in industrialized countries (CDC, 2008; Fiore, 2000). Cigarette smoking is associated with increased risks for lung and pancreas cancer as well as coronary heart disease, and stroke.

Neuronal nAChRs are expressed throughout the central nervous system, in particular, the mesolimbic pathway that is implicated in nicotine addiction. nAChRs in the ventral tegmental area (VTA) are stimulated by Nic causing the release of dopamine in the nucleus accumbens (nAcc), from where signals are sent to the prefrontal cortex resulting in addiction (**Fig. 1.8**) (Corrigal *et al.*, 1994).

A substantial body of experimental evidence supports the view that nAChRs containing  $\alpha 4$  or  $\beta 2$  subunits are necessary and sufficient for the rewarding and reinforcing effects of Nic. Thus,  $\alpha 4\beta 2$  nAChRs have been shown to exhibit the highest affinity for Nic of all brain nAChRs and to be involved in cognitive pathways central to reward and addiction (Picciotto *et al.* 2001). Studies that used  $\beta 2(-)$  knock out mice suggested a central role in nicotine addiction for receptors featuring this subunit as these mice do not self-administer nicotine (Picciotto *et al.*, 1999). Also, in these animals Nic does not appear to exert any effect on dopamine release in the VTA or NAcc (Picciotto *et al.*, 1999). Crucially, if the  $\beta 2$  subunit is restored in these knock out mice, Nic self-administration behaviour is introduced alongside nicotine determined dopamine release in the VTA and NAcc (Maskos *et al.*, 2005). Also, an  $\alpha 4L9A$  mutation in the M2 of the  $\alpha 4$  subunit increases receptor sensitivity to activation by nicotine and induces Nic-addiction behaviours at a Nic concentration 50-fold lower than the concentration needed to induce the same response in wild type mice. As other nAChRs are not activated at the concentration causing the above effects, it is clear that the effects are caused by receptors containing  $\alpha 4$  subunits (Tapper *et al.*, 2004). Receptors containing  $\alpha 4$  and  $\beta 2$  subunits also appear to be implicated in memories associated with smoking that reinforces the addictive behaviour as Nic-evoked ACh release in hippocampal synaptosomes is driven by the  $\alpha 4\beta 2$  receptor subtype (Wilkie *et al.*, 1996) also implicating this subtype in learning and memory processes.

Work with mice lacking the  $\alpha 5$  subunit has suggested that this type of  $\alpha 4\beta 2^*$  nAChRs may be implicated in Nic addiction liability as  $\alpha 5(-)$  mice display a decrease in the affinity for acute nicotine administration (Kedmi *et al.*, 2004). A single-nucleotide polymorphism in the gene coding for the  $\alpha 5$  subunit (CHRNA5) has been linked to propensity to nicotine addiction although how this polymorphism may affect the addiction and reward pathways is unknown (Kuryatov *et al.*, 2011). More recent studies have shown that a group of  $\alpha 5$  nAChR subunit-expressing neurones in the midbrain interpeduncular nucleus increase the expression of genes that regulate feedback inhibition of the medial habenula when exposed chronically to Nic (Ables *et al.*, 2017) (**Fig. 1.7**). Reducing expression of these genes in these neurones blocks the rewarding effects of Nic. These studies therefore give an insight into the molecular mechanisms that may make humans genetically predisposed to smoking addiction (Ables *et al.*, 2017).



Interestingly, chronic exposure to Nic upregulates  $\alpha 4\beta 2$  nAChRs in the brain of mice, rats (Schwartz and Kellar, 1983; Marks *et al.*, 1983) as well as humans (Benwell *et al.*, 1988; Breese *et al.*, 1997; Perry *et al.*, 1999). By using recombinant  $\alpha 4\beta 2$  nAChRs expressed heterologously in clonal cell lines (Nelson *et al.*, 2003; Kuryatov *et al.*, 2005; Fox-Loe *et al.*, 2017) or *Xenopus* oocytes (Moroni *et al.*, 2006), it has been shown that chronic exposure to Nic favours the assembly of the high sensitivity isoform  $(\alpha 4\beta 2)_2\beta 2$  over the low sensitivity form  $(\alpha 4\beta 2)_2\alpha 4$ . The biological effects of up-regulation have not been elucidated, although it is tempting to suggest that it may be to upset the generalised receptor desensitisation caused by chronic exposure to nicotine.

An interesting aspect of nicotine addiction is that chronic exposure to Nic, as it occurs in the smoker, causes receptor desensitisation, a receptor state in which the pore is closed, even though the agonist is still bound (Albuquerque *et al.*, 2009). When these receptors undergo such effects and are temporarily non-functional, it reduces the activation of inhibitory GABAergic neurones in the VTA. This will cause a down-stream effect of diminished inhibition of the dopaminergic signalling in the VTA and NAcc, thus increasing and maintaining high levels of activity in the reward pathway, also caused by the initial activation of pre-synaptic  $\alpha 4\beta 2$  nAChRs of the dopaminergic neurons in these regions (Mansvelder and McGhee, 2002; Laviolette and Van der Kooy, 2004; Exley *et al.*, 2008; Wooltorton *et al.*, 2003). It is likely that both activation and desensitisation of  $\alpha 4\beta 2$  nAChR contribute to nicotine addiction through addiction, reward, withdrawal and tolerance (Mansvelder and McGhee, 2002; Picciotto *et al.*, 2008).

$\alpha 4\beta 2$  nAChR partial agonists may help people stop smoking by maintaining moderate levels of dopamine to counteract withdrawal symptoms. For example, Cytisine (Cyt), an  $\alpha 4\beta 2$  nAChR partial agonist, which is only available in central and eastern European countries. The most widely-available treatment is the nAChR partial agonist varenicline (Var) (Chantix™), which is available world-wide as an aid for quitting smoking. However, the US Food and Drug Administration (FDA) posted a warning that Var may increase the risk of heart complications (such as a heart attack) in people who have existing cardiovascular disease. Moreover, there have been various reports of a possible link between Var and behavioural or mood changes including hostility, agitation, depressed mood, suicidal thoughts and attempted suicide (Moore *et al.*, 2011).

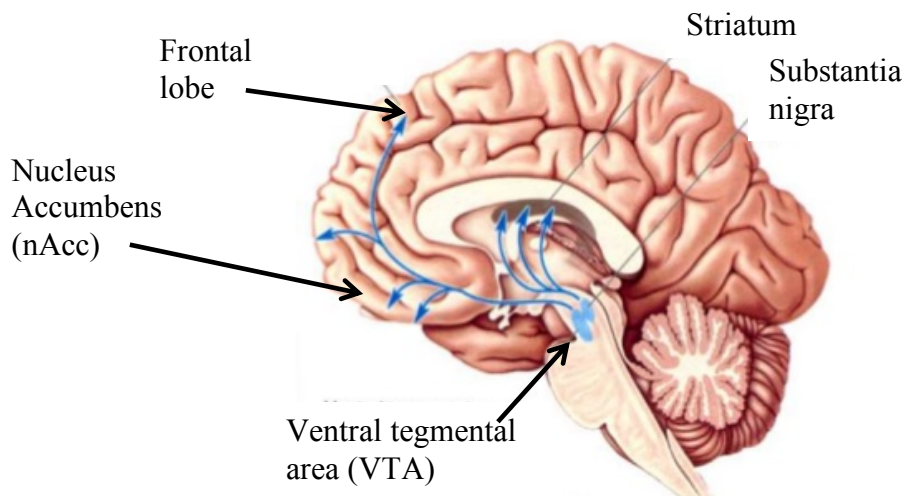


**Figure 1.9 The mesocorticolimbic “reward” circuitry.** The mesocorticolimbic “reward” circuitry of  $\alpha 4\beta 2$  nAChR in the VTA is stimulated by Nic causing the release of dopamine in the nAcc. Signals to the prefrontal cortex result in addictive behaviour.

### 1.3.2.b Depression

Depression is one of the most common psychiatric illnesses in the world and has a significant public health impact (McLaughlin KA, 2011). Although serotonergic and noradrenergic signalling are the primary target for chemical intervention in depression,  $\alpha 4\beta 2^*$  nAChRs have been implicated in the mood functions of the brain, making them additional targets for drug therapy of anxiety and depressive disorders (Levin and Simon, 1998; Mineur and Picciotto, 2010; Mantione *et al.*, 2012).

The possible involvement of cholinergic signalling in depression was first suggested by Janowsky in 1972, who proposed that hyperactivity in brain cholinergic systems induced depression. Since then evidence has grown that  $\alpha 4\beta 2^*$  nAChRs may be involved in mood. Critically, presynaptic  $\alpha 4\beta 2^*$  nAChRs are expressed within brain regions highly associated with mood and stress such as the VTA, NAcc, locus coeruleus, dorsal raphe nucleus, prefrontal cortex, amygdala and hippocampus, from where they have been shown to modulate

the release of ACh and neurotransmitters involved in mood such as serotonin, GABA, and dopamine (Picciotto *et al.*, 2012; Garduno *et al.*, 2012). Also,  $\alpha 4$  subunits have point mutations leading to hypersensitivity display dopaminergic impairment in the substantia nigra alongside altered basal levels of anxiety (Labarca *et al.*, 2001), supporting links between  $\alpha 4\beta 2$  nAChRs, dopamine and depression. Deletion of the  $\alpha 4$  subunit increases sensitivity to nicotinic-induced depression (Markett *et al.*, 2011). Moreover, a polymorphism in the  $\alpha 4$  subunit gene (CHRNA4, rs1044396) is associated with depression (Markett *et al.*, 2011).

Concerning the use of  $\alpha 4\beta 2$  nAChRs as targets for anti-depressive medication, available pre-clinical and clinical evidence supports the view of Janowsky (1972) that hyperactivity of the cholinergic system is linked to depression. The specific  $\alpha 4\beta 2$  nAChR competitive antagonist Dh $\beta$ E, displays antidepressant-like effects in mice (Andreasen *et al.*, 2009). Also, the non-selective nAChR channel blocker mecamylamine reduces depressive-like behaviours in wild type mice (Rabenstein *et al.*, 2006; Andreasen *et al.*, 2009) but not in  $\beta 2(-)$  knock out mice. Also, chronic exposure to Nic causes antidepressant effects and enhances the outcomes of treatment with antidepressants in mice (Andreasen *et al.*, 2006). Partial agonists, such as Var (Rollema *et al.*, 2009) and cytisine (Cyt) (Mineur and Picciotto, 2010) also exert antidepressant effects. Together, these findings suggest that a reduction in the activity of  $\alpha 4\beta 2^*$  nAChRs activity is key to diminish of depressive behaviours.

Interestingly, depression is linked to smoking. The incidence of smoking in depressed individuals is 49% compared to 22–30% in the general population (Breslau, 1995). Moreover, smokers with a history of depression suffer more significant depressive symptoms immediately after quitting (Glassman *et al.*, 1990) showing a connection between smoking and depression. Smoking produces an upregulation of nAChRs maintained for at least 2 weeks following cessation, explaining the presence of depressive symptoms following abstinence (Staley *et al.*, 2006).

### **1.3.2.c Analgesia**

Reduced nociception in mice lacking the  $\alpha 4$  or  $\beta 2$  nAChRs (Picciotto *et al.*, 1999) and absence of analgesic effects of Nic in  $\alpha 5$  nAChR subunit knock out mice (Jackson *et al.*, 2010), together with the analgesic effects of  $\alpha 4\beta 2$  nAChR agonists such as Nic and epibatidine (Daly *et al.*, 2000), have established  $\alpha 4\beta 2$  and  $\alpha 5\alpha 4\beta 2$  nAChRs as valid targets for therapeutic reduction of nociception.

The role of  $\alpha 4\beta 2/\alpha 5\alpha 4\beta 2$  nAChRs in nociception may be mediated through activation or desensitisation, as suggested by activation of  $\alpha 4\beta 2$  nAChRs being necessary but not sufficient to produce analgesia *in vivo* (Gao *et al.*, 2010). Additionally, compounds that more potently desensitise  $\alpha 4\beta 2$  nAChRs are more effective at producing analgesia, suggesting that desensitisation contributes to the efficacy of nicotinic analgesics (Zhang *et al.*, 2012).

### 1.3.2.d Alzheimer's Disease

Alzheimer's disease is the most common neurodegenerative disorder and the most common type (70%) of dementia in the elderly. Symptoms are a progressive deterioration of memory and cognitive function. Also, symptoms include impaired attention, language disturbances and emotional instability (Zarotovsky *et al.*, 2003).

$\alpha 4\beta 2^*$  nAChRs have been implicated in Alzheimer's diseases due to their role in memory and cognition (Jensen *et al.*, 2005). These receptors are highly represented in brain areas such as the prefrontal cortex and hippocampus and dysfunction of these regions is linked with cognitive deficit (Yakel, 2013). Moreover, there is a deficit in cholinergic innervation in the hippocampus and cerebral cortex in Alzheimer's disease, as judged by a significant reduction (up to 90%) in acetylcholinesterase (AChE) and choline acetyltransferase activity in these regions. These two enzymes are involved in the degradation and synthesis of ACh respectively. Studies also show that nicotinic  $\alpha 4$ -containing receptors are selectively reduced around 30-40% in Alzheimer's diseased brains (Guan *et al.*, 2000).

As mentioned above, the loss of cholinergic transmission in the brain plays an important part in Alzheimer's disease, but it is not the only factor involved. There are also abnormalities in glutamatergic, noradrenergic, serotonergic and dopaminergic transmission (Doggreli and Evans, 2003).

Current therapies focus on alleviating symptoms by replacing loss of cholinergic activity but the progression of the disease can only be slowed, not stopped. In strategies to reinforce nicotinic neurotransmission, the action of endogenous ACh is enhanced by administration of inhibitors of AChE (Giacobini and Michel, 1998). Inhibitors of AChE used in the palliative

treatment of Alzheimer's disease include, Tacrine, Physostigmine or Donezapil. ACh transmission is not affected in muscles of AD patients so the overstimulation of cholinergic systems outside the brain cause several side effects including bradycardia, insomnia, agitation, nausea and vomiting (Grutzendler and Morris, 2001).

Future treatments may include cholinergic agonists such as Nic, which appears to improve some forms of attentional function in Alzheimer's disease (Sacco *et al.*, 2004). The short half-life of Nic as well as the cardiovascular side effects and risk of addiction reduce the possibilities as a therapeutic agent. However, the most predominant metabolite of Nic, cotinine, has advantages over Nic in terms of much longer half-life and lower risk of abuse (Benowitz, 1996). Cotinine has neuroprotective effects (Rosecrans, 1979), it prevented memory loss in an Alzheimer's disease mouse model (Echeverria *et al.*, 2011; Patel *et al.*, 2014) and improved working/short term memory in monkeys (Terry *et al.*, 2005). There is also evidence that some agonist and allosteric modulators of nAChRs improve cognitive function in preclinical models and clinical trials (Timmermann *et al.*, 2012; Taly *et al.*, 2009). An example of which is the allosteric modulator of the  $\alpha 4\beta 2$  nAChR physostigmine (Zwart *et al.*, 2000).

### **1.3.2.e Parkinson's disease**

Parkinson's disease is the second most common neurodegenerative disorder after Alzheimer's disease, and affects 2% of people over the age of 60 (Mayeux, 2003). Parkinson's disease is a debilitating neurodegenerative movement disorder characterised by damage to the nigrostriatal dopaminergic system. The disorder produces severe motor dysfunction, characterised by tremor, postural imbalance, slowness of movement, and rigidity.

Current therapies use levodopa (L-dopa), the precursor to the neurotransmitter dopamine that can cross the protective blood brain barrier (Haddad F *et al.*, 2017). L-dopa is used to increase dopamine concentrations in the treatment of Parkinson's disease. Nic administration has been reported as an adjunct therapy to minimise L-Dopa-induced dyskinesias, a troubling side effect of L-Dopa therapy (Quik and Wonnacott, 2011). The first evidence that the use of nicotinic drugs could be useful in treating Parkinson's disease emerged from epidemiological studies developed during early 1960s, which showed a negative correlation between smoking and the incidence of Parkinson's disease (Dani, 2001; Hernan *et al.*, 2001). Also, Nicotine

could exert a neuroprotective effect in Parkinson's disease through the downstream pathway including PARP-1. PARP-1 has DNA binding domains that detect DNA damage and facilitate repair (Lu *et al.*, 2017). It is not clear which receptor may be the target of the nicotinic drugs, but because the striatum contains  $\alpha 4\beta 2^*$  nAChRs, it is thought that nicotinic drugs may exert their effects, at least partly, through them.

### **1.3.2.f Schizophrenia**

Schizophrenia is a chronic neuropsychiatric and mental disorder. Schizophrenia affects 1% of the world population and it is characterised by deficits in neurocognition, hallucinations and delusions (Saha *et al.*, 2005).

The incidence of Nic consumption (and vulnerability to Nic addiction) is higher in schizophrenia patients compared to normal individuals (Volkow, 2009). For example, the incidence of tobacco smoking in individuals with schizophrenia is estimated to be 80–90% versus 20–30% in the general population (de Leon and Diaz, 2005). It has been suggested that a higher Nic use may represent an attempt to restore nAChR function (Yakel, 2013).

It is not clear whether only one or several types of nAChR may be implicated in schizophrenia. It is interesting that a non-coding single nucleotide polymorphism within the nAChR  $\alpha 4$  subunit gene (CHRNA4) has been found to be associated with neurological and behavioural phenotypes including schizophrenia (Eggert *et al.*, 2015). In addition, post-mortem studies suggest a dysregulation of  $\beta 2$ -containing nAChRs as there are low levels of  $\beta 2^*$ -containing nAChR in smokers with schizophrenia, compared to smokers without schizophrenia (Brašić *et al.*, 2012). There is also evidence that the  $\alpha 7$  nAChRs are involved in the regulation of sensory gating, a function that seems to be dysfunctional in the schizophrenia brain (Yakel, 2013).

### **1.3.2.g Autosomal dominant nocturnal frontal lobe epilepsy**

Autosomal dominant nocturnal frontal lobe epilepsy (ADNFLE) is a focal epilepsy with seizures typically arising from the frontal lobe during non-rapid eye movement (NREM) sleep. It is characterised by clusters of complex and stereotyped hypermotor seizures,

frequently accompanied by sudden arousals (Scheffer *et al.*, 1995). Neurocognitive deficits or psychiatric effects may be also occur (Steinlein *et al.*, 1995; Bertrand *et al.*, 2005).

Approximately 12% of the ADNFLE families carry mutations on genes coding for subunits of the heteromeric nAChRs. Single point mutations to either the  $\alpha 4$  or  $\beta 2$  subunits appear to mediate ADNFLE (Eggert *et al.*, 2015). The desensitisation in nAChRs modulate the frequency of the ion channel conducting states and has been suggested to play an important role in neuronal networks associated with memory and learning (Dehaene and Changeaux, 1991). In fact, altered desensitization mechanisms correlate with ADNFLE (Bertrand *et al.*, 1998). Regulation of the conformational transitions, including desensitization, by allosteric modulators could be a potentially good pharmacological strategy for brain pathologies (Arias, 1998).

### 1.3.3 The Pharmacology of $\alpha 4\beta 2$ nAChRs

The pharmacology of  $\alpha 4\beta 2$  nAChRs has been intensively and extensively examined using recombinant receptors expressed in *Xenopus* oocytes or clonal cell lines, as well as a variety of native receptor preparations from whole animals. A summary of the pharmacological profile of  $\alpha 4\beta 2$  nAChRs is discussed below. The main drugs that affect  $\alpha 4\beta 2$  nAChR function are summarised in **Table 1.2, 1.3**.

#### 1.3.3.1 Agonists

Agonists are a class of ligands that by binding the pocket activate the agonist binding-transduction pathway that gates the ion channel. Examples of classical  $\alpha 4\beta 2$  nAChRs agonists are discussed below.

**Acetylcholine (ACh).** This ligand is an ester formed from choline and acetic acid that serves as the neurotransmitter of the cholinergic system in the central and peripheral nervous systems. It is the main neurotransmitter in the parasympathetic system and at the neuromuscular junction. Although ACh is a non-specific agonist, it shows selectivity towards  $\alpha 4(+)/\beta 2(-)$  and  $\alpha 4(+)/\alpha 4(-)$  agonist sites (Harpsøe *et al.*, 2011; Mazzaferro *et al.*, 2011).

**Nicotine (Nic).** It is a natural compound found in tobacco plants (*Solanaceae* family). Nic is a partial agonist of  $\alpha 4\beta 2$  nAChRs. This receptor type has high affinity for Nic, with a binding affinity ( $K_i$ ) at the nanomolar level (Jensen *et al.*, 2005). Nic also activates most other nAChRs, albeit with reduced potency, compared to  $\alpha 4\beta 2$  nAChRs (Jensen *et al.*, 2005). At  $\alpha 9\alpha 10$  nAChRs, Nic behaves as an antagonist (IUPHAR Database).

**Varenicline (Var).** As mentioned previously, Var (Chantix<sup>TM</sup>) is used as a smoking cessation medication (Coe *et al.*, 2005). Var is a partial agonist of  $\alpha 4\beta 2^*$  nAChRs that leads to the release of dopamine in the nucleus accumbens, reducing the feelings of craving and withdrawal. Var displays lower efficacy at  $(\alpha 4\beta 2)_2\beta 2$  and  $(\alpha 4\beta 2)_2\alpha 5$  nAChRs than at  $(\alpha 4\beta 2)_2\alpha 4$  nAChRs. Var is however also a full agonist at  $\alpha 7$  nAChRs.

**Cytisine (Cyt).** It is an alkaloid from a plant used for smoking cessation in Eastern Europe and it has antidepressant effects in animal models of depression (Mineur and Picciotto, 2010). Its molecular structure has some similarity to that of Nic and it has similar pharmacological effects. Cyt shows low nano-molar affinity for  $\alpha 4\beta 2^*$  nAChRs and low micro-molar affinity at the  $\alpha 7$  subtype (Slater *et al.*, 2003). It displays higher efficacy at  $(\alpha 4\beta 2)_2\alpha 4$  compared to  $(\alpha 4\beta 2)_2\beta 2$  or  $(\alpha 4\beta 2)_2\alpha 5$  nAChRs (Moroni *et al.*, 2006; Carbone *et al.*, 2009).

**4-(5-ethoxy-3-pyridinyl)-N-methyl-(3E)-3-buten-1-amine difumarate (TC2559).** This compound is a superagonist (its efficacy is 4 times greater than that of the full agonist ACh) on  $(\alpha 4\beta 2)_2\beta 2$  but behaves as partial agonist on  $(\alpha 4\beta 2)_2\alpha 4$  (Zwart *et al.*, 2006; Carbone *et al.*, 2009). Interestingly, this compound binds the agonist sites on the  $\alpha 4/\beta 2$  interfaces but not that on the  $\alpha 4(+)/\alpha 4(-)$  interface of the  $(\alpha 4\beta 2)_2\alpha 4$  nAChR (Mazzaferro *et al.*, 2011), making it an excellent tool to study the function and modulation of the agonist sites on  $\alpha 4(+)/\beta 2(-)$  interfaces. Steric restrictions from H142 on the (-) side of the  $\alpha 4(+)/\alpha 4(+)$  interface have been shown to be the structural determinant for the inability of TC2559 to access the agonist site on this interface (Mazzaferro *et al.*, 2014).

**Sazetidline-A (Saz-A).** This compound is a full agonist on  $(\alpha 4\beta 2)_2\beta 2$  but a partial agonist on  $(\alpha 4\beta 2)_2\alpha 4$  (Zwart *et al.*, 2008). As for TC2559, Saz-A does not bind the  $\alpha 4(+)/\alpha 4(-)$  interface of the  $(\alpha 4\beta 2)_2\alpha 4$  nAChR, which accounts for its partial agonism at this receptor type (Mazzaferro *et al.*, 2011). As for TC2559, H142 on (-) side of the  $\alpha 4(+)/\alpha 4(-)$  interface blocks Saz-A accessing the agonist site on this interface (Mazzaferro *et al.*, 2014).



### 1.3.3.2 Antagonist

Antagonists inhibit the receptor function by recognising the same orthosteric site as an agonist without activation (competitive ligands) or by occupying other sites (non-competitive antagonists). Examples of classical  $\alpha 4\beta 2$  nAChRs antagonists are discussed below.

**Dihydro- $\beta$ -erythroidine (DH $\beta$ E).** This compound was first isolated from *Erythrina americana* seeds. It is a competitive antagonist of nAChRs. DH $\beta$ E preferentially blocks  $\beta 2$ -containing nAChRs; thus, DH $\beta$ E displays high potency at  $\alpha 4\beta 2$  and  $\alpha 3\beta 2$  nAChRs, whereas the potency at  $\alpha 7$  and at  $\alpha 3\beta 4$  nAChRs is considerably decreased (10-50 fold less) (Jensen *et al.*, 2005). In particular, DH $\beta$ E is more potent at  $(\alpha 4\beta 2)_2\beta 2$  and  $(\alpha 4\beta 2)_2\alpha 5$  nAChRs than at  $(\alpha 4\beta 2)_2\alpha 4$  nAChRs (Mantione *et al.*, 2012). Dh $\beta$ E shows antidepressant effects in mice (Mineur and Picciotto, 2010).

**Mecamylamine (Mec).** This ligand behaves as a non-selective, non-competitive antagonist of nAChRs and is used as an antihypertensive drug (Vecamyl<sup>TM</sup>). Mec inhibits  $\alpha/\beta$  heteromeric nAChRs at low micromolar concentrations (IC<sub>50</sub> values between 0.1-10  $\mu$ M), whereas it is less potent at homomeric  $\alpha 7$  nAChRs (Jensen *et al.*, 2005).

**Bupropion.** A non-competitive antagonist of  $\alpha 4\beta 2$ ,  $\alpha 3\beta 2$  and  $\alpha 7$  nAChRs (Jensen *et al.*, 2005). It is used as an antidepressant because it inhibits dopamine and noradrenaline transporters and as an aid in smoking cessation (Zyban<sup>TM</sup>).

### 1.3.3.3 Allosteric modulators

Allosteric modulators are ligands that bind at distinct locations away from the agonist binding site of receptors and modulate function without direct activation. The allosteric site can be adjacent to the agonist site or tens of angstroms away in the protein, including sites located in the TMD. They can positively modulate (positive allosteric modulator, PAM) or negatively modulate (negative allosteric modulator, NAM) the protein's activity. By potentiating the action of an agonist through binding to an allosteric site, a PAM can enhance cholinergic neurotransmission, thus compensating for compromised neuronal communication in a pathophysiological setting.

Allosteric modulators stabilise receptors in specific conformational states. PAMs can increase agonist potency by enhancing agonist binding to the receptor resting state (e.g., benzodiazepine effects in GABA<sub>A</sub> receptors) (Twyman *et al.*, 1989). PAMs can also increase efficacy by reducing the energy of the transition between the closed and open states (e.g., barbiturate effects on GABA<sub>A</sub> receptors) (Taly *et al.*, 2009; Mantione *et al.*, 2012). In contrast, NAMs can increase the energy barrier for activation and thus decrease or inhibit the effect of agonists (Burford *et al.*, 2011). Alternatively, NAMs can decrease the energy barrier to enter desensitisation, which leads to physiological inactivation.

The pharmacological advantages of allosteric modulators over agonists include minimal interference with spatial and temporal aspects of neurotransmission (Sarter and Bruno, 1997). Also, they present a higher subtype selectivity among the various nAChR subtypes (Pandya and Yakel, 2011), resulting in high clinical efficacy with minimal adverse effects. Below a number of allosteric modulators of the  $\alpha 4\beta 2$  nAChR are described (**Table 1.3**).

**Calcium (Ca<sup>2+</sup>).** At millimolar concentrations Ca<sup>2+</sup> potentiates most neuronal nAChRs (Mulle *et al.* 1992). It binds to sites located at the ECD, below the ACh site near the TMD (Le Novere *et al.*, 2002).

**NS 9283.** This compound was developed by NeuroSearch. It enhances the agonist- evoked responses of  $(\alpha 4\beta 2)_2\alpha 4$ ,  $(\alpha 2\beta 2)_2\alpha 2$  and  $(\alpha 4\beta 4)_2\alpha 4$  receptors (Timmermann *et al.*, 2012) but not those of nAChRs with the stoichiometry  $(\alpha 4\beta 2)_2\beta 2$  or containing  $\alpha 3$  subunits. It was associated with improvements in animal models of attention, social recognition memory and spatial reference memory (Timmermann *et al.*, 2012). NS9283 has also been shown to have beneficial analgesic effects in a number of preclinical pain models (e.g., neuropathic and inflammatory pain) when the compound was co-administered with the  $\alpha 4\beta 2$  nAChR agonist ABT-594 (Lee *et al.*, 2011; Zhu *et al.*, 2011) or the  $\alpha 4\beta 2$  partial agonist NS3956 (Rode *et al.*, 2012).

**Zinc (Zn<sup>2+</sup>).** This divalent cation is present in neurons throughout the brain, especially in the cerebral cortex and the hippocampus. Zn<sup>2+</sup> potentiates the low affinity stoichiometry  $((\alpha 4\beta 2)_2\alpha 4)$  but also inhibits both low and high affinity stoichiometries. This is because there is an inhibition site on both isoforms at  $\beta 2(+)/\alpha 4(-)$  and a potentiation site only in the low affinity receptor at the  $\alpha 4(+)/\alpha 4(-)$  subunit interface (Moroni *et al.*, 2008). Thus, Zn<sup>2+</sup> potentiates or

inhibits, depending on its concentration, the function of  $(\alpha 4\beta 2)_2\alpha 4$  nAChRs (Moroni *et al.*, 2008). The effects of  $Zn^{2+}$  on nAChRs are likely to be not physiologically relevant since the concentrations at which  $Zn^{2+}$  exerts its effect on  $\alpha 4\beta 2$  nAChRs are above the levels found in the external medium or at synapses. Nevertheless,  $Zn^{2+}$  is a good pharmacological tool to study the function of  $\alpha 4\beta 2$  nAChRs.

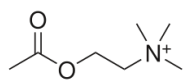
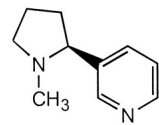
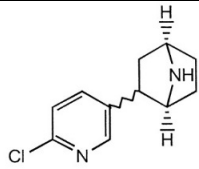
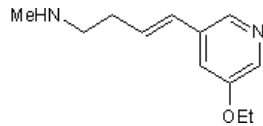
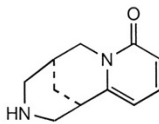
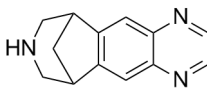
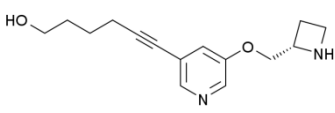
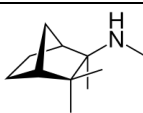
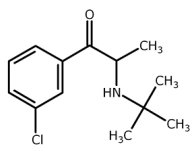
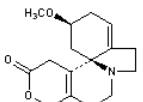
**Desformylflustrabromine hydrochloride (dFBr).** This ligand is a metabolite of the marine bryozoan *Flustra foliacea* which is common in the North Sea (Lysek *et al.*, 2002). When co-applied with ACh, it increases the potency and efficacy of the effects of ACh on  $\alpha 4\beta 2$  nAChRs (Kim *et al.*, 2007). Potentiation occurs at nano-molar range ( $EC_{50} = 120$  nM) but at concentrations higher than  $100 \mu M$  it inhibits the receptors, likely by ion channel blockade (Kim *et al.*, 2007; Weltzin and Schulte, 2010). dFBr also enhances the function of other heteromeric nAChRs such as  $\alpha 2\beta 2$  and  $\alpha 3\beta 2$  nAChRs (Pandya and Yakel, 2011).

Recently, it was found that the potentiating effect of dFBr is exerted by binding to a site in the TMD of the  $\alpha 4$  subunit, specifically in a cavity between M3 and M4 (Alcaino *et al.*, 2017), which is conserved in the pLGIC family (Corringer *et al.*, 2012).

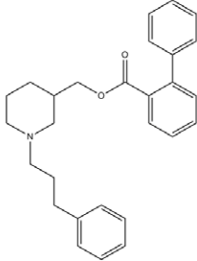
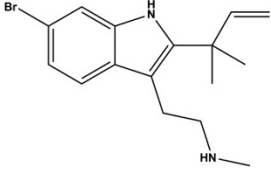
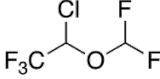
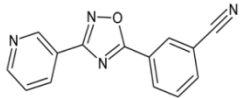
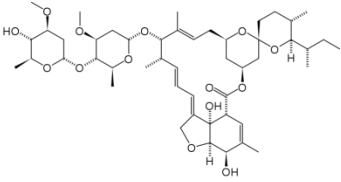
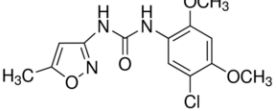
**General anesthetics (GAs).** GAs are allosteric inhibitors of nAChRs, whereas they potentiate receptors such as the  $GABA_A$  and GluCl receptors (Corringer *et al.*, 2012). Interestingly, GAs bind to a conserved site within the upper part of the TMD inside a cavity accessible to phospholipids from the lipid bilayer in all pLGICs (Nury *et al.*, 2011). One example is Isoflurane which binds to nAChR transmembrane domain (Brannigan *et al.*, 2010).

**KAB-18.** A selective  $\alpha 4\beta 2^*$  nAChR NAM (Henderson *et al.*, 2010). KAB-18 inhibits  $\alpha 4\beta 2$  nAChRs in the low micromolar range and its binding site is located in the  $\alpha/\beta$  interface approximately  $10 \text{ \AA}$  away from the agonist-binding pocket; where it appears to interact with residues Phe118, Glu60, and Thr58 on the  $\beta 2$  subunit (Pavlovicz *et al.*, 2011; Henderson *et al.*, 2012).

**Table 1.2. Classical  $\alpha 4\beta 2$  nAChRs competitive ligands.** The ligands shown bind the canonical agonist sites of the  $\alpha 4\beta 2$  nAChRs located at the  $\alpha 4/\beta 2$  interfaces of the receptors.

Compound	Classification	Chemical Structure
Acetylcholine (ACh)	Endogenous agonist	
Nicotine (Nic)	Agonist	
Epibatidine	Agonist	
TC2559	Agonist	
Cytisine (Cyt)	Agonist	
Varenicline (Var)	Agonist	
Sazetine-A (Saz-A)	Agonist	
Mecamylamine (Mec)	Antagonist	
Bupropion	Antagonist	
Dihidro- $\beta$ -Eritroidine (Dh $\beta$ E)	Antagonist	

**Table 1.3. Allosteric modulators of  $\alpha 4\beta 2$  nAChRs.** The ligands shown are not competitive; they bind regions far away from the canonical agonist sites.

Compound	Classification	Chemical Structure
<b>KAB-18</b>	Allosteric modulator	
<b>Desformylflustrabromine hydrochloride (dFBr)</b>	Allosteric modulator	
<b>General anesthetics (GAs)</b> Isoflurane	Allosteric modulator	
<b>NS 9283</b>	Allosteric modulator	
<b>Zn<sup>2+</sup></b>	Allosteric modulator	
<b>Ca<sup>2+</sup></b>	Allosteric modulator	
<b>Ivermectin</b>	Allosteric modulator	
<b>PNU-120596</b>	Allosteric modulator	

### 1.3.4 Alternate forms of the $\alpha 4\beta 2$ nAChR

As mentioned previously, the  $\alpha 4\beta 2$  nAChR exists in two alternate forms, the  $(\alpha 4\beta 2)_2\beta 2$  and  $(\alpha 4\beta 2)_2\alpha 4$  nAChRs (Nelson *et al.*, 2003; Moroni *et al.*, 2006) (**Fig. 1.9 A, B**). The alternate forms arise because the fifth subunit of the receptor can be an  $\alpha 4$  or  $\beta 2$  subunit. The alternate receptors display different sensitivities to activation by ACh and other agonists or allosteric modulators (see **Table 1.2,1.3**) (Nelson *et al.*, 2003; Moroni *et al.*, 2006; Harpsøe *et al.*, 2011; Mazzaferro *et al.*, 2011; Timmermann *et al.*, 2012; Absalom *et al.*, 2013; Lucero *et al.*, 2016), high-affinity desensitization (Marks *et al.*, 2010; Benallegue *et al.*, 2013), sensitivity to allosteric modulators (Moroni *et al.*, 2008; Alcaino *et al.*, 2017; Jin *et al.*, 2017) and single channel properties (Mazzaferro *et al.*, 2017). An additional agonist site on the signature  $\alpha 4(+)/\alpha 4(-)$  interface of the  $(\alpha 4\beta 2)_2\alpha 4$  isoform partly accounts for these differences (Harpsøe *et al.*, 2011; Mazzaferro *et al.*, 2011). Structurally, the agonist binding sites at the  $\alpha 4/\beta 2$  interfaces are equivalent. However, the agonist site at the  $\alpha 4(+)/\alpha 4(-)$  interface differs as the complementary side of this site is contributed by an  $\alpha 4$  subunit, resulting in pharmacological differences between the sites (Mazzaferro *et al.*, 2014). For example, as mentioned previously, agonist sites at  $\alpha 4/\beta 2$  interfaces bind Saz-A and TC2559, whereas the agonist site at the  $\alpha 4(+)/\alpha 4(-)$  interface does not. This is due to a histidine residue (H1412) in the complementary side of the agonist site on the  $\alpha 4(+)/\alpha 4(-)$  interface that blocks the entrance to the site to ligands of a certain size (Mazzaferro *et al.*, 2014). Additionally, a triad of non-conserved E loop residues on the complementary side of the agonist site on the  $\alpha 4(+)/\alpha 4(-)$  interface has been identified as critical in determining the agonist sensitivity differences between the  $(\alpha 4\beta 2)_2\beta 2$  and  $(\alpha 4\beta 2)_2\alpha 4$  receptors:  $\alpha 4$ H142,  $\alpha 4$ Q150 and  $\alpha 4$ T152 (Harpsøe *et al.*, 2011; Lucero *et al.*, 2016). Subsequent studies by New and collaborators (2017) found that the  $\beta 2/\beta 2$  interface of the  $(\alpha 4\beta 2)_2\beta 2$  nAChR affected the amplitude of the maximal agonist responses without changes in agonist sensitivity. Thus, overall these studies highlight the  $\alpha 4(+)/\alpha 4(-)$  and  $\beta 2/\beta 2$  interfaces in the  $\alpha 4\beta 2$  nAChRs as key players in the shaping of the receptor functional properties. The elucidation of how these interfaces impact receptor function should provide a new impetus to drug discovery programs that target  $\alpha 4\beta 2$  nAChRs.

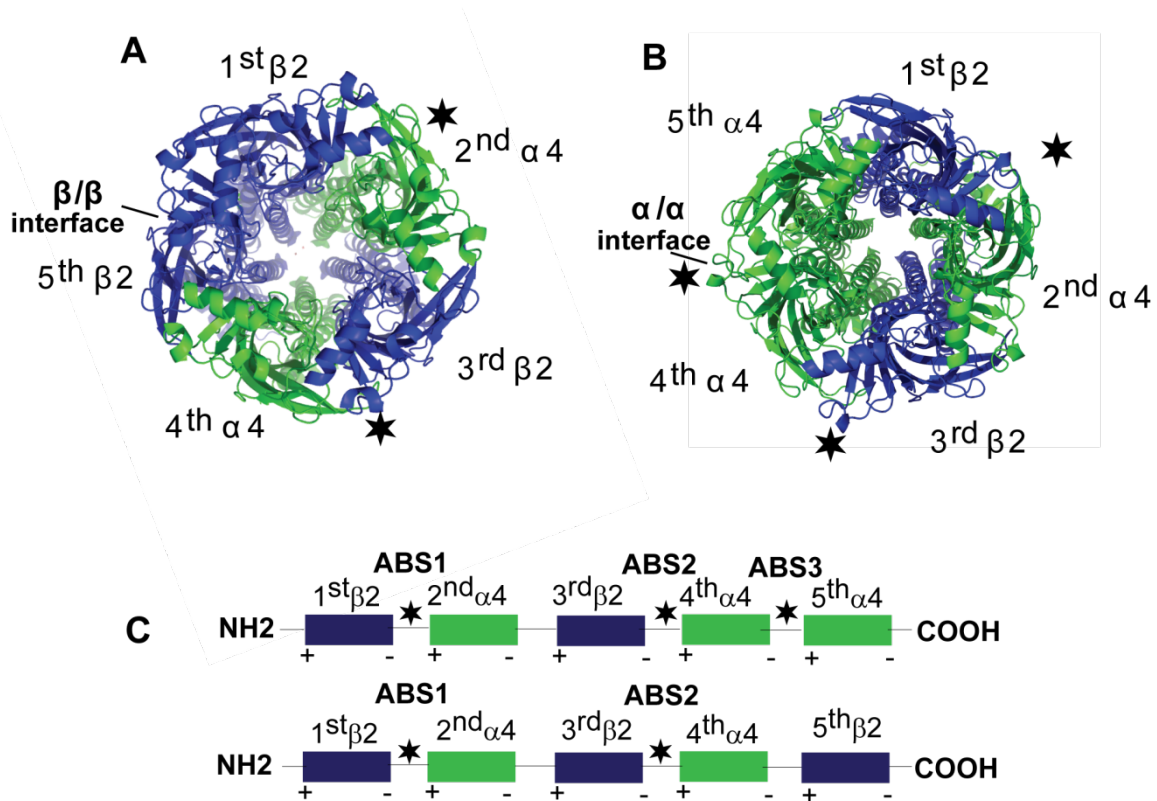


**Figure 1.10. Alternate forms of the  $\alpha 4\beta 2$  nAChR.** A, B) Diagram representing the two stoichiometries of  $\alpha 4\beta 2$  nAChRs. Subunits are distinguished by colour (green,  $\alpha 4$  and, blue,  $\beta 2$ ). C) The  $(\alpha 4\beta 2)_2\alpha 4$  and  $(\alpha 4\beta 2)_2\beta 2$  concatenated nAChR receptor. The star represents binding sites (ABS1, ABS2 and ABS3).

### 1.3.5 Concatenated $\alpha 4\beta 2$ receptors

Significant insights into the role of the  $\alpha 4(+)/\alpha 4(-)$  and  $\beta 2/\beta 2$  interfaces of the alternate  $\alpha 4\beta 2$  nAChRs has been achieved by using fully (Mazzaferro *et al.*, 2011; 2014; Lucero *et al.*, 2016; New *et al.*, 2017) or partially (Jain *et al.*, 2016) concatenated  $\alpha 4$  and  $\beta 2$  subunits. The function of multimeric LGICs is difficult to analyse by recombinant expression of a mixture of loose single subunits because multiple receptor subtypes with different subunit stoichiometry can be formed (Zwart and Vijverberg, 1998; Minier and Sigel, 2004; Moroni *et al.*, 2006). Thus, a key advantage of concatenated receptors is that it is possible to express only one type of receptor stoichiometry. Another important advantage, which particularly applies to receptors made of two different subunits such as the  $\alpha 4\beta 2$  nAChR, is that mutations can be introduced in defined subunits of the pentamer. This permits studies of the role of specific subunits or subunit interfaces (Mazzaferro *et al.*, 2011; 2014).

The studies reported in this thesis were carried out using fully concatenated  $(\alpha 4\beta 2)_2\beta 2$  and  $(\alpha 4\beta 2)_2\alpha 4$  receptors (Carbone *et al.*, 2009) (**Fig 1.9, C**). Concatemeric receptors containing two non-consecutive  $\alpha 4$  and three  $\beta 2$  subunits activate in response to low concentrations of ACh, and mimic the high agonist sensitivity of non-concatenated  $(\alpha 4\beta 2)_2\beta 2$  receptors, whereas concatemeric receptors containing three  $\alpha 4$  and two non-consecutive  $\beta 2$  subunits activate in response to high concentrations of Ach (Carbone *et al.*, 2009; Mazzaferro *et al.*, 2011; 2014). The use of concatenated receptors must be carefully considered. The linked subunits can orient themselves readily in both clockwise and counterclockwise directions. The linker lengths in concatenated nAChRs is important to ensure the expression of a specific concatemer (Ahring *et al.*, 2018).Concatameric  $\alpha 4\beta 2$  nAChRs used in this project replicate the sensitivity of their non-concatenated counterparts to other nicotinic ligands, including agonist, antagonists and allosteric modulators. For example, agonists Saz-A and TC2559 activate concatemeric  $(\alpha 4\beta 2)_2\beta 2$  receptors, but not concatemeric  $(\alpha 4\beta 2)_2\alpha 4$  receptors, in accord with their effects on non-concatenated  $\alpha 4\beta 2$  nAChRs (Moroni *et al.*, 2006; Zwart *et al.*, 2006; Carbone *et al.*, 2009). Also,  $Zn^{2+}$  enhances the agonist responses of concatenated  $(\alpha 4\beta 2)_2\alpha 4$  receptors, but only inhibits the agonist responses of concatenated  $(\alpha 4\beta 2)_2\beta 2$  receptors (Carbone *et al.*, 2009), which is in good agreement with studies of receptors assembled in the presence of an excess of either  $\alpha 4$  or  $\beta 2$  subunits, respectively (Moroni *et al.*, 2008).

Partially (Zhou *et al.*, 2003) or fully (Carbone *et al.*, 2009) concatenated  $\alpha 4\beta 2$  nAChRs have had a significant impact in our understanding of this receptor family, particularly in the role of the accessory subunit (**Fig 1.9**) in the function of the alternate stoichiometric ensembles of the  $\alpha 4\beta 2$  nAChR (Mazzaferro *et al.*, 2011; Benallegue *et al.*, 2013; Mazzaferro *et al.*, 2014; New *et al.*, 2017). Concatemeric  $\alpha 4\beta 2$  nAChRs have also shed light on the critical role of the E loop in the  $\alpha 4(+)/\alpha 4(-)$  interface of the  $(\alpha 4\beta 2)_2\alpha 4$  receptor in defining the pharmacology of this receptor stoichiometry (Harpsøe *et al.*, 2011; Mazzaferro *et al.*, 2011; 2014; Lucero *et al.*, 2016). Also, using concatenated nAChRs, Lindstrom and his team (Jain *et al.*, 2016) were able to demonstrate that the  $\alpha 5$  and  $\beta 3$  subunits are considered as non agonist binding subunits, can contribute to operational agonist sites in  $\alpha 4\beta 2^*$  nAChRs (Jain *et al.*, 2016).

Fully concatenated receptors with substituted cysteine residues were subjected to chemical modifications by MTSET. The substituted cysteine accessibility method (SCAM) was first



applied to pLGIC to identify the amino acid residues lining the ion channel of the muscle nAChR (Karlin and Akabas, 1998). Since then, SCAM has become an established experimental approach to study pLGICs function and structure in real time. Thus, SCAM has been successfully applied to gain invaluable insights into diverse aspects of pLGICs, including amino acid residues contributing to competitive or allosteric ligand bindings, pLGICs structure (e.g., Boileau *et al.*, 1999; Holden and Czajkowski, 2002; Alcaïno *et al.*, 2016), conformational changes induced by agonist or allosteric modulators (Barron *et al.*, 2009), secondary structure of functional domains (Mercado and Czajkowski, 2008) and presence of operational agonist sites (Mazzaferro *et al.*, 2011, 2014).

Interestingly, the use of concatenated  $\alpha 4\beta 2$  nAChRs have shown that the agonist sites on the  $\alpha 4(+)/\beta 2(-)$  interfaces function asymmetrically, despite them being structurally equivalent (Mazzaferro *et al.*, 2011; Lucero *et al.*, 2016; New *et al.*, 2017). This finding suggests that different subunit environments surrounding the agonist sites result in functional differences. A subunit that defines the differences in agonist binding environment is the fifth or accessory subunit (Mazzaferro *et al.*, 2011). More recently, New and collaborators (2017) have shown that the fifth subunit links asymmetrically to the agonist sites in the  $(\alpha 4\beta 2)_2\beta 2$  receptor but the pathway linking these regions was not identified. This thesis focuses on this issue: the link between the fifth subunit and the agonist sites on the  $\alpha 4(+)/\beta 2(-)$  interfaces in the  $\alpha 4\beta 2$  nAChRs.

## 1.4 Thesis rationale

In the last seven years it has become increasingly certain that the agonist sites in the alternate forms of the  $\alpha 4\beta 2$  nAChR function asymmetrically. In the case of the agonist site formed at the  $\alpha 4(+)/\alpha 4(-)$  interface, the differences underlying asymmetry are straightforward: the complementary side of the agonist site is contributed by an  $\alpha 4$  subunit, whereas in the agonist sites present in  $\alpha 4(+)/\beta 2(-)$  interfaces the complementary side is provided by  $\beta 2$ . Although the conserved aromatic residues that line the agonist binding pocket are present in both  $\alpha 4$  and  $\beta 2$ , other residues that are part of the agonist sites are not, giving rise to important differences. A region that has been shown to be pharmacology-defining is the E loop. This region defines the agonist sensitivity to activation of the  $(\alpha 4\beta 2)_2\alpha 4$  receptor (Harpsøe *et al.*, 2011; Mazzaferro *et al.*, 2014; Lucero *et al.*, 2016). More recent studies by New and collaborators (2017) have shown that the fifth subunit links asymmetrically with the agonist

binding sites in the  $(\alpha 4\beta 2)_2\beta 2$  stoichiometry, showing for the first time long-range communication between the fifth subunit and agonist sites. The challenge today is to map and identify the pathways that link the fifth subunits to the agonist sites on the  $\alpha 4(+)/\beta 2(-)$  interfaces. Insights into these pathways and their functional roles will provide exquisite insight on how these proteins work. It may also lead to the development of stoichiometry-specific  $\alpha 4\beta 2$  drugs.

The studies that will be described in this thesis have used the concatemeric  $\alpha 4\beta 2$  nAChRs to address how the signature  $\beta 2(+)/\beta 2(-)$  and  $\alpha 4(+)/\alpha 4(-)$  interfaces may link to agonist sites to define the asymmetric function of those structures. By using available structural data, subunit-targeted mutagenesis and the covalent modification of substituted cysteines by a methanethiosulphonate reagent, it was found that the fifth subunit confers functional signatures to the  $(\alpha 4\beta 2)_2\alpha 4$  nAChR through “gain of function” effects (e.g., additional agonist site,  $Zn^{2+}$  potentiating binding site) but also by modulating the function of adjacent agonist sites. The modulatory effects of the fifth subunit appear to be exerted through two distinct pathways. One pathway links the agonist sites on the  $\alpha 4(+)/\alpha 4(-)$  and  $\alpha 4/\beta 2-1$  interface through a pathway that starts at loop C in the  $\alpha 4(+)/\alpha 4(-)$  interface and that requires the site at the  $\alpha 4(+)/\alpha 4(-)$  interface to be agonist-bound. The other pathway likely involves a modulatory site at the  $\beta 2/\alpha 4$  interface or inter-subunit interactions between agonist-bound  $\alpha 4/\beta 2-1$  interface and the adjacent fifth subunit. The studies presented here could not distinguish between these two possibilities.

By using similar experimental strategies used for the  $(\alpha 4\beta 2)_2\alpha 4$  receptor, this study found that conserved loop B and Loop E residues in the  $\beta 2/\beta 2$  interact to modulate the amplitude of maximal agonist responses. The interactions between loop B and loop E residues modify agonist efficacy but not potency. By using a M2 reporter mutation (L9'T) in combination with double mutant cycle analysis, it was established that the conserved residues are functionally linked to M2, suggesting that the conserved residues may modulate gating. This is the first time that agonist efficacy is shown to be modulated by non-agonist binding. The results are discussed in terms of their significance for gating and agonist efficacy.

## 1.5 Aims of the thesis

The overall aim of this PhD study was to advance our understanding of how the signature  $\beta 2/\beta 2$  and  $\alpha 4/\alpha 4$  interfaces of  $(\alpha 4\beta 2)_2\beta 2$  and  $(\alpha 4\beta 2)_2\alpha 4$  nAChRs respectively affect the function of neighbouring  $\alpha 4\beta 2$  nAChRs. In line with this, the research question this thesis addressed were:

- A) Do the agonist sites on the  $(\alpha 4\beta 2)_2\alpha 4$  receptor function asymmetrically?
- B) Does the  $\alpha 4(+)/\alpha 4(-)$  interface communicate with adjacent agonist sites?
- C) Do conserved residues in loops A and B of the  $\beta 2(+)/\beta 2(-)$  interface interact to modulate the function of neighbouring agonist sites?
- D) Are conserved residues in loop A and Loop B that affect agonist efficacy functionally linked?
- E) Do  $\beta 2(+)/\alpha 4(-)$  interfaces in the  $(\alpha 4\beta 2)_2\beta 2$  and  $(\alpha 4\beta 2)_2\alpha 4$  nAChRs affect receptor function, as judged by changes in agonist efficacy and potency?



# **Chapter 2**

## **Materials and Methods**



## 2.1 Reagents

Standard laboratory chemicals were of Analar grade. Collagenase (Type 1 C-0130), acetylcholine (ACh), terrific medium for bacterial growth, antibiotic/antimycotic mixture (10,000 units penicillin, 10 mg streptomycin and 25 µg amphotericin B per mL), tricaine, and amikacin were purchased from Sigma-Aldrich (UK). Cyt. Var, Saz-A TC2559 were purchased from Tocris Chemicals (UK). Methanenosulphate reagents (MTS) aminoethyl methanethiosulfonate (MTSEA) and [2-(Trimethylammonium) ethyl] methanethiosulfonate (MTSET) were purchased from Toronto Chemicals (Canada).

## 2.2 Animals

All animal care and experimental procedures followed the guideline from the UK Home Office at the Biomedical Services, University of Oxford. Adult female *Xenopus laevis* toads were purchased from Xenopus1 (MI, USA) or Nasco (WI, USA). *Xenopus* toads were housed in a climate-controlled, light-regulated room. Toads were anaesthetised by immersion in 0.5% tricaine until non-responsive to toe pinch. Toads were then decapitated and ovarian lobes harvested and defolliculated by incubation in 2 mg/ml collagenase. Defolliculated stage V-VI oocytes were sorted and injected with 100 ng of wild type or mutant concatemeric  $\alpha 4\beta 2$  nAChR-cRNA, as previously described (Carbone *et al.*, 2009). Injected oocytes were incubated until use at 18 °C in Barth's solution: 88 mM NaCl, 1 mM KCl, 0.33 mM Ca(NO<sub>3</sub>)<sub>2</sub>, 0.41 mM CaCl<sub>2</sub>, 0.82 mM MgSO<sub>4</sub>, 2.4 mM NaHCO<sub>3</sub>, 10 mM HEPES, supplemented with antibiotic/antimycotic mixture (1%) and 50 µg/mL neomycin or amikacin (100 µg/mL) (pH 7.5, with 5 M NaOH).

## 2.3 Molecular Biology

Standard molecular cloning techniques, including DNA ligations, maintenance and growth of *Escherichia coli* bacterial strains and the use of digestion restriction enzymes were carried out following the procedures described by Sambrook *et al.*, (1989). Plasmid isolation and DNA gel purification were carried out using commercially available kits (Promega, UK). Capped cRNA coding for wild type or mutant concatameric receptors was synthesised by *in vitro* transcription from SwaI-linearised cDNA template using the mMessage mMachine T7 kit (Ambion, UK).

### 2.3.1 Single Point Mutations

Point mutations were introduced into  $\alpha 4$  or  $\beta 2$  subunits using the QuikChange™, site-Directed Mutagenesis Kit (Stratagene, The Netherlands). Oligonucleotides for polymerase chain reactions (PCRs) were purchased from Eurofins (UK). In order to increase the number of positive transformants, the protocol used was slightly modified from the manufacturer's instructions, as described below.

- 1) Oligonucleotides primers (35 to 45 long, Melting  $T^\circ < 80\text{ C}^\circ$ ) were synthesised carrying the desired mutations in the middle.
- 2) The synthesised primers were diluted to a final concentration of 125 ng/ $\mu\text{l}$  and used in the subsequent PCR reaction.

- 3) The PCR mix consisted of the following:

5  $\mu\text{l}$  Pfu Buffer 10X

1  $\mu\text{l}$  DNA template (stock 50 ng/ $\mu\text{l}$ )

1  $\mu\text{l}$  of sense primer (125 ng)

1  $\mu\text{l}$  of antisense primer (125 ng)

3  $\mu\text{l}$  dimethyl sulphoxide

5  $\mu\text{l}$  dNTPs (from 2 mM stocks)

1  $\mu\text{l}$  High Fidelity Pfu enzyme

33  $\mu\text{l}$  Nuclease free water

- 4) The parameters for the PCR run were as follows:

PCR Segment	Number of Cycles	Holding Temperature (C)	Time (minutes)
1	1	95	1
2	16	95	0.5
		55	1
		68	1 min per kbp
3	1	68	1 min per kbp

- 5) 1  $\mu\text{l}$  of the enzyme DpnI was added to the PCR mixture in order to degrade the parental methylated DNA, which corresponds to the template (non-mutated DNA), and to leave intact only the newly formed DNA (non-methylated and likely containing the desired mutation).



6) X-Gold Competent cells (Invitrogen, UK) were transformed with 30  $\mu$ l of the digestion product. After overnight incubation at 37 C°, 3 colonies were picked and amplified by growing them in 10 ml of Terrific medium (Sigma-Aldrich, UK) at 37 C°. After overnight growth, the plasmid was isolated from the bacteria using commercially available DNA purification kits (Promega, UK), and fully sequenced to confirm the presence of the desired mutation and verified the sequence of the non-mutated regions.

The full-length sequence of wild type and mutated subunit cDNAs were verified by DNA sequencing (BiosourceScience, Oxford or Eurofins, Germany). The residue numbering used throughout this thesis includes the signal sequence. To obtain the position in the mature form, subtract 28 for  $\alpha$ 4 and 26 for  $\beta$ 2.

### 2.3.2 Concatameric $\alpha$ 4 $\beta$ 2 receptors

The fully concatenated form of the  $(\alpha$ 4 $\beta$ 2)<sub>2</sub> $\beta$ 2 and  $(\alpha$ 4 $\beta$ 2)<sub>2</sub> $\alpha$ 4 isoforms were engineered as previously described by Carbone *et al.* (2009). Briefly, the signal peptide and start codon were removed from all the subunits but the first (a  $\beta$ 2 subunit) and the subunits were bridged by Alanine, Glycine and Serine (AGS) linkers. The number of AGS linkers was 6 between  $\beta$ 2 and  $\alpha$ 4 subunits, and 9 between  $\alpha$ 4 and  $\beta$ 2 subunits or between  $\alpha$ 4 subunits. Only the last subunit in the construct ( $\beta$ 2 or  $\alpha$ 4 subunit) contained a stop codon. The subunits were subcloned into a modified pCI plasmid vector (Promega, UK) using unique restriction enzyme sites flanking the N- and C-terminals of each subunit. Wild type or mutant concatenated receptors were assayed for integrity by determining the ACh sensitivity of concatenated receptors co-expressed with an excess of  $\beta$ 2 or  $\alpha$ 4 monomers carrying a reporter mutation in the ion channel (L9'T in the second transmembrane domain). (For further information on this reporter mutation, see section 2.9 of this Chapter). No changes in EC<sub>50</sub> values were observed in comparison to constructs expressed alone. This indicates that the constructs used in this study did not degrade into lower-order concatamers or monomers as such degradation products would incorporate the  $\beta$ 2L9'T or  $\alpha$ 4L9'T monomers into receptors of higher sensitivity to ACh than the intact concatenated  $(\alpha$ 4 $\beta$ 2)<sub>2</sub> $\alpha$ 4 receptors (Groot-Kormelink *et al.*, 2004).

Henceforth, concatenated  $(\alpha$ 4 $\beta$ 2)<sub>2</sub> $\beta$ 2 or  $(\alpha$ 4 $\beta$ 2)<sub>2</sub> $\alpha$ 4 receptors will be referred to as  $\beta$ 2\_ $\alpha$ 4\_ $\beta$ 2\_ $\alpha$ 4\_ $\beta$ 2 or  $\beta$ 2\_ $\alpha$ 4\_ $\beta$ 2\_ $\alpha$ 4\_ $\alpha$ 4, respectively.

### 2.3.3 Engineering mutant concatenated $\alpha 4\beta 2$ receptors

To introduce mutations into specific subunits of  $\beta 2\_ \alpha 4\_ \beta 2\_ \alpha 4\_ \alpha 4$  receptors, the mutation was first introduced into the appropriate individual subunit subcloned into a modified pCI plasmid. After confirming the presence of the desired mutation and verifying the sequence of the non-mutated regions, the subunit cDNA was digested with appropriate unique flanking restriction enzymes and then ligated into the desired position in the concatamer using standard cDNA ligation protocols with T4 ligase (New England Biolabs, UK). The presence of the mutated subunit was also confirmed by DNA sequencing. Following ligation and DNA amplification, the appropriate subunit was cut by enzyme restriction digestion from the concatamer and sequenced by standard DNA sequencing.

For clarity, mutations in the concatameric receptors are shown as superscript positioned in the (+) or (-) face of the mutated subunit e.g., in  $\beta 2^{L146C}\_ \alpha 4\_ \beta 2\_ \alpha 4\_ \alpha 4$  the mutation L146C is located in the (-) face of the  $\beta 2$  subunit occupying the first position of the linear sequence of the concatamer. Wild-type and mutant  $\beta 2\_ \alpha 4\_ \beta 2\_ \alpha 4\_ \alpha 4$  nAChR cRNA were then prepared and injected into the cytoplasm of *Xenopus* oocytes as described by Mazzaferro *et al.* (2011).

### 2.4 Microinjection of cRNA

Needles for microinjection were prepared from Drummond glass capillaries (Sartorius, UK), which were pulled in one stage using a vertical microelectrode puller (Narishige PC-10). Prior to use, the tip of a selected needle was broken using fine forceps to give a narrow tip length of approximately 3 mm with an external ranging from 1.0 to 1.5  $\mu\text{m}$ . The needle was back-filled with light mineral oil and loaded on to a Nanoject II microinjector (Drummond, USA). Wild type or mutant concatameric receptor (**Fig.2.1.B**) cRNA were injected into the oocyte cytoplasm (50.6 nl at 0.1 ng/nl) as illustrated in **Fig.2.1.A**. Injected oocytes were transferred to 96 well sterile dish (one oocyte per well) containing modified Barth's solution and incubated at 18 C° for a maximum of 5 days.

Two to three days after injection, *Xenopus* oocytes expressed functional wild type (WT) or mutant  $\beta 2\_ \alpha 4\_ \beta 2\_ \alpha 4\_ \alpha 4$  receptors, which were used to examine receptor function.

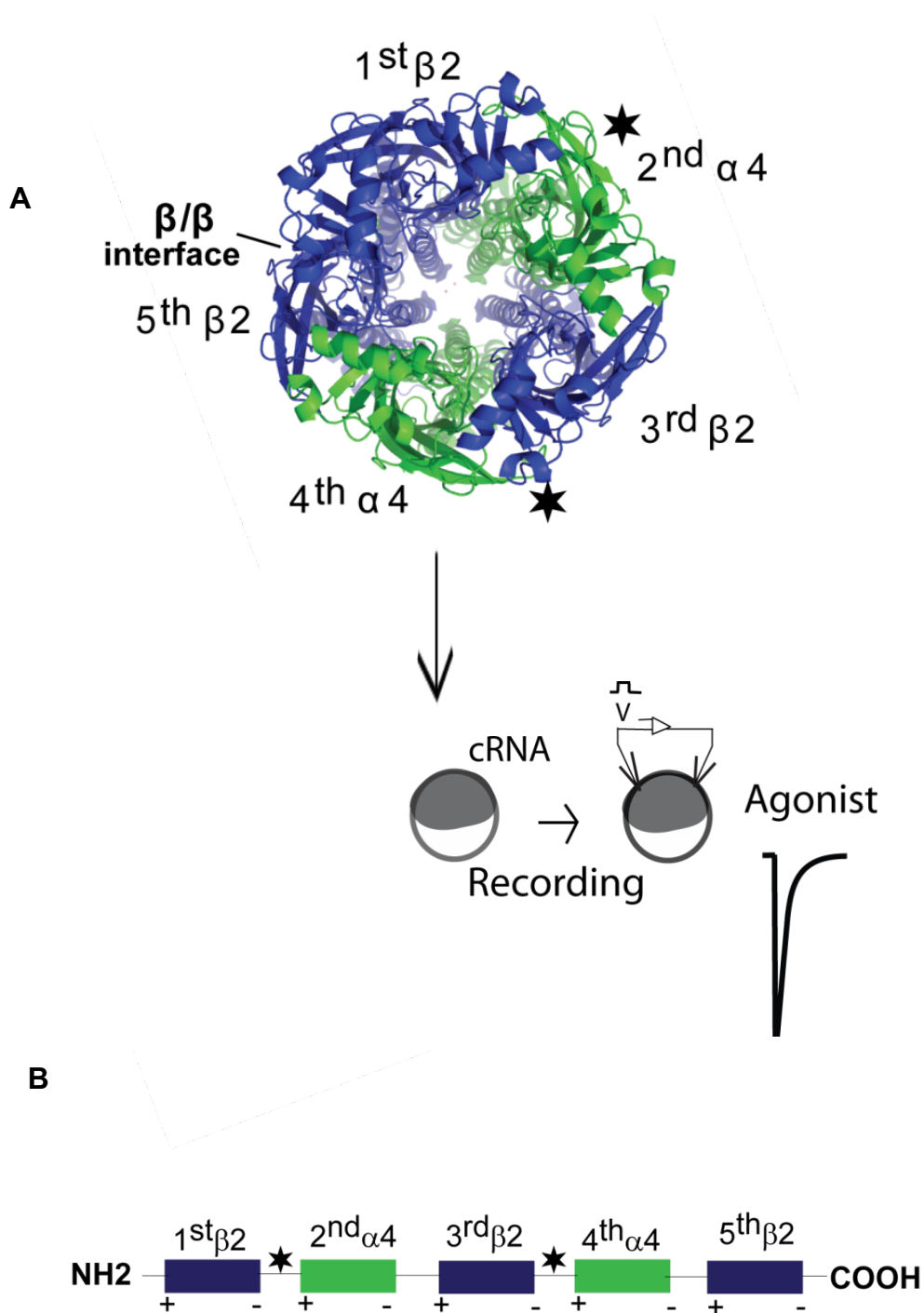


**Figure 2.1. Diagram showing  $\alpha 4\beta 2$  cRNA injection into *Xenopus* oocytes. A)**  $\alpha 4\beta 2$  cRNA injection into *Xenopus* oocytes. After 2-3 days post-injection, currents were recorded using two-electrode voltage clamp technique. **B)** The  $(\alpha 4\beta 2)_2\beta 2$  concatenated nAChR receptor. The star represents binding sites.

## 2.5 Electrophysiological Recordings

The functional characterisation of the receptors expressed in this study at the surface of oocytes was carried out using two electrode voltage-clamping. In this approach, the potential of the oocyte is held constant by means of an electronic circuit and the current required for holding the cell at the chosen potential is then measured. Measurement of the current in the absence or presence of a known concentration of agonist provides, by subtraction, a direct measurement of the current flowing through the ion channel of the activated receptor. The sensitivity of this technique allows current measurements of tens of nA to  $\mu$ A during whole cell recording.

After 2-3 days post-injection oocytes were selected according to their appearance. Only oocytes with integral membrane and no signs of degradation were chosen for electrophysiological recordings. Oocyte isolation and two-electrode voltage-clamp recordings on oocytes were carried out as previously described (Carbone *et al.*, 2009, Moroni *et al.*, 2008). Oocytes were placed in a 30 $\mu$ l recording chamber (Digitimer Ltd, UK) and bathed with a modified Ringer solution (in mM: NaCl 150, KCl 2.8, HEPES 10, BaCl<sub>2</sub> 1.8; pH 7.2, adjusted with NaOH). A gravity driven perfusion system was used for all the experiments. All solutions were freshly made prior to recordings.

Oocytes were impaled by two electrodes connected to a Geneclamp 500B (Molecular Devices, USA) for standard voltage clamp recordings (voltage-clamped at -60 mV) and pCLAMP 6 software (Molecular Devices, Sunnyvale, CA). Briefly, electrodes were made from borosilicate capillary glass (Harvard Apparatus, GC 150 TF) using a vertical two stage electrode puller (Narishige PP-83) to give a top diameter of 1-2 $\mu$ m. Prior to recordings electrodes were filled with 3 M KCl and only electrodes with a resistance between 0.5 and 2 M $\Omega$  were used for voltage clamping. Traces were filtered at 1 kHz during recording and digitized at 0.5 to 5 kHz using a DigiData 1200 interface (Molecular Devices, Sunnyvale, CA). All experiments were carried out at room temperature. Oocytes were continually perfused with fresh Ringer solution at a rate of 10 ml/min. Manually activated valves allowed switching between different solutions.

## 2.6 Agonist concentration response curves

Concentration-response curves (CRC) for agonists were obtained by normalizing agonist-induced responses to the control responses induced by a near-maximum effective agonist concentration, as previously described (Carbone *et al.*, 2009, Moroni *et al.*, 2008). A minimum interval of 5 min was allowed between agonist applications to ensure reproducible recordings. The agonist CRC data were first fitted to the one-component Hill equation (Eq. 1):

$$I = I_{max} / [1 + (EC_{50}/x)^{nH}] \quad (\text{Eq. 1})$$

where  $EC_{50}$  represents the concentration of agonist inducing 50% of the maximal response ( $I_{max}$ ),  $x$  is the agonist concentration and  $nH$  the Hill coefficient.  $EC_{50}$  is the concentration of agonist needed to elicit half-maximal response from the receptor and the Hill coefficient is the slope of the curve and a measure of cooperativity.  $EC_{50}$  values are commonly used for functional comparisons: increases in  $EC_{50}$  values correspond to a loss-of-function (more agonist is needed to open the same number of channels) and decreases in  $EC_{50}$  values correspond to a gain-of-function (less agonist is needed to open the same number of channels). The  $EC_{50}$  is a composite measurement of agonist binding and functional coupling. In addition,  $EC_{50}$  values are also influenced by receptor desensitisation and ion channel blockade (Colquhoun, 1998). Despite being composite receptor metrics,  $EC_{50}$  values are useful for comparisons between wild type and mutant receptors or for establishing the macroscopic potency and maximal effects of ligands acting on receptors.

When ACh induced biphasic receptor activation, the CRC data were fitted with the two-component Hill equation shown below (Eq. 2).

$$I = \text{Top-Bottom} + \text{Span} * \text{Frac} / (1+10^{((\text{LogEC}_{50\_1}-X) * nH1)}) + \text{Span} * (1-\text{Frac}) / (1+10^{((\text{LogEC}_{50\_2}-X) * nH2)}) \quad (\text{Eq. 2})$$

where Top and Bottom are the plateaus at the left and right ends of the curve, in the same units as  $I$ ,  $\text{LogEC}_{50\_1}$  and  $\text{LogEC}_{50\_2}$  are the concentrations that give half-maximal high sensitivity or low- sensitivity stimulatory effects, respectively,  $nH1$  and  $nH2$  are the Hill coefficients,  $\text{Frac}$  is the proportion of maximal response due to the higher sensitivity

component and  $Span$  is a fitted coefficient between 0 and 1 that gives the weight of the first component.

For some studies, the effect of  $Zn^{2+}$  potentiation on concatenated  $(\alpha4\beta2)_2\alpha4$  nAChRs was assayed. The sensitivity to  $Zn^{2+}$  was assessed by co-applying a range of  $Zn^{2+}$  concentrations with 10  $\mu$ M ACh at  $(\alpha4\beta2)_2\alpha4$  nAChRs receptors (the ACh  $EC_{10}$  at  $(\alpha4\beta2)_2\alpha4$  nAChRs). In order for  $Zn^{2+}$  to attain equilibrium around impaled oocytes,  $Zn^{2+}$  was pre-applied for 30 s to the cell before co-applications of ACh and  $Zn^{2+}$ . Concentration-response relationships for  $Zn^{2+}$  were obtained using this protocol and the peak responses elicited by ACh +  $Zn^{2+}$  were normalised to the peak response of the appropriate ACh alone. Where a single component concentration-response relationship was evident, data were fitted to the Hill equation shown above. When  $Zn^{2+}$  produced both a potentiating and inhibiting effect the data were fitted to the following equation (Eq. 3) which has been designed by Harvey *et al.* (1999) to account for the potentiating and inhibitory effects of  $Zn^{2+}$  on glycine receptors assuming this cation binds to two distinct sites:

$$I = I_{\min} + (I_{\max} - I_{\min}) \left\{ \frac{1}{1 + (EC_{50}/X)^{nH_{\text{pot}}}} - \frac{1}{1 + (IC_{50}/X)^{nH_{\text{inh}}}} \right\} \quad (\text{Eq. 3})$$

where  $I$  represents the current responses at a given  $Zn^{2+}$  concentration ( $X$ ),  $I_{\min}$  the control ACh response in the absence of  $Zn^{2+}$  and was set to 1.  $I_{\max}$  represents the maximally potentiated peak,  $EC_{50}$  and  $IC_{50}$  are the concentrations of  $Zn^{2+}$  inducing half-maximal potentiation and inhibition, respectively, and  $nH_{\text{pot}}$  and  $nH_{\text{inh}}$  are the Hill coefficients for potentiation and inhibition, respectively (Moroni *et al.*, 2008). F tests were always performed to assess the fitting of the data; the simpler one-component model was preferred unless the extra sum-of-squares F test had a value of  $p$  less than 0.05.

## 2.7 Substituted cysteine accessibility method

The substituted cysteine accessibility method (SCAM) involves the introduction of cysteines, one at a time, into a region and the subsequent application of thiol-specific (e.g., MTS)

reagents to the engineered residues to covalently modify the substituted cysteine residue (Karlin and Akabas, 1998) (**Fig. 2.2**). The introduced cysteines should not affect the responses of the receptors. If the cysteine is accessible to the MTS reagent, it will be oxidised and, if the position occupied by the modified cysteine affects structure or function, or both, the responses of the receptor will be either enhanced or decreased. Modification of the introduced cysteine is monitored using electrophysiological or biochemical assays.

### **2.7.1 Maximal effects of MTSET- modification of substituted cysteines**

In this study, MTSET was used to modify free cysteine residues introduced one at a time at the (+) or (-) side of the  $\alpha 4$  or  $\beta 2$  subunits in fully concatenated  $\alpha 4\beta 2$  nAChRs. The amino acids mutated to cysteine were E loop residues  $\beta 2L146$  and  $\alpha 4T152$ . Previous studies have shown that both  $\beta 2L146$  and  $\alpha 4T152$  are suited for SCAM-based studies (Papke *et al.*, 2011; Mazzaferro *et al.*, 2011, 2014; New *et al.*, 2017). Neither  $\beta 2L146C$  nor  $\alpha 4T152C$  have significant impact on receptor function, as judged by ACh  $EC_{50}$  values, but in the presence of MTS reagents, they produce a profound decrease in the maximal responses of  $\alpha 4\beta 2$ -cysteine substituted receptors to ACh (Papke *et al.*, 2011; Mazzaferro *et al.*, 2011, 2014; New *et al.*, 2017).

Wild type and cysteine substituted concatenated  $\alpha 4\beta 2$  nAChRs were expressed in *Xenopus* oocytes and subsequently characterised using two electrode voltage clamping procedures, as described above.

The effect of the MTSET reagent on agonist responses was assessed as shown in **Fig. 2.2**. Briefly, oocytes expressing receptors with a free cysteine or wild type receptors were first challenged with a control agonist (ACh, Cyt, Var, TC2559) concentration every 5 min until a stable response was obtained. Oocytes were then perfused with Ringer's solution containing MTSET (1 mM) for 120 s after which time the impaled cells were washed with Ringer's solution for 90 s. After washing, the agonist was applied again every 5 min until the amplitude of the responses was constant to determine accessibility to the modified cysteine residue by the MTS reagent. The average of the current amplitudes prior to application of MTS was the control response current ( $I_{initial}$ ), and the average of current amplitudes after

rinsing was the average response after MTSET application ( $I_{\text{after MTS}}$ ). The effect of the MTS reagents was estimated using the following equation (Eq.4):

$$\% \text{ Change} = (I_{\text{after MTS}}/I_{\text{initial}}) - 1 \times 100 \quad (\text{Eq. 4})$$

For both mutants, ( $\beta_2\_ \alpha_4\_ \beta_2\_ \alpha_4^{\text{T152C}}\_ \alpha_4$  and  $\beta_2^{\text{L146C}}\_ \alpha_4\_ \beta_2\_ \alpha_4\_ \alpha$  and wild type ( $\beta_2\_ \alpha_4\_ \beta_2\_ \alpha_4$ ) receptors, the concentration of MTSET used were 1mM (the optimal concentration for MTSET; Zhang and Karlin 1997).

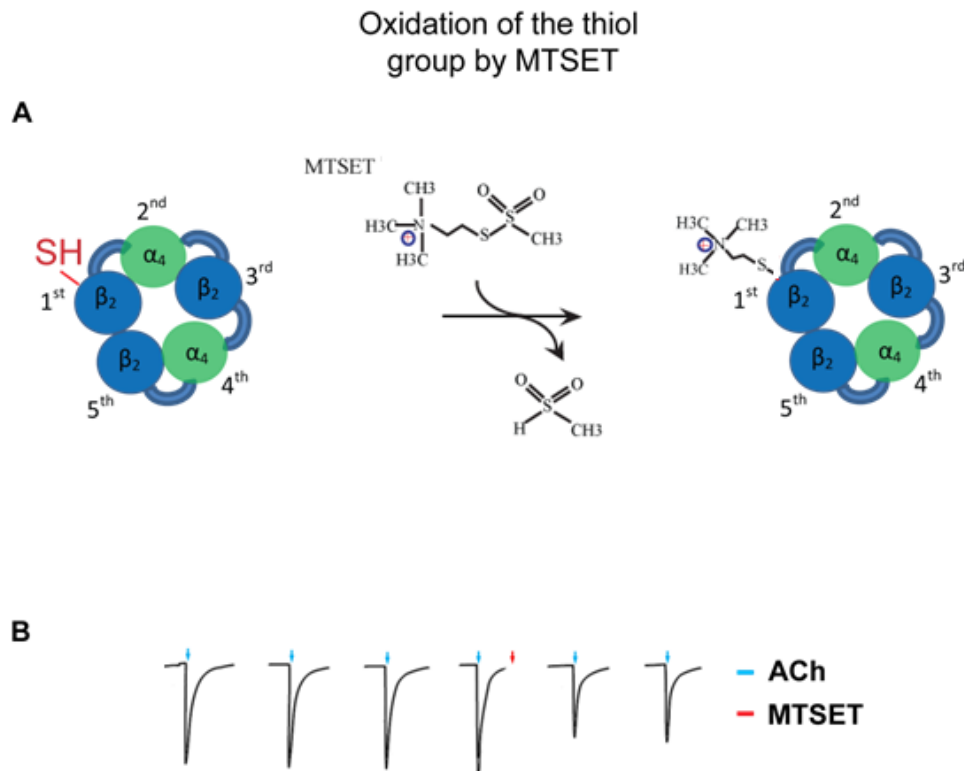


**Figure 2.2 Covalent MTS modification of substituted cysteine** **A)** Using concatenated  $\alpha_4\beta_2$  nAChRs it is possible to introduce single point mutations at an identified subunit interface. There is a reaction between the thiolic group of the cysteine and MTSET **B)** Representative traces that shows max inhibition of ACh current (blue arrows) after maximal MTSET concentration (1mM) treatment. MTSET is applied for 120 s (red arrow).



## 2.7.2 Rates of MTSET reaction

To determine whether nicotinic ligands affect the covalent modification of introduced free cysteines, and distinguish differences between the agonist sites on  $\alpha 4(+)/\beta 2(-)$  sites, the effect of nicotinic ligands on the rate of MTSET modification was determined. These studies were termed “protection assays” (**Figure 2.3**). If in the presence of reversible ligands the rate of reactions is modified, it is considered that the ligand changes the accessibility of the introduced free cysteine to MTSET. Accessibility may be altered by steric hindrance, changes in the electrostatic environment close to the substituted cysteine or changes in the conformation of the region harbouring the substituted cysteine (Newell and Czajkowski, 2007). Henceforth, the ligand (ACh) used in the SCAM studies will be referred to as protectants.

The rate of MTSET modification of introduced cysteines was first determined by measuring the effect of sequential applications of sub-saturating concentrations of MTSET on IACH responses. The concentration of MTSET reagent used was 1  $\mu\text{M}$  for wild type or mutant concatenated  $(\alpha 4\beta 2)_2\alpha 4$  or 10  $\mu\text{M}$  for wild type or mutant concatenated  $(\alpha 4\beta 2)_2\beta 2$ . Preliminary experiments established that these concentrations of MTSET were optimal to describe adequately the early and plateau phases of the MTSET reaction rate data. Because  $\alpha 4\beta 2$  nAChRs are highly prone to long-term desensitisation when exposed to agonists (Marks *et al.*, 2010; Benallegue *et al.*, 2013), the protectant was applied in the rate experiments prior to MTSET to correct for any process of desensitisation that could develop during the protection assays, when the protectant is added together with the MTSET reagent.

Responses to ACh prior to MTSET reagent application were first stabilised as follows:

1. ACh ( $\text{EC}_{50} \times 5$ ) pulses were applied for 5 s
  2. Step 1 was followed by a recovery time of 125 s
  3. The protectant ( $\text{EC}_{50} \times 5$ ) was then applied for 10 s
  4. Step 3 was followed by a washing period of 3 min and 40 s with ringer solution.
- The cycle 6 min total was repeated until the responses to Ach were stable (<5% on four successive applications of  $\text{EC}_{50} \times 5$  ACh).

MTS reagent was then applied using the following sequence of reactions:

1. At time 0, ACh ( $EC_{50} \times 5$ ) was applied for 5 s
  2. Step one was followed by a period of recovery of 95 s
  3. MTSET was then applied for 10 s
  4. Step 3 was then followed by a recovery period of 20 s.
  5. Immediately after the recovery time, the protectant ( $EC_{50} \times 5$ ) was applied for 10s
  6. Cell then were washed with Ringer's solution for 3 min and 40s.
- The 6 min total cycle was repeated until MTSET applications produced less than 5% changes in IACH on four successive applications of  $EC_{80}$  ACh).

MTSET application was repeated 9 times to give a total accumulative application time of 90s. To confirm that any observed decrease in  $I_{ACh}$  was due to the effects of MTSET and not to receptor desensitisation, ACh and protectant pulses (following the same scheme used to stabilize the ACh responses prior the MTSET application) were applied at the end of the protocol as illustrated in **Figure. 2.3**.

### 2.7.3 Protection assays

The effects of agonists and antagonists on the rate of MTSET modification were tested by co-applying MTSET with agonist ( $EC_{50} \times 5$ ). The protocol used was identical to the one used to determine the rate of MTSET reaction, except that the reversible ligand (protectant) was co-applied with MTSET reagent. The sequence of steps illustrated in **Figure 2.5** was as follows:

IACH was stabilised by:

1. Applying  $EC_{80}$  pulses of ACh for 5 s
2. Step 1 was followed by a 95s period of recovery
3. The protectant was then applied for 10s
4. Step 3 was followed by a recovery period of 4 min and 10s
5. This cycle was repeated until stability was achieved. (<5%change in IACH elicited by four successive applications of  $EC_{80}$  ACh).

The sequence of MTSET reactions was as follows:

1. At time 0, ACh ( $5 \times EC_{50}$ ) was applied (5 s)
2. Step 1 was then followed by a brief period of recovery (95 s)
3. MTSET and the protectant were co-applied for 10 s
4. Step 3 was followed by a recovery period of 4 min and 10 s. This cycle was repeated until the application of MTSET produced no further changes in I<sub>ACh</sub> (<5% on four successive applications of EC<sub>80</sub> ACh).

To exclude receptor desensitisation as responsible for decreases in I<sub>ACh</sub>, ACh and protectant pulses (following the same scheme used to stabilize the ACh responses prior the MTSET application) were applied at the end of the protocol as a control (**Figure. 2.3**).

The change in current was plotted versus cumulative time of MTSET exposure. A pseudo-first-order rate constant was calculated from the change in I<sub>ACh</sub>. Peak values at each time point were normalised to the initial peak at time 0 s, and a pseudo-first-order rate constant ( $k_1$ ) was determined by fitting the data with a single exponential decay equation:  $y = \text{span} \times e^{-kt} + \text{plateau}$  using Prism v.5.0 (GraphPad Software). Because the data are normalised to values at time 0,  $\text{span} = 1 - \text{plateau}$ . The second order rate constant ( $k_2$ ) for MTSET reaction was determined by dividing the calculated pseudo-first-order rate constant by the concentration of MTSET reagent used.

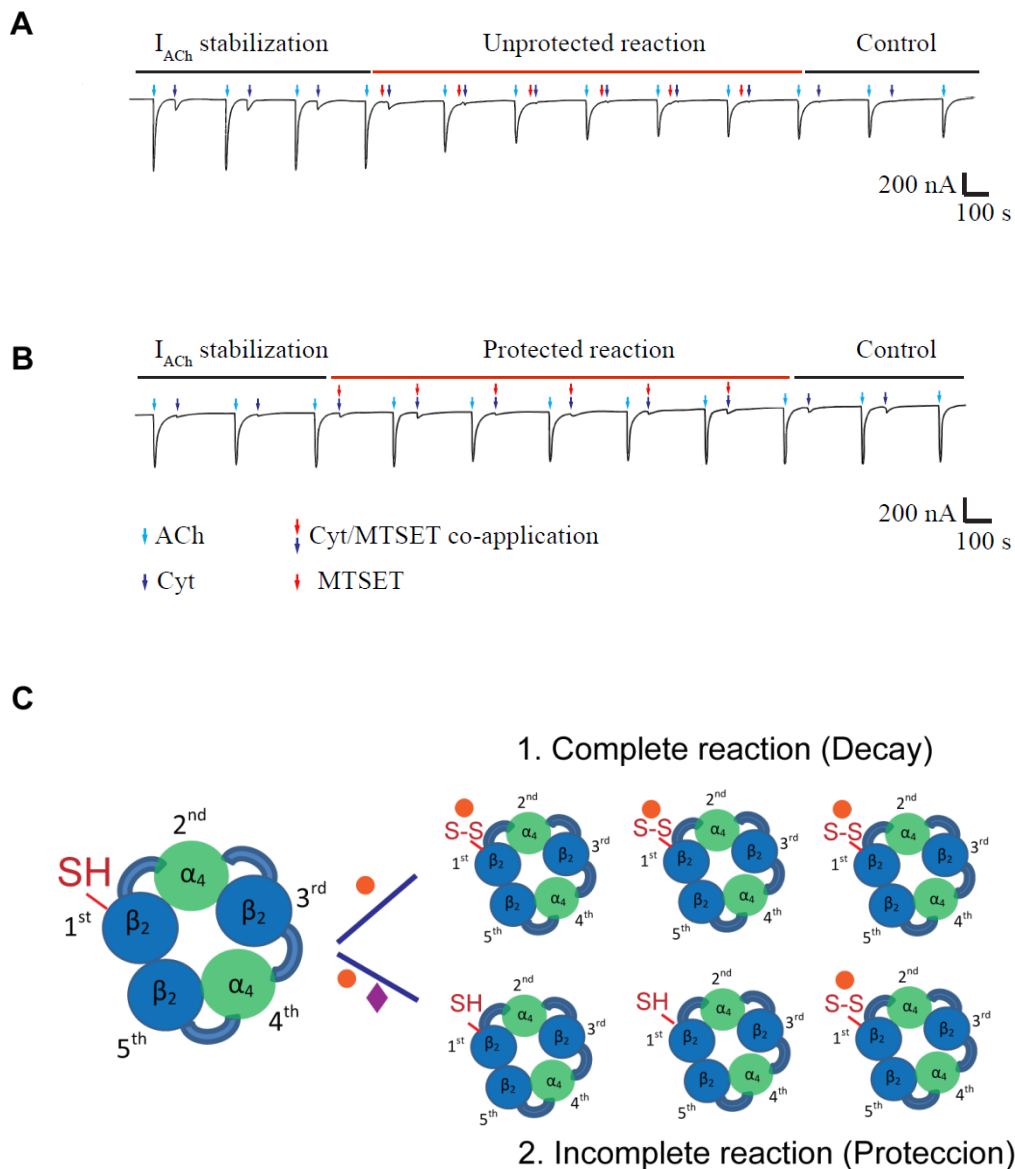


**Figure 2.3. Decay and Protection assay.** **A)** Representative traces of ACh responses prior, during and after cumulative MTSET application to determine the  $k_1$  for the exponential decay of  $I_{ACh}$  (azure arrows) in presence of the partial agonist Cyt (blue arrows). MTSET (red arrows) was applied prior to Cyt. **B)** When Cyt and MTSET were co-applied (protected reaction), MTSET did not impair the  $I_{ACh}$  currents. **C)** General scheme of the protection assay experiment. After cumulative MTSET (orange circle) application, the reaction is complete (**C, 1**) and the result is a decrease of the  $I_{ACh}$  current. However, when MTSET is co-applied with a ligand (purple diamond) that competes or impedes the MTSET reaction with the free cysteine introduced in the agonist site at the  $\alpha_4(+)/\beta_2(-)$  interface, the reaction rate is slower (**C, 2**).

## 2.8 Double mutant Cycle Analysis.

To assess whether E loop and B loop residues in non-agonist binding subunit interfaces in concatenated  $\alpha 4\beta 2$  nAChR affect agonist binding or the functional response of these receptors, the double mutant cycle analyses strategy was used. Typically, a double-mutant cycle analyses involves wild-type protein, two single mutants and the corresponding double mutant protein. If the change in free energy associated with a structural or functional property of the protein upon a double mutation differs from the sum of changes in free energy due to the single mutations, then the residues at the two positions are coupled. Such coupling reflects either direct or indirect interactions between these residues. In the absence of coupling between residues, prediction of mutational effects is possible by assuming their additivity. The function estimated is  $\Omega$ , the coupling parameter, which in the studies reported here is given in terms of the parameter  $EC_{50}$  (**Fig. 2.4**). If the two perturbations are independent of one another,  $\Omega$  should be  $\sim 1$ . That is, for independence the individual mutations' effects on functional parameters should be additive. On the other hand, if  $\Omega$  deviates significantly from 1, an interaction between the perturbed sites is established. Typically, a value of  $\Omega > 2$  is considered as significant coupling. This method has been used to establish stabilising interactions such as salt bridges in LGICs (Hidalgo and MacKinnon, 1995; Faiman and Horovitz, 1996; Venkatachalan and Czajkowski, 2008).

In the present study, since mutations to E loop or B loop residues in non-agonist binding interfaces change the maximal agonist responses without significant changes to  $EC_{50}$  values, mutations to these residues were paired with a reporter mutation in the ion channel known to induce a gain of function in the Cys loop family of LGICs. The reporter mutation used was the highly conserved leucine 9' (the 9<sup>th</sup> residue downstream from the proximal end of TM2). The precise role of this conserved leucine has not been resolved but it is well known that swapping the hydrophobic leucine with a more hydrophilic amino acid such as serine or threonine leads to an increase in the agonist  $EC_{50}$  (Chang and Weiss, 1999; Revah *et al.*, 1991; Moroni *et al.*, 2006). This approach was developed by Dennis Dougherty and his team to probe long range coupling between residues in agonist binding sites and other domains of the muscle nAChR (Gleitsman *et al.*, 2009).

Estimated  $EC_{50}$  values were used to calculate the coupling parameter ( $\Omega$ ) using the equation 5 (Eq.5), where  $EC_{50}(AB)$  is the wild type value,  $EC_{50}(A'B')$  is the  $EC_{50}$  for receptors

containing the double mutation,  $EC_{50}(A'B)$  is the  $EC_{50}$  for receptors containing the target mutation and  $EC_{50}(AB')$  is the  $EC_{50}$  determined for receptors containing the reporter mutation.

$$\Omega = \frac{EC_{50}(AB) * EC_{50}(A'B')}{EC_{50}(A'B) * EC_{50}(AB')} \quad (\text{Eq.5})$$

## 2.9 Comparative Modeling

The published structure of the  $(\alpha 4\beta 2)_2\beta 2$  nAChR containing 2 copies of the  $\alpha 4$  subunit and 3 copies of  $\beta 2$  (PDB ID 5kxi; Morales-Pérez *et al.*, 2016) was viewed and figures were made using Pymol (<http://www.pymol.org>).

## 2.10 Statistical analysis

The data and statistical analysis comply with the recommendations on experimental design and analysis in pharmacology (Curtis *et al.*, 2015). Data for wild type or each mutant receptor studied were obtained from oocytes from at least five different donors. Statistical and non-linear regression analyses of the data from concentration response curves and MTSET modification were performed using Prism 5 (GraphPad, San Diego, CA). An F-test determined whether the one-site or biphasic model best fit the concentration response data; the simpler one-component model was preferred unless the extra sum-of-squares F test had a value of  $p$  less than 0.05. One-way ANOVA with post-hoc Dunnett's test was used for comparison involving more than two groups. Unpaired Student's  $t$ -tests were used for comparison between two groups (control and test). Values are presented as arithmetic mean  $\pm$  SEM of at least 5 independent experiments. Statistical tests with  $p < 0.05$  were considered significant. For all data analysis, post-hoc tests (Dunnett's tests) were used only if after analysis of variance  $p < 0.05$  and there was no significant variance in data homogeneity.

## **Chapter 3**

**The fifth subunit in  $(\alpha_4\beta_2)_2\alpha_4$  receptors  
modulates the function of canonical  
agonist sites**





### 3.1 Introduction

The alternate forms of the  $\alpha 4\beta 2$  nAChR have a pair of canonical agonist binding sites located at  $\alpha 4(+)/\beta 2(-)$  interfaces and two  $\beta 2(+)/\alpha 4(-)$  interfaces, interposed between the agonist sites (**Fig. 3.1**). Conserved aromatic residues line the cavity between the  $\beta 2(+)$  and the  $\alpha 4(-)$  sides, as they do in the agonist binding interfaces  $\alpha 4(+)/\beta 2(-)$  (Morales-Pérez *et al.*, 2016). However, conserved aromatic residues in  $\beta 2(+)$  are unlikely to bind agonists because their side chain orientates away from the aromatic pocket (Morales- Pérez *et al.*, 2016). The fifth subunit in the alternate  $\alpha 4\beta 2$  nAChRs plays a pivotal role in distinguishing the two receptor types, defining agonist potency and efficacy, sensitivity to allosteric modulators and desensitisation (Harpsøe *et al.*, 2011; Mazzaferro *et al.*, 2011; Benallegue *et al.*, 2013; Wang *et al.*, 2015). In  $(\alpha 4\beta 2)_2\beta 2$ , the fifth subunit is a  $\beta 2$  subunit that interfaces with another  $\beta 2$  to form  $\beta 2(+)\beta 2(-)$ , the signature subunit interface of this receptor type. Recently,  $\beta 2(+)/\beta 2(-)$  was found to modulate the maximal agonist responses of  $(\alpha 4\beta 2)_2\beta 2$  through a long-range coupling pathway linking the E loop of the fifth subunit to one of the canonical agonist sites (New *et al.*, 2017). In the  $(\alpha 4\beta 2)_2\alpha 4$  receptor, the fifth subunit is an  $\alpha 4$  subunit; this subunit interfaces with another  $\alpha 4$  subunit to form the signature  $\alpha 4(+)/\alpha 4(-)$  interface of  $(\alpha 4\beta 2)_2\alpha 4$  (Moroni *et al.*, 2008; Harpsøe *et al.*, 2011; Mazzaferro *et al.*, 2011). A distinct structural and functional feature of  $\alpha 4(+)/\alpha 4(-)$  is the presence of an operational agonist binding site (Harpsøe *et al.*, 2011; Mazzaferro *et al.*, 2011).

The  $\alpha 4(+)/\alpha 4(-)$  interface binds ACh in a region homologous to the canonical agonist sites in the  $\alpha 4(+)/\beta 2(-)$  interfaces (Harpsøe *et al.*, 2011; Mazzaferro *et al.*, 2011). This site binds ACh with lower affinity than the canonical sites, which account for the biphasic nature of the ACh concentration response curve (CRC) of  $(\alpha 4\beta 2)_2\alpha 4$  receptors (Harpsøe *et al.*, 2011; Mazzaferro *et al.*, 2011). The molecular mechanisms underlying the biphasic nature of the ACh CRC are not known, as yet. However, on the basis of the ACh potency at  $(\alpha 4\beta 2)_2\beta 2$  receptors, it is thought that at low  $\mu\text{M}$  ACh concentrations, the canonical agonist sites are first occupied; this level of occupancy is sufficient to induce efficacious gating. At higher ACh concentrations, the site at the  $\alpha 4(+)/\alpha 4(-)$  interfaces becomes occupied, increasing agonist efficacy but decreasing overall ACh potency (Harpsøe *et al.*, 2011; Mazzaferro *et al.*, 2011; Indurthi *et al.*, 2016). In this model the agonist sites are independent of each other; however, several observations suggest they are not. First, ACh efficacy at concentrations that fully activate the

$(\alpha 4\beta 2)_2\beta 2$  are not as efficacious as they are in the  $(\alpha 4\beta 2)_2\alpha 4$  receptor (Harpsoe *et al.*, 2011; Mazzaferro *et al.*, 2011). Secondly, agonists that bind only canonical agonist sites in the alternate receptors (e.g., TC2559 and Saz-A) have remarkably different efficacy between the two different stoichiometries (Moroni *et al.*, 2006; Carbone *et al.*, 2009; Mazzaferro *et al.*, 2014). Thirdly, when the  $\alpha 4(+)/\alpha 4(-)$  site is modified to allow binding of agonists excluded from the wild type site, the efficacy of the agonists, although increased, remains significantly different from that displayed at  $(\alpha 4\beta 2)_2\beta 2$  receptors (Mazzaferro *et al.*, 2011). Fourthly, analysis of the distribution of open channel durations shows that occupation of the  $\alpha 4(+)/\alpha 4(-)$  site reduces the duration of the open channels markedly in comparison to those mediated by occupation of canonical agonist sites (Mazzaferro *et al.*, 2017). Thus, the presence of an agonist site at the  $\alpha 4(+)/\alpha 4(-)$  interface appears to have an allosteric effect on the agonist sites at  $\alpha 4(+)/\beta 2(-)$  interfaces (Mazzaferro *et al.*, 2011, 2014, 2017).

Allosteric communication between  $\alpha 4(+)/\alpha 4(-)$  and  $\alpha 4(+)/\beta 2(-)$  interfaces implies that there are intersubunit pathways linking the subunits. The canonical sites are separated from the  $\alpha 4(+)/\alpha 4(-)$  site by  $\beta 2(+)/\alpha 4(-)$  interfaces (**Fig. 3.1**), and these interfaces could represent the key allosteric connectors between the agonist binding sites. The  $\beta 2(+)/\alpha 4(-)$  interface of nAChRs such as the  $\alpha 4\beta 2$  and  $\alpha 3\beta 2$  nAChRs, contains residues that are essential for the action of allosteric modulators and, when altered by mutagenesis, these residues alter the potency and efficacy of ACh (Moroni *et al.*, 2008; Seo *et al.*, 2009; Weltzin and Schulte, 2015; Lucero *et al.*, 2016), suggesting they impact overall receptor function.

This Chapter focuses on examining the possibility that the interface contributed by the (-) side of the fifth subunit and the (+) side of a  $\beta 2$  contributing to a canonical site is part of an allosteric pathway linking the canonical site and the  $\alpha 4(+)/\alpha 4(-)$  site. By introducing cysteines in the agonist sites of the  $(\alpha 4\beta 2)_2\alpha 4$  receptor it was first established that all three agonist sites respond asymmetrically to agonists.

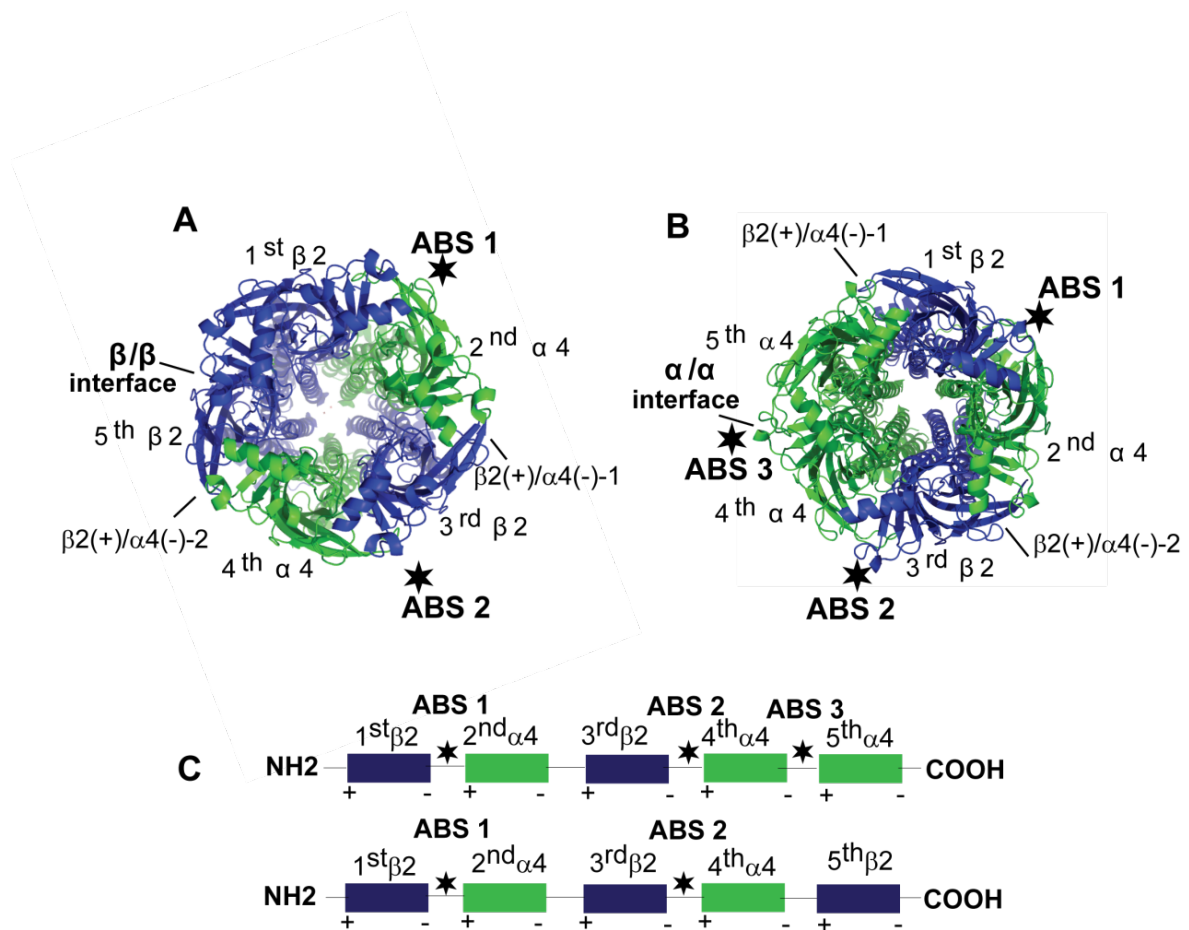


**Figure 3.1. Subunit position and orientation in concatenated  $\alpha 4\beta 2$  nAChRs.** **A, B)** Top view of  $(\alpha 4\beta 2)_2\beta 2$  and  $(\alpha 4\beta 2)_2\alpha 4$  nAChRs. Subunits are numbered according to their position in the linear sequence of the concatenated constructs **C)** The subunit that occupies the fifth position in the linear sequence of the concatemers is the “accessory” or fifth subunit of the  $\alpha 4\beta 2$  nAChRs. The stoichiometry specific subunit interfaces  $\beta 2(+)/\beta 2(-)$  and  $\alpha 4(+)/\alpha 4(-)$  are shown in **A**. The orientation of the principal and complementary side of the subunits is shown. The position of the canonical agonist binding sites (ABS) is shown by asterisks in **A** and **B**.  $\beta 2(+)/\alpha 4(-)$  interfaces are shown in **A** and **B**.

## 3.2 Results

### 3.2.1 Agonist sites and subunit interfaces in $\alpha 4\beta 2$ nAChRs

The studies that will be described in the results chapter focus on examining prospective pathways linking agonist sites on  $\alpha 4(+)/\beta 2(-)$  interfaces to  $\alpha 4(+)/\alpha 4(-)$ , a critical function-defining element in this receptor type. To circumvent ambiguities in data analysis brought about by expression of a mixed population of the alternate stoichiometries of  $\alpha 4\beta 2$  nAChRs, the studies described in the Results Chapters were carried out using fully concatenated  $(\alpha 4\beta 2)_2\beta 2$  and  $(\alpha 4\beta 2)_2\alpha 4$  nAChRs, respectively  $\beta 2\_ \alpha 4\_ \beta 2\_ \alpha 4\_ \beta 2$  and  $\beta 2\_ \alpha 4\_ \beta 2\_ \alpha 4\_ \alpha 4$  nAChRs (Carbone *et al.*, 2009).

For clarity, the subunits in the concatamers are termed according to their position in the linear sequence of the construct, i.e., first subunit, second subunit (**Fig. 3.1 A, B**). Concatenated  $(\alpha 4\beta 2)_2\alpha 4$  and  $(\alpha 4\beta 2)_2\beta 2$  receptors consist of the subunit cassette  $\beta 2\_ \alpha 4\_ \beta 2\_ \alpha 4$  and a fifth subunit. If the fifth subunit is  $\beta 2$ , the resulting concatamer  $\beta 2\_ \alpha 4\_ \beta 2\_ \alpha 4\_ \beta 2$  is equivalent to the  $(\alpha 4\beta 2)_2\beta 2$  receptor isoform. If the fifth subunit is  $\alpha 4$ , the concatamer becomes  $\beta 2\_ \alpha 4\_ \beta 2\_ \alpha 4\_ \alpha 4$ , the  $(\alpha 4\beta 2)_2\alpha 4$  receptor isoform (**Fig. 3.1 C**). Canonical agonist sites (i.e., agonist sites on  $\alpha(+)/\beta(-)$  interfaces) in both concatamers are found in the  $\beta 2\_ \alpha 4\_ \beta 2\_ \alpha 4$  subunit cassette: one site is in the interface between the first subunit (a  $\beta 2$ ) and the second subunit (an  $\alpha 4$ ) and, the other between the third subunit (a  $\beta 2$ ) and the fourth (an  $\alpha 4$ ) subunit. Henceforth, the canonical agonist sites will be termed respectively, ABS 1 and ABS 2 (**Fig. 3.1 C**). In the case of the concatenated  $(\alpha 4\beta 2)_2\alpha 4$  nAChR, the fifth subunit (an  $\alpha 4$ ) interfaces with the 4<sup>th</sup> subunit (an  $\alpha 4$ ) to form the  $\alpha 4(+)/\alpha 4(-)$  interface; as mentioned in the Introduction section of this Chapter, this interface contains an operational agonist site; the fifth subunit contributes the (+) side of this agonist site, whereas the fourth provides the (-) side (Mazzaferro *et al.*, 2011). Thus, this agonist site will be referred to as ABS 3 (**Fig. 3.1**). In the concatenated  $(\alpha 4\beta 2)_2\beta 2$  nAChR, the first subunit (a  $\beta 2$  subunit) interfaces with the fifth subunit (a  $\beta 2$  subunit), forming the signature  $\beta 2(+)/\beta 2(-)$  interface of this receptor type (**Fig. 3.1**). The concatamers also contain interfaces between the (+) side of  $\beta 2$  and the (-) side of  $\alpha 4$ ; these are termed  $\beta 2(+)/\alpha 4(-)$  and are numbered according to their position in the concatamer. In  $\beta 2\_ \alpha 4\_ \beta 2\_ \alpha 4\_ \alpha 4$ , the (-) side of the fifth subunit and the (+) side of the first subunit form  $\beta 2(+)/\alpha 4(-)$ -1, whilst the (-) side in the second subunit (an  $\alpha 4$ ) interfaces with the (+) side of the third subunit (a  $\beta 2$ ) to form  $\beta 2(+)/\alpha 4(-)$ -2 (**Fig. 3.1**). In concatamer

$\beta 2\_ \alpha 4\_ \beta 2\_ \alpha 4\_ \beta 2$ ,  $\beta 2(+)/\alpha 4(-)$ -1 is between the second subunit and the third and;  $\beta 2(+)/\alpha 4(-)$ -2 is between the fourth and fifth subunits (**Fig. 3.1**).

### 3.2.2 Functional asymmetry of agonist binding sites

To assess the function of individual agonist sites, both the ACh sensitivity and the pattern of reaction with MTSET of receptors with mutant agonist sites were assessed. Agonist binding sites were cysteine substituted, one at a time. For canonical sites, the residue substituted was  $\beta 2$ L146 and for the site on  $\alpha 4(+)/\alpha 4(-)$  the residue was  $\alpha 4$ T152. These residues lie in Loop E, at the top of the agonist sites. They have been used previously to study the function of the  $\alpha 4\beta 2$  nAChRs (Mazzaferro *et al.*, 2011, 2014; New *et al.*, 2017). As previously shown, cysteine substitution of  $\beta 2$ L146 or  $\alpha 4$ T152 in the agonist sites of the concatenated  $(\alpha 4\beta 2)_2\alpha 4$  receptor did not ablate functional expression (**Fig. 3.2; Table 3.1**), further confirming that these substitutions are well tolerated (Mazzaferro *et al.*, 2011, 2014; New *et al.*, 2017). In accord with previous studies (Mazzaferro *et al.*, 2011, 2014), the ACh CRC for wild type  $\beta 2\_ \alpha 4\_ \beta 2\_ \alpha 4\_ \alpha 4$  receptors was biphasic, comprising a high-affinity and low-affinity component (**Fig. 3.2, Table 3.1**). Substituted cysteines affect ACh response, depending on which agonist sites the cysteine was incorporated (**Fig. 3.1; Table 3.1**). For  $\beta 2\_ \alpha 4\_ \beta 2\_ \alpha 4^{T152C}\_ \alpha 4$  receptors, the ACh CRC was monophasic and shifted to the right by 2.4-fold, compared to wild type. For  $\beta 2^{L146C}\_ \alpha 4\_ \beta 2\_ \alpha 4\_ \alpha 4$  receptors, the biphasic nature of the ACh CRC was maintained, but the  $EC_{50}$  values for the two curve components were significantly different from wild type ( $p < 0.05$ ; ANOVA). These findings confirm previous studies that the agonist site in  $\alpha 4(+)/\alpha 4(-)$  respond differently to E loop substitutions, compared to ABS 1 (Mazzaferro *et al.*, 2011; 2014). Surprisingly, for  $\beta 2\_ \alpha 4\_ \beta 2^{L146C}\_ \alpha 4\_ \alpha 4$ , the ACh CRC was no different from wild type. This finding is significant because ABS 1 and ABS 2 are structurally equivalent.

To further examine the agonist responses of the cysteine substituted  $\beta 2\_ \alpha 4\_ \beta 2\_ \alpha 4\_ \alpha 4$  receptors, the receptors were tested for their sensitivity to  $\alpha 4\beta 2$ -selective agonists Cys, Var, Saz-A and TC2559. These agonists behave as partial agonists of the  $(\alpha 4\beta 2)_2\alpha 4$  nAChR, compared to the full agonist nature of ACh (Moroni *et al.*, 2006; Zwart *et al.*, 2008; Carbone *et al.*, 2009). **Table 3.1** summarises the findings of these studies. For  $\beta 2\_ \alpha 4\_ \beta 2\_ \alpha 4^{T152C}\_ \alpha 4$  receptors, the  $EC_{50}$  for Cys or TC2559 was not different from wild type but the  $EC_{50}$  for varenicline was 4-fold lower. By comparison,  $\beta 2^{L146C}\_ \alpha 4\_ \beta 2\_ \alpha 4\_ \alpha 4$  receptors retained wild

type sensitivity for Var but displayed reduced sensitivity for Cys and TC2559. Agonist efficacy was not altered in  $\beta_2\_ \alpha_4\_ \beta_2\_ \alpha_4^{T152C}\_ \alpha_4$  or  $\beta_2^{L146C}\_ \alpha_4\_ \beta_2\_ \alpha_4\_ \alpha_4$  receptors. These findings confirm the pharmacological profile of  $\beta_2^{L146C}\_ \alpha_4\_ \beta_2\_ \alpha_4\_ \alpha_4$  and  $\beta_2\_ \alpha_4\_ \beta_2\_ \alpha_4^{T152C}\_ \alpha_4$  receptors published by Mazzaferro *et al.* (2014). At  $\beta_2\_ \alpha_4\_ \beta_2^{L146C}\_ \alpha_4\_ \alpha_4$ , Cys, Var and TC2559 produced biphasic responses and, the efficacy of these agonists was reduced, compared to wild type. Thus, the agonist profile of  $\beta_2\_ \alpha_4\_ \beta_2^{L146C}\_ \alpha_4\_ \alpha_4$ , is not only different from wild type and  $\beta_2\_ \alpha_4\_ \beta_2\_ \alpha_4^{T152C}\_ \alpha_4$  but also from  $\beta_2^{L146C}\_ \alpha_4\_ \beta_2\_ \alpha_4\_ \alpha_4$ . These findings indicate that canonical agonist sites and the agonist site on  $\alpha_4(+)/\alpha_4(-)$  function asymmetrically, which is expected because the (-) side of these agonist sites are structurally different. More intriguingly, the findings also show for the first time in the nAChR family that structurally equivalent agonist sites function asymmetrically.

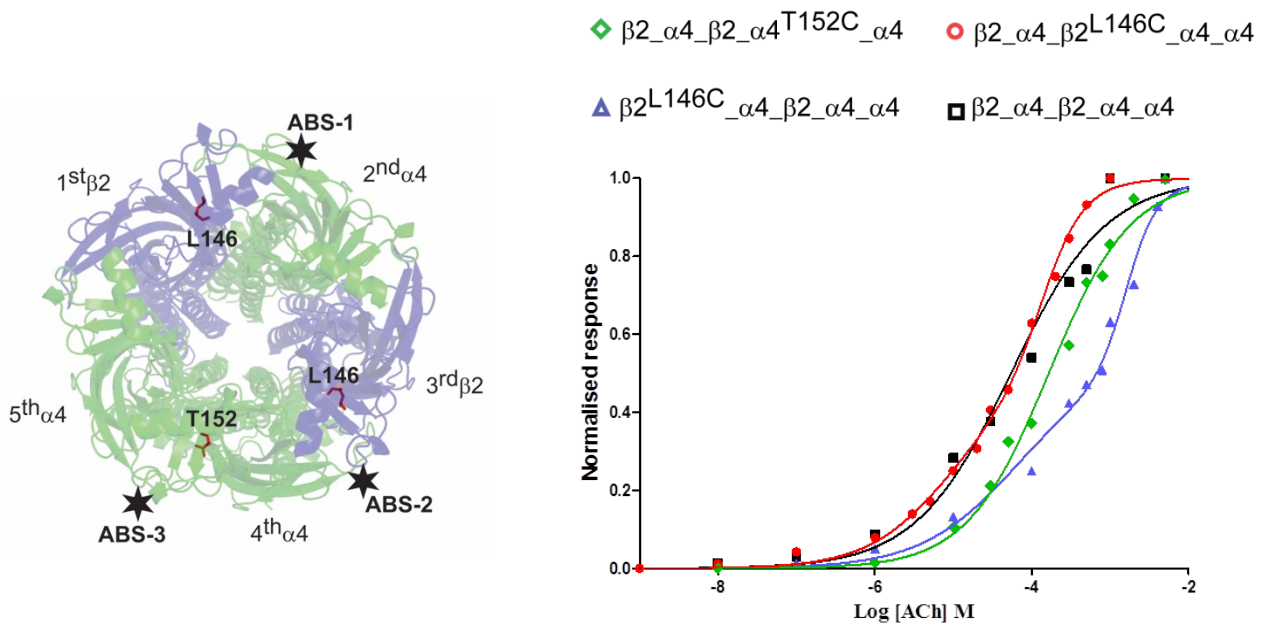


**Figure 3.2. Effects of ACh on wild type and mutant  $(\alpha_4\beta_2)_2\alpha_4$  receptors.** ACh CRC for wild type and mutant  $(\alpha_4\beta_2)_2\alpha_4$  receptors were obtained as described in Chapter 3 expressed heterologously in *Xenopus* oocytes. CRCs were fitted to monophasic and biphasic Hill equations, as described in the Materials and Methods Chapter. The best fit was determined by F-tests; the simpler one-component model was preferred unless the extra sum-of-squares F test had a value of  $p < 0.05$ .

**Table 3.1. Agonist potency (EC<sub>50</sub>) and efficacy (I/I<sub>AChmax</sub>) on wild type and mutant concatenated (α4β2)<sub>2</sub>α4 nAChRs.** Recordings were performed under two-electrode voltage clamp. EC<sub>50</sub> values represent the mean plus 95% confidence interval of n= 6-8 independent experiments. All other values represent the mean ± SEM of n= 6-8 independent experiments. Abbreviations: Cyt, cytisine; Var, varenicline; Saz-A, sazetidine-A; ND, not determined because the amplitude of the agonist responses were too small for reliable measurements. CRCs were fitted to monophasic and biphasic Hill equations, as described in the Materials and Methods Chapter. The best fit was determined by F-tests; the simpler one-component model was preferred unless the extra sum-of-squares F test had a value of *p* less than 0.05, noted by +. Statistical analysis was carried out by Anova with post-hoc Dunnet's test; differences between data were considered significant if *p* < 0.05 (noted by \*).

Receptor		ACh	Cyt	Var	TC2555 9	Saz-A
β2_α4_β2_α4_α4	EC <sub>50</sub> μM	15 (6.3-23.7)  294 (280-308) +	7.27 (2.39- 12.16)	9.52 (5.44- 13.59)	5.99 (4.04- 7.78)	0.9 0.6-1.10)
	I/I <sub>max</sub>	1	0.2±0.06	0.3±0.11	0.22±0.09	0.12±0.06
β2_α4_β2_α4 <sup>T152C</sup> _α4	EC <sub>50</sub> μM	206* (35-337)	10.91 (4.56- 17.27)	2.42 (1.53- 3.32)*	3.06 (1.57- 4.55)	ND
	I/I <sub>max</sub>	1	0.2±0.09	0.23±0.0 7	0.12±0.09	0.10±0.01
β2 <sup>L146C</sup> _α4_β2_α4_α4	EC <sub>50</sub> μM	54 (31-96)  1600±880 (1175- 2028)+,*	19* (11-26)	9 (4.2-13)	13 (9-16)*	ND
	I/I <sub>max</sub>	1	0.08±0.02*	0.29±0.1	0.13±0.09	0.03±0.01
β2_α4_β2 <sup>L146C</sup> _α4_α4	EC <sub>50</sub> μM	12 (8.6-15.7)  155 (133-177) +	4.9 (2.4-7.4)  51 (46-55) +, *	2 (0.3-4)  23 (14-33) +, *	7.75 (5.1-10.4)  16.4 (10.6- 21.7)+, *	ND
	I/I <sub>max</sub>	1	0.06±0.001 *	0.25 ± 0.08	0.08±0.00 6*	0.09±0.01

### 3.2.3 Effects of MTSET on cysteine substituted $\beta_2\_ \alpha_4\_ \beta_2\_ \alpha_4\_ \alpha_4$ nAChRs

The findings described above suggest that agonists interact asymmetrically with the agonist sites in  $(\alpha_4\beta_2)_2\alpha_4$  receptors. This could happen if the overall conformation of the sites somehow differs. This could alter the accessibility of residues to the agonists or to thiol reagents. To examine this possibility further, the cysteine substituted agonist sites were covalently modified by MTSET. Accessibility to MTS reagents is an established strategy to establish differences, structural or environmental (e.g., electronegativity, etc) between receptor regions or loci (Karlin and Akabas, 1998). This approach has been successfully used to identify the agonist site on the  $\alpha_4(+)/\alpha_4(-)$  interface and its pharmacology (Mazzaferro *et al.*, 2011, 2014) and, more recently, long-range coupling between the  $\beta_2(+)/\beta_2(-)$  interface in the  $(\alpha_4\beta_2)_2\beta_2$  receptor (New *et al.*, 2017).

#### 3.2.3.a Maximal effects of MTSET

Accessibility of the substituted cysteines to MTSET was established by exposing the cysteine substituted receptors to 1 mM MTSET, a saturating concentration for MTSET on nAChRs (Karlin and Akabas, 1998), using the procedures described in the Materials and Methods Chapter. As shown in **Fig. 3.3**, the  $EC_{50} \times 5$  ACh responses of  $\beta_2^{L146C}\_ \alpha_4\_ \beta_2\_ \alpha_4\_ \alpha_4$  receptors were almost two-fold more reduced than those of  $\beta_2\_ \alpha_4\_ \beta_2\_ \alpha_4^{T152C}\_ \alpha_4$  receptors (**Fig. 3.3**) following exposure to MTSET, in accord with previously published data (Mazzaferro *et al.*, 2011, 2014). Interestingly, exposure to MTSET reduced the amplitude of the  $EC_{50} \times 5$  ACh responses of  $\beta_2\_ \alpha_4\_ \beta_2^{L146C}\_ \alpha_4\_ \alpha_4$  to the same extent as of those of  $\beta_2\_ \alpha_4\_ \beta_2\_ \alpha_4^{T152C}\_ \alpha_4$  receptors (**Fig. 3.3**), further highlighting differences between the agonist sites. The ACh responses of  $\beta_2\_ \alpha_4\_ \beta_2\_ \alpha_4\_ \alpha_4$  (wild type) receptors were not affected by exposure to MTSET (**Fig. 3.3, C**), demonstrating that the changes in the amplitude of the ACh responses of the mutant receptors following MTSET exposure were due to the reaction between MTSET and the substituted cysteines.



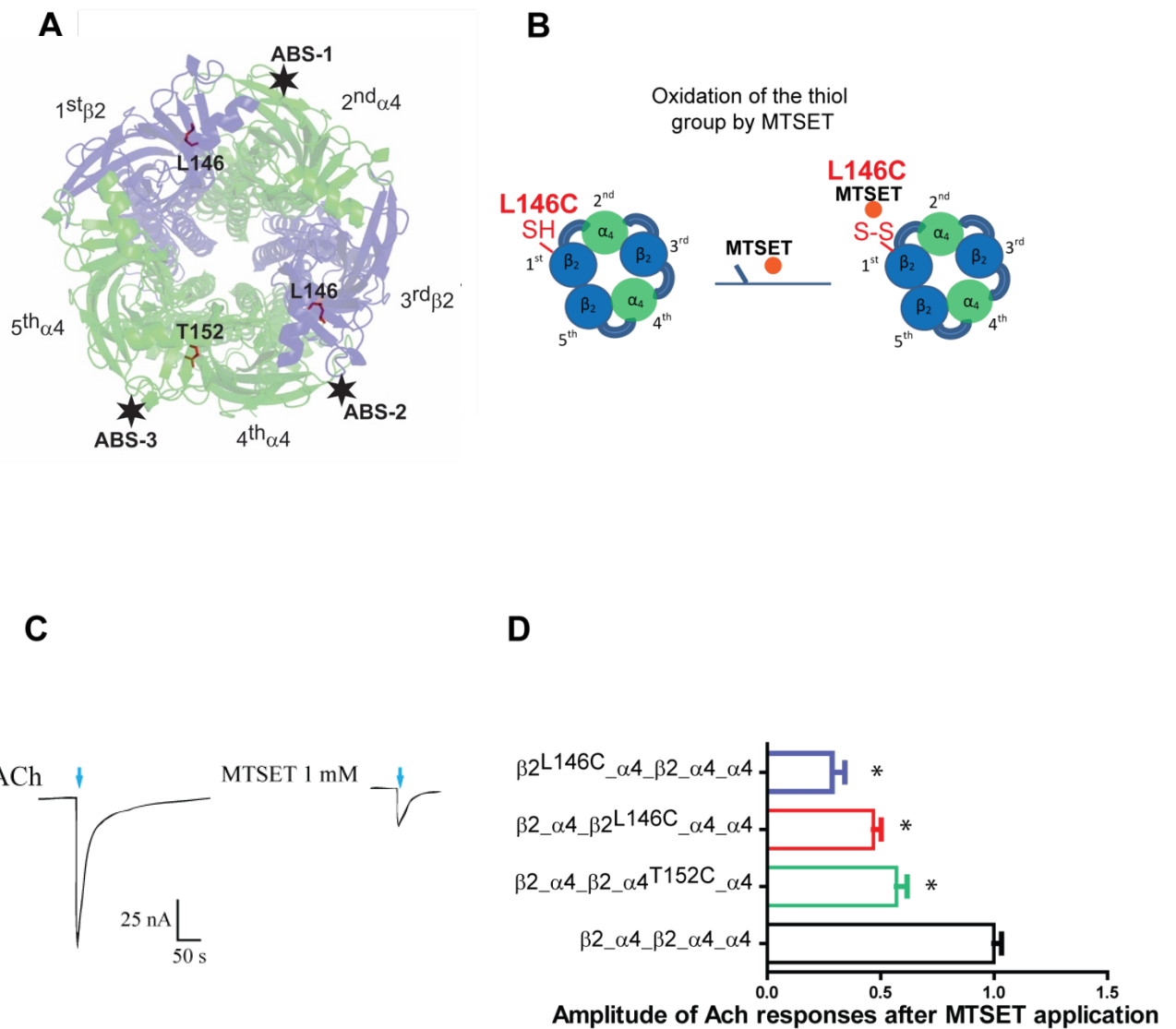


**Figure 3.3 Amplitude of ACh responses after maximum MTSET application. A)** Top view of the  $(\alpha 4\beta 2)_2\alpha 4$ , as viewed from the extracellular side. Subunits are numbered according to their position in the linear sequence of the concatenated constructs. Binding sites are represented by asterisks. **B)** Reaction between the thiolic group of the cysteine and MTSET. **C)** Representative traces of the responses elicited by ACh before and after application of MTSET at  $\beta 2^{L146C}\text{-}\alpha 4\text{-}\beta 2\text{-}\alpha 4\text{-}\alpha 4$ . **D)** Amplitude of ACh responses after maximum MTSET application. Longer periods of MTSET applications produced no further changes in the ACh responses. Significant differences to wild type were determined using one way ANOVA tests with post-hoc Dunnet's test; \* correspond to  $p < 0.05$ .

### 3.2.3.b Rate of MTSET Reaction and Protection Assays

To further explore differences between the agonist sites of  $\beta_2\_ \alpha_4\_ \beta_2\_ \alpha_4\_ \alpha_4$  receptors, the rates of covalent modification of the introduced cysteines were determined by measuring the effect of successive subsaturating applications of MTSET on ACh current responses using the protocol described in Chapter 2. The decrease in ACh current responses was plotted against cumulative duration of MTSET exposure and fit with a single exponential decay curve, which yields a pseudo-first-order rate constant ( $k_1$ ). To correct for the concentration dependence of the rate (Mercado and Czajlowski, 2006), a second order rate constant ( $k_2$ ) was calculated by dividing  $k_1$  by the concentration of MTSET used. This correction was needed to compare the rate of MTSET reactions on the agonist sites. For all mutant receptors, the control MTSET reaction rate was not affected by the application of ACh during the stabilisation of the ACh responses, which proves that any changes in the responses to ACh pulses observed during the protection assays are due to changes in MTSET reaction rates and not to processes such as desensitisation.

As shown in **Fig. 3.4** (rate constants summarised in **Table 3.2**), the fastest reaction of MTSET occurred at  $\beta_2\_ \alpha_4\_ \beta_2\_ \alpha_4^{T152C}\_ \alpha_4$  receptors, suggesting that  $\alpha_4T152C$  is more accessible than  $\beta_2L146$ . Interestingly, the rate of MTSET reaction determined for  $\beta_2^{L146C}\_ \alpha_4\_ \beta_2\_ \alpha_4\_ \alpha_4$  receptors was four times slower than that estimated for  $\beta_2\_ \alpha_4\_ \beta_2^{L146C}\_ \alpha_4\_ \alpha_4$  (**Fig. 3.4, Table 3.2**), suggesting that  $\beta_2$  is less accessible when incorporated in ABS 1. This pattern of accessibility was also observed when the rates of reaction were measured in the presence of ACh (protected rate of reaction assays).

The co-application with agonists should slow the rate of MTSET reaction with substituted cysteines, if the co-applied agonists compete with MTSET for access to the substituted cysteine. As shown in **Table 3.2**, the rates of MTSET reaction slowed down when ACh was co-applied with ACh. As for the rates of reaction in the absence of ACh, the rate of reaction was fastest in  $\beta_2\_ \alpha_4\_ \beta_2\_ \alpha_4^{T152C}\_ \alpha_4$  receptors than in the L146C-labelled receptors and, the rate of reaction of  $\beta_2\_ \alpha_4\_ \beta_2^{L146C}\_ \alpha_4\_ \alpha_4$  was fastest than that of  $\beta_2^{L146C}\_ \alpha_4\_ \beta_2\_ \alpha_4\_ \alpha_4$  receptors (**Fig. 3.4, Table 3.2**).

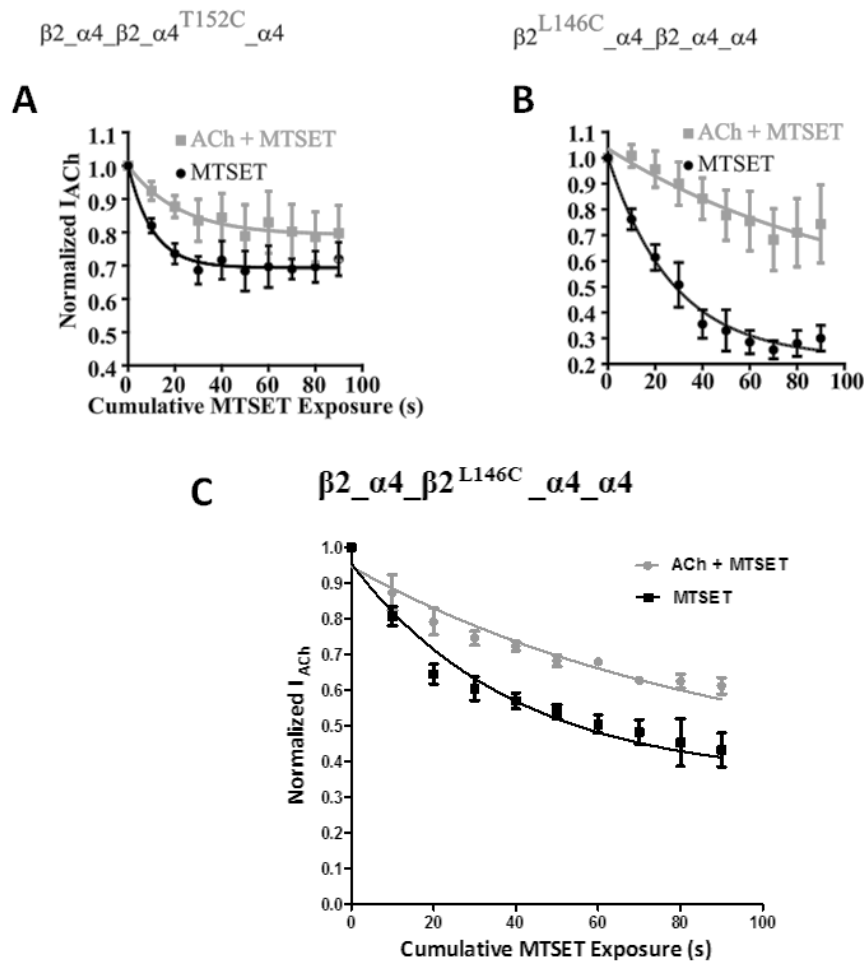


**Figure 3.4. Rates of covalent modification of cysteine substituted concatenated ( $\alpha_4\beta_2$ ) $_2\alpha_4$  nAChRs.** **A)** Normalised ACh currents in the absence and presence of agonist on  $\beta_2\_ \alpha_4\_ \beta_2\_ \alpha_4^{T152C}\_ \alpha_4$  (Mazzaferro *et al.*, 2014) **B)**  $\beta_2^{L146C}\_ \alpha_4\_ \beta_2\_ \alpha_4\_ \alpha_4$  (Mazzaferro *et al.*, 2014) and **C)**  $\beta_2\_ \alpha_4\_ \beta_2^{L146C}\_ \alpha_4\_ \alpha_4$  receptors. Agonist (ACh) used in the protection assays were applied during the stabilisation of the responses to ACh to correct for any process of desensitisation that may have occurred during the assay. In the protection assay the protectant (ACh) was co-applied with MTSET. Data points were normalised to ACh currents at time 0 and are the mean  $\pm$  SEM of at least 4 experiments.

**Table 3.2. Rates of MTSET-covalent modification of cysteine substituted concatenated ( $\alpha 4\beta 2$ ) $_2\alpha 4$  nAChRs.** The protectant used was ACh and the protection assays were carried out as described in Materials and Methods. Significant differences to wild type were determined using one way ANOVA tests; \* correspond to  $p < 0.05$ .  $n \geq 5$

Receptor	Control rate $k_2 \times 10^{-3} \text{M}$ ( $\text{M}^{-1} \text{s}^{-1}$ )	Protection Assay $k_2 \times 10^{-3} \text{M}$ ( $\text{M}^{-1} \text{s}^{-1}$ )
$\beta 2_{\alpha 4} \beta 2_{\alpha 4} \text{T}152\text{C}_{\alpha 4}$	100 $\pm$ 15 *	21 $\pm$ 7.5 *
$\beta 2^{\text{L}146\text{C}}_{\alpha 4} \beta 2_{\alpha 4} \alpha 4$	6.4 $\pm$ 0.9 *	1.4 $\pm$ 0.5 *
$\beta 2_{\alpha 4} \beta 2^{\text{L}146\text{C}}_{\alpha 4} \alpha 4$	25 $\pm$ 4.3 *	10.85 $\pm$ 1.7 *

### 3.2.4 Do $\beta 2(+)/\alpha 4(-)$ interfaces contain elements of intersubunit communication?

Taken together, the data indicate that structurally equivalent agonist sites in ( $\alpha 4\beta 2$ ) $_2\alpha 4$  function asymmetrically. ABSs in the ( $\alpha 4\beta 2$ ) $_2\alpha 4$  differ in terms of the subunit flanking them: ABS 1 is flanked on its right by the (+) side of a  $\beta 2$  subunit and on its left by the (-) side of the fifth  $\alpha 4$  subunit (**Fig. 3.1**). In contrast, ABS 2 is flanked on both sites by the (-) side of  $\alpha 4$  subunits (**Fig. 3.1**). The different flanking environments may affect the function of the individual sites; for example, it may affect the conformation of residues in the agonist binding pocket, which would affect agonist binding and/or the binding-coupling gating pathway. If flanking subunits are critical for the asymmetrical function of ABSs, there must be intersubunit interactions through which the flanking subunits communicate with ABSs. To test this possibility, residues in the ABS flanking subunit interfaces were replaced by alanine and the effects of these replacements on ACh sensitivity were assayed using two-electrode voltage clamping procedures, as described in Materials and Methods.

Visual examination of a homology model of the ( $\alpha 4\beta 2$ ) $_2\alpha 4$  suggested conserved agonist binding residues W176 and Y120 in  $\beta 2(+)$  and W88 and T152 in  $\alpha 4(-)$  as residues that could interact (**Fig 3.5, A**).  $\beta 2\text{W}176$  and  $\beta 2\text{Y}120$  are equivalent to  $\alpha 4\text{W}182$  and  $\alpha 4\text{Y}126$ , both of which bind agonists across the nAChR family (Albuquerque *et al.*, 2009).  $\alpha 4\text{W}88$  is

equivalent to  $\beta 2 W 8 2$ , which is also a conserved agonist binding residue in nAChRs.  $\alpha 4 T 1 5 2$  is equivalent to  $\beta 2 L 1 4 6$ , an E loop residue that forms the hydrophobic top of  $\alpha (+) / \beta (-)$  agonist sites. W176, Y120 and T152 are structurally close and their side chains extend towards the space separating the interfacing subunits (**Fig. 3.5**). Alanine substitutions were introduced into the concatamers to engineer:  $^{W 1 7 6 A} \beta 2 \_ \alpha 4 \_ \beta 2 \_ \alpha 4 \_ \alpha 4$ ,  $^{Y 1 2 0 A} \beta 2 \_ \alpha 4 \_ \beta 2 \_ \alpha 4 \_ \alpha 4$ ,  $\beta 2 \_ \alpha 4 \_ ^{W 1 7 6 A} \beta 2 \_ \alpha 4 \_ \alpha 4$ ,  $\beta 2 \_ \alpha 4 \_ ^{Y 1 2 0 A} \beta 2 \_ \alpha 4 \_ \alpha 4$ ,  $\beta 2 \_ \alpha 4 \_ \beta 2 \_ \alpha 4 \_ \alpha 4 ^{W 8 8 A}$ ,  $\beta 2 \_ \alpha 4 ^{W 8 8 A} \_ \beta 2 \_ \alpha 4 \_ \alpha 4$ ,  $\beta 2 \_ \alpha 4 ^{T 1 5 2 A} \_ \beta 2 \_ \alpha 4 \_ \alpha 4$  and  $\beta 2 \_ \alpha 4 \_ \beta 2 \_ \alpha 4 \_ \alpha 4 ^{T 1 5 2 A}$ . As shown in **Table 3.3**, all of these mutations altered the ACh sensitivity of the  $\beta 2 \_ \alpha 4 \_ \beta 2 \_ \alpha 4 \_ \alpha 4$  receptor with the exception of the  $\beta 2 \_ \alpha 4 \_ \beta 2 \_ \alpha 4 \_ \alpha 4 ^{W 8 8 A}$ . Interestingly, Y120, W176 and T152A abolished the high-sensitivity component of the wild type ACh CRC, with no significant changes in the low-sensitivity biphasic component of the ACh CRC, regardless of which position they occupied the concatamers (**Fig 3.5, Table 3.3**). In contrast,  $\alpha 4 W 8 8 A$  abolished the high sensitivity component when positioned in  $\beta 2 (+) / \alpha 4 (-) - 2$  only. Overall, these findings suggest that conserved residues in  $\beta 2 (+) / \alpha 4 (-)$  interfaces impact agonist effects even though they are not part of an agonist binding interface. These residues appear to impact only the high-sensitivity component of the ACh CRC. Since the high-affinity component of the ACh CRC of  $(\alpha 4 \beta 2)_2 \alpha 4$  nACRs reflects binding to agonist sites on the  $\alpha 4 (+) / \beta 2 (-)$  interfaces (ABSs) (Harpsoe *et al.*, 2011; Indurthi *et al.*, 2016; Mazzaferro *et al.*, 2017), the findings suggest that  $\beta (+) / \alpha 4 (-)$  may contain elements of pathways modulating the function of agonist sites on  $\alpha 4 (+) / \beta 2 (-)$  interfaces.

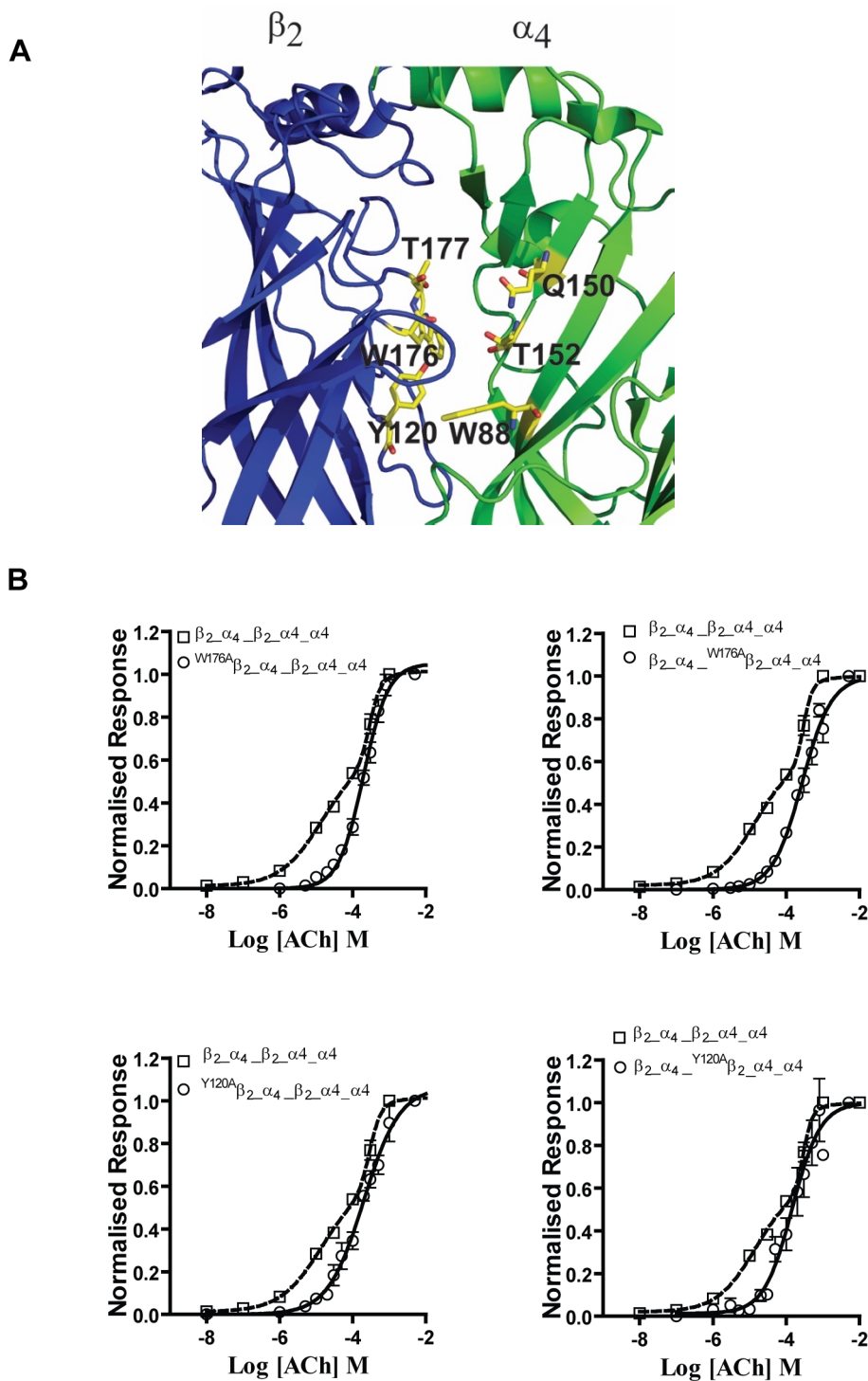


**Figure 3.5. Effect on the ACh sensitivity on concatenated ( $\alpha_4\beta_2$ ) $_2\alpha_4$  nAChRs. A)**  $\beta_2(+)/\alpha_4(-)$  interface showing conserved amino acids. Images were generated using Pymol from the X-ray structure of the ( $\alpha_4\beta_2$ ) $_2\beta_2$  nAChR. PDB ID 5kxi. (Morales-Pérez *et al.*, 2016) **B)** ACh concentrations response curves of singles alanine substitution of conserved aromatic residues at the  $\beta_2(+)/\alpha_4(-)$  interfaces of the  $\beta_2_{\alpha_4}_{\beta_2_{\alpha_4}_{\alpha_4}}$  receptor. The best fit was determined by F-tests; the simpler one-component model was preferred unless the extra sum-of-squares F test had a value of  $p < 0.05$ .

**Table 3.3. Relative potency and efficacy of ACh on concatenated ( $\alpha 4\beta 2$ ) $_2\alpha 4$  nAChRs.** Recordings were performed under two-electrode voltage clamp. EC<sub>50</sub> values are in  $\mu$ M and they represent the mean  $\pm$  SEM of at least five independent experiments. CRCs were fitted to monophasic and biphasic Hill equations, as described in the Materials and Methods Chapter. The best fit was determined by F-tests; the simpler one-component model was preferred unless the extra sum-of-squares F test had a value of p less than 0.05, noted by +. Statistical differences were determined by ANOVA. Significant differences, compared to control were considered as significant if p < 0.05 (noted by \*).

Receptor	EC <sub>50</sub> $\pm$ SEM $\mu$ M
$\beta 2_{\alpha 4}\beta 2_{\alpha 4}_{\alpha 4}$	15 $\pm$ 3 294 $\pm$ 105 +
<sup>W176A</sup> $\beta 2_{\alpha 4}\beta 2_{\alpha 4}_{\alpha 4}$	213 $\pm$ 78*
$\beta 2_{\alpha 4}_{\sup{W176A}}\beta 2_{\alpha 4}_{\alpha 4}$	257 $\pm$ 53*
<sup>Y120A</sup> $\beta 2_{\alpha 4}\beta 2_{\alpha 4}_{\alpha 4}$	207 $\pm$ 86*
$\beta 2_{\alpha 4}_{\sup{Y120A}}\beta 2_{\alpha 4}_{\alpha 4}$	118 $\pm$ 99*
$\beta 2_{\alpha 4}\beta 2_{\alpha 4}_{\alpha 4}\sup{W88A}$	5 $\pm$ 2 533 $\pm$ 12 +
$\beta 2_{\alpha 4}\sup{W82A}\beta 2_{\alpha 4}_{\alpha 4}$	236 $\pm$ 58*
$\beta 2_{\alpha 4}\sup{T152A}\beta 2_{\alpha 4}_{\alpha 4}$	185 $\pm$ 34*
$\beta 2_{\alpha 4}\beta 2_{\alpha 4}_{\alpha 4}\sup{T152A}$	81 $\pm$ 15*
$\beta 2_{\alpha 4}\beta 2_{\alpha 4}_{\alpha 4}\sup{K186A}$	292 $\pm$ 0.04*
$\beta 2_{\alpha 4}\beta 2_{\alpha 4}_{\alpha 4}\sup{E92A}$	120.7 $\pm$ 0.03*
$\beta 2_{\alpha 4}\beta 2_{\alpha 4}_{\alpha 4}\sup{K188A}$	216.7 $\pm$ 0.04*
$\beta 2_{\alpha 4}\beta 2_{\alpha 4}_{\alpha 4}\sup{D190A}$	99.9 $\pm$ 0.09*
$\beta 2_{\alpha 4}\beta 2_{\alpha 4}_{\alpha 4}\sup{D60A}$	105.5 $\pm$ 0.05*
$\beta 2_{\alpha 4}\beta 2_{\alpha 4}_{\alpha 4}\sup{R65A}$	267.3 $\pm$ 0.02*

### 3.2.5 Zn<sup>2+</sup> potentiating pathway

Because occupation of the agonist site on  $\alpha 4(+)/\alpha 4(-)$  appears to allosterically modify the duration mean open times (Mazzaferro *et al.*, 2017). To explore this possibility, the homology model of the  $(\alpha 4\beta 2)_2\alpha 4$  receptor was further examined for residues that could be part of a pathway connecting the  $\alpha 4(+)/\alpha 4(-)$  interface to  $\beta 2(+)/\alpha 4(-)$  interfaces, focusing on residues that could link the (+) side of  $\alpha 4(+)/\alpha 4(-)$  to  $\beta 2(+)/\alpha 4(-)$ -1. In addition to the residues already tested, this approach revealed a number of non-consecutive residues that could interact through salt bridges or electrostatic interactions to link the (+) side of  $\alpha 4(+)/\alpha 4(-)$  to  $\beta 2(+)/\alpha 4(-)$ -1. Starting from loop C in the fifth subunit, the residues are as follows.  $\alpha 4E228$ ,  $\alpha 4K186$ ,  $\alpha 4K188$ ,  $\alpha 4D190$ ,  $\alpha 4R65$  and  $\alpha 4D60$ . (**Fig. 3.6**). The residues are close enough to engage in interactions such as hydrogen bonding (2.5 Å), salt bridges (5 Å), and  $\pi$ -cation (6.6 Å). As shown in **Table 3.3**, alanine replacements of  $\alpha 4E228$ ,  $\alpha 4K186$ ,  $\alpha 4K188$ ,  $\alpha 4D190$ ,  $\alpha 4R65$  and  $\alpha 4D60$  eliminated the high-affinity component of the ACh CRC without significant changes on the low sensitivity component. These findings support the view that the residues mutated may contribute to linking ABS 3 to ABS 1. To examine this possibility, the effects of the alanine replacements on potentiation of ACh responses by Zn<sup>2+</sup> were assayed. The  $(\alpha 4\beta 2)_2\alpha 4$  nAChR is allosterically potentiated by Zn<sup>2+</sup> through a Zn<sup>2+</sup> binding site located in  $\alpha 4(+)/\alpha 4(-)$ , and a key Zn<sup>2+</sup>-chelating residue in this site is E224 on loop C of the (+) side of the fifth subunit (Moroni *et al.*, 2008). Conceivably, if the putative pathway linking ABS 1 to  $\alpha 4(+)/\alpha 4(-)$  is operational, alanine replacements of the prospective pathway residues should affect Zn<sup>2+</sup> potentiation of the receptors.

As shown in **Fig. 3.7** (data summarised in **Table 3.4**), alanine replacement of E228, K186, K188, D190, R65 and D60 in the fifth subunit decreased significantly the efficacy of Zn<sup>2+</sup> potentiation. The extent of Zn<sup>2+</sup> potentiation varied from about 70% to almost elimination (E92, K186, K188). None of the mutations modified the potency of Zn<sup>2+</sup> potentiation (**Table 3.4**), showing that none of the residues are part of a potentiating Zn<sup>2+</sup> binding site. Interestingly, Zn<sup>2+</sup> potentiation was reduced in mutants <sup>W176A</sup> $\beta 2\_ \alpha 4\_ \beta 2\_ \alpha 4\_ \alpha 4$  and  $\beta 2\_ \alpha 4\_ \beta 2\_ \alpha 4\_ \alpha 4^{\text{W88A}}$  ( $p < 0.05$ ) but not in  $\beta 2\_ \alpha 4\_ ^{\text{W176A}}\beta 2\_ \alpha 4\_ \alpha 4$  or  $\beta 2\_ \alpha 4^{\text{W88A}}\_ \beta 2\_ \alpha 4\_ \alpha 4$  receptor (**Table 3.4**), suggesting that these residues impact Zn<sup>2+</sup> potentiation only when present in interface  $\beta 2(+)/\alpha 4(-)$ -2. Y120A affected Zn<sup>2+</sup> potentiation in both  $\beta 2(+)/\alpha 4(-)$  interfaces ( $p < 0.05$ ).



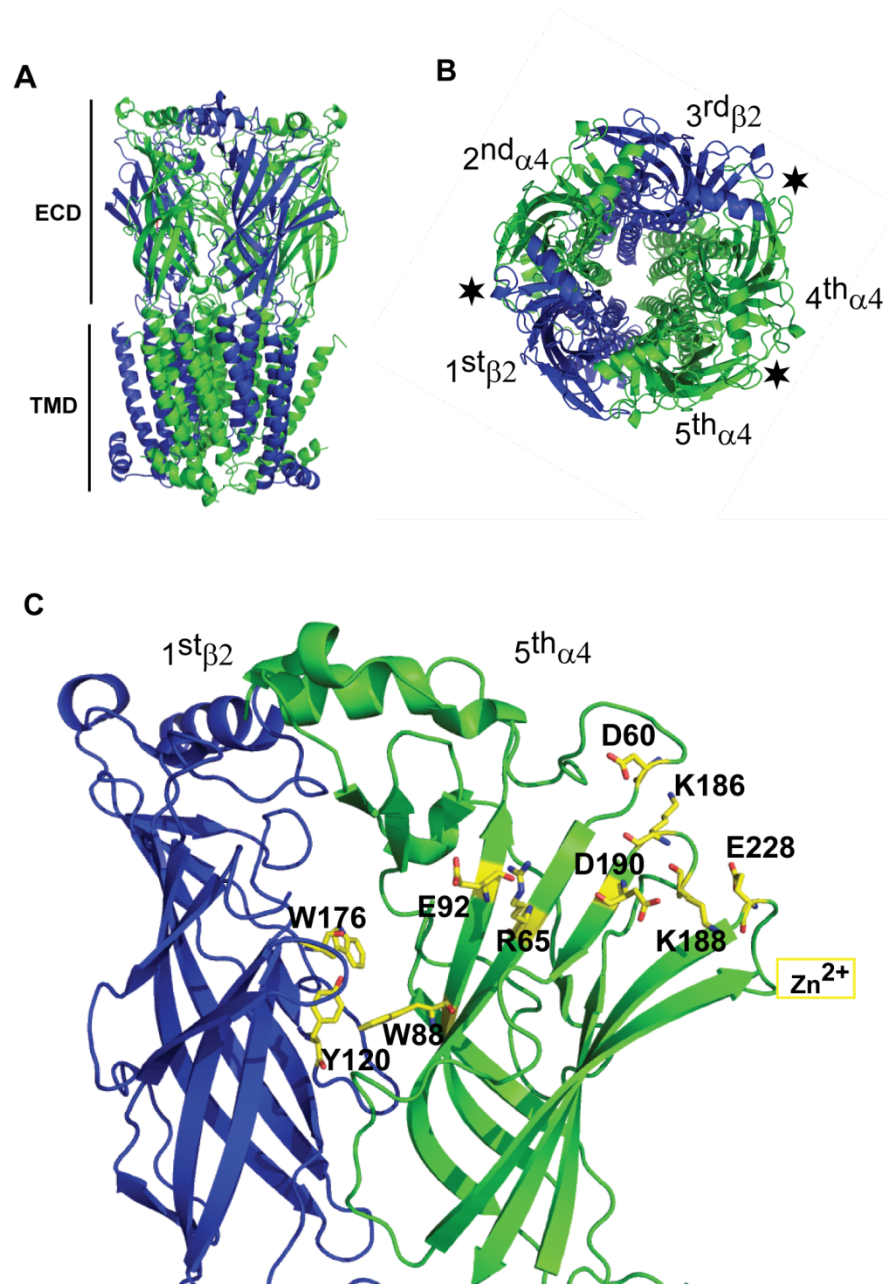


**Figure 3.6. Zn<sup>2+</sup> pathway in (α4β2)<sub>2</sub>α<sub>4</sub> nAChR.** A) Whole assembly, lateral side view, showing the ECD and TMD domains of the receptor B) Top view of the (α4β2)<sub>2</sub>α<sub>4</sub>, as viewed from the extracellular side. Subunits are numbered according to their position in the linear sequence of the concatenated constructs. Binding sites are represented by asterisks. C) Representation of Zn<sup>2+</sup> pathway in (α4β2)<sub>2</sub>α<sub>4</sub> nAChR. Images were generated using Pymol from the X-ray structure of the (α4β2)<sub>2</sub>β<sub>2</sub> nAChR. PDB ID 5kxi. (Morales- Pérez *et al.*, 2016).

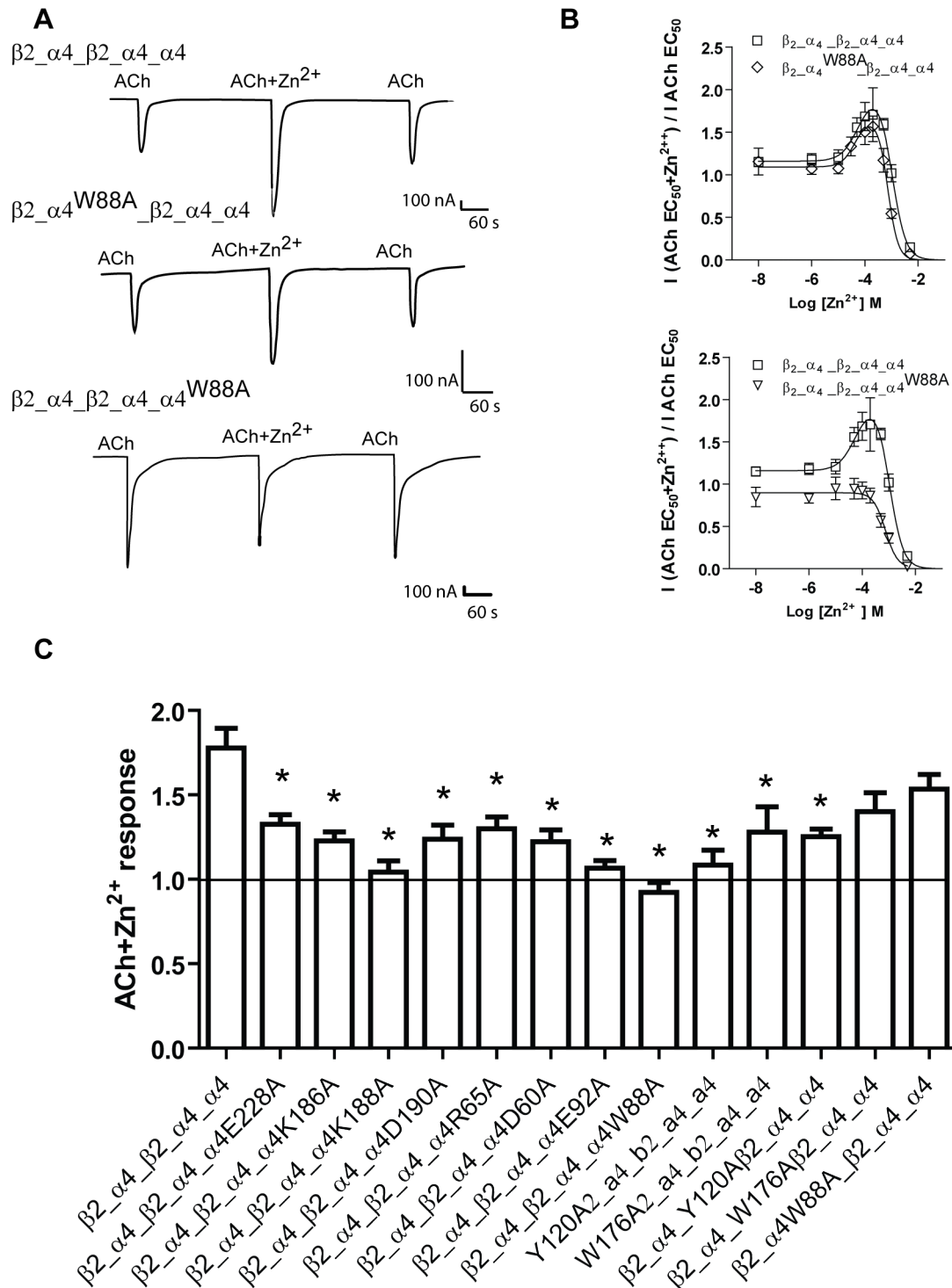


**Figure 3.7. Maximal potentiation of Zn<sup>2+</sup>.** **A)** Representative traces of the responses elicited by ACh and coplication of ACh+Zn<sup>2+</sup> at  $\beta_2\_alpha4\_beta2\_alpha4\_alpha4$ ,  $\beta_2\_alpha4^{W88A}\_beta2\_alpha4\_alpha4$  and  $\beta_2\_alpha4\_beta2\_alpha4\_alpha4^{W88A}$  concatenated receptors expressed heterologously in *Xenopus* oocytes. **B)** Concentration response curve representing the potentiation of Zn<sup>2+</sup> at  $\beta_2\_alpha4\_beta2\_alpha4\_alpha4$ ,  $\beta_2\_alpha4^{W88A}\_beta2\_alpha4\_alpha4$  and  $\beta_2\_alpha4\_beta2\_alpha4\_alpha4^{W88A}$  concatenated receptors. The data were fit to a bell Hill equation to take into account potentiation and inhibition, as mentioned in Chapter 2. **C)** Maximal potentiation of Zn<sup>2+</sup>. The mutations introduced in that  $\beta_2/\alpha_4$ -1 interface had a profound effect on Zn<sup>2+</sup> potentiation. The mutations in the interface  $\beta_2/\alpha_4$ -2 had little impact on Zn<sup>2+</sup> potentiation. ANOVA tests (\*,  $p < 0.05$ ).

**Table 3.4. Zn<sup>2+</sup> potentiation of ACh responses of concatenated (α4β2)<sub>2</sub>α4 receptors.** ACh EC<sub>50</sub> responses were recorded in the presence or absence of Zn<sup>2+</sup>, as described in Chapter 2. Maximal potentiation by Zn<sup>2+</sup> (I(ACh+Zn<sup>2+</sup>)/I<sub>ACh</sub>) and Zn<sup>2+</sup> EC<sub>50</sub> values were estimated from Zn<sup>2+</sup> CRC data. Statistical differences to control were estimated by ANOVA and values were considered significant if p < 0.05 (\*). ND, not determined because potentiation was too low for reliable measurements. Data points represent the mean ±SEM from at least 10 independent experiments.

Receptor	Zn <sup>2+</sup> EC <sub>50</sub> ±SEM μM	I(ACh+Zn <sup>2+</sup> )/I <sub>ACh</sub>
β2_α4_β2_α4_α4	59 ± 12	1.78 ± 0.7
<sup>W176A</sup> β2_α4_β2_α4_α4	110 ± 58	1.41 ± 0.1*
β2_α4_ <sup>W176A</sup> β2_α4_α4	59.2 ± 7.9	1.58 ± 0.9
<sup>Y120A</sup> β2_α4_β2_α4_α4	ND	1.15 ± 0.4*
β2_α4_ <sup>Y120A</sup> β2_α4_α4	21.7 ± 7	1.25 ± 0.4*
β2_α4_β2_α4_α4 <sup>E228A</sup>	29 ± 12	1.33 ± 0.5*
β2_α4_β2_α4_α4 <sup>K186A</sup>	57.5 ± 13	1.23 ± 0.4*
β2_α4_β2_α4_α4 <sup>E92A</sup>	ND	1.06 ± 0.4*
β2_α4_β2_α4_α4 <sup>K188A</sup>	ND	1.043 ± 0.3*
β2_α4_β2_α4_α4 <sup>D190A</sup>	34 ± 10	1.24 ± 0.4*
β2_α4_β2_α4_α4 <sup>D60A</sup>	52 ± 9	1.22 ± 0.3*
β2_α4_β2_α4_α4 <sup>R65A</sup>	64 ± 18	1.40 ± 0.2*
β2_α4_β2_α4_α4 <sup>W88A</sup>	ND	1.08 ± 0.1
β2_α4 <sup>W88A</sup> _β2_α4_α4	33 ± 11	1.53 ± 0.3*

### 3.3 Discussion

Previous work of  $(\alpha 4\beta 2)_2\alpha 4$  nAChR that used mutagenesis and/or SCAM approaches established that the  $\alpha 4(+)/\alpha 4(-)$  interface of this receptor type houses an additional agonist site that is structurally and functionally different from the agonist sites on  $\alpha 4(+)/\beta 2(-)$  interfaces (Harpsoe *et al.*, 2011; Mazzaferro *et al.*, 2011, 2014; Lucero *et al.*, 2016). The present results, based on agonist-elicited macroscopic responses of mutant receptors, establish that the canonical agonist binding sites in the  $(\alpha 4\beta 2)_2\alpha 4$  nAChR function asymmetrically. Functionally asymmetry in structurally equivalent agonist sites have been reported for the GABA<sub>A</sub>  $\alpha 1\beta 2\gamma 2s$  (Baumann *et al.*, 2003) and the  $(\alpha 4\beta 2)_2\beta 2$  nAChR receptors (New *et al.*, 2017). Functional asymmetry likely stems from the different subunits flanking the canonical sites. Differences in flanking subunits appear to produce intersubunit communications that regulate function in an agonist binding site dependent manner. The overall results of this study provide evidence for interdependent subunit contributions to receptor function and pharmacology.

While residues in the (+) side of the agonist site are conserved, residues on the (-) side differ markedly between ABS1-2 and ABS 3 and play a critical role in defining the pharmacology of the receptor (Harpsoe *et al.*, 2011; Mazzaferro *et al.*, 2014).  $\alpha 4$  is more hydrophilic due to residues H142, Q150 and T152 in the (-) side compared to  $\beta 2$ , which contains hydrophobic V136, F144 and L146 in its (-) side (Harpsoe *et al.*, 2011; Mazzaferro *et al.*, 2014). The importance of the complementary side for the pharmacology of agonist sites has been studied extensively in the muscle nAChR; the complementary face of the agonist sites in muscle nAChRs also differs (i.e.,  $\alpha 1\delta$  versus  $\alpha 1\gamma/\epsilon$ ) and this produces distinct pharmacological phenotypes in the sites (for a review, see Arias, 1998)).

Agonist sites on  $\alpha 4(+)/\beta 2(-)$  receptors are structurally equivalent, yet this study shows that they function non-equivalently. Thus, cysteine substituted ABSs were modified by MTSET in the presence or absence of agonist, at different rates. Since the rate of substituted cysteines and MTS reagents is determined by how accessible the substituted cysteine is to the thiol reagent (Karlin and Akabas, 1998), it seems reasonable to surmise that the accessibility of L146 in the agonist binding sites varies. This may be due to differences in the physico-chemical environments around the agonist binding residues or residues that contribute indirectly to agonist binding. Subunit interfaces flanking the complementary side of the

agonist sites may induce ABS-selective structural re-arrangements in the ABSs resulting in physico-chemical changes. Intersubunit interactions transmitted along downstream pathways to L146 or around L146 could change the accessibility of this residue. Support for such a scenario comes from studies of the GABA<sub>A</sub> receptor that have shown agonist-induced (Eaton *et al.*, 2012) and benzodiazepine-induced changes (Sancar and Czajkowski, 2011) in the rate of MTS modification of residues in the complementary side ( $\alpha 1$ ) of GABA agonist sites, suggesting that occupation of the agonist or benzodiazepine sites induces structural movements in the  $\alpha 1/\gamma$  interface. More recently, New *et al.* (2017) showed that the  $\beta 2(+)/\beta 2(-)$  interface modulates the agonist responses of the receptor through asymmetric intersubunit modulatory pathways. Thus, although the fifth subunit is quite distant from ABS ( $< 80\text{\AA}$ ) and separated from them by intersubunit spaces, long-range intramolecular communication is possible.

ABSs also appeared to differ in how they bind agonists, as judged by the effects of ABS-alanine replacements on agonist responses. It is possible that as for the accessibility of residues to MTS, the orientation of the side chains of the residues contributing to the agonist site differ, which could lead to differences in agonist binding and hence agonist effects. Consistent with this view, it has been reported that the binding of the agonist Cys on  $\alpha 4/\beta 2$  interfaces differ (Rucktooa *et al.*, 2012).

The fifth subunit (an  $\alpha 4$ ) of the  $(\alpha 4\beta 2)_2\alpha 4$  nAChR is necessary and sufficient to define the relative sensitivity of this receptor type (Harpsoe *et al.*, 2011; Mazzaferro *et al.*, 2011; 2014; Timmermann *et al.*, 2012; Lucero *et al.*, 2016). The fifth subunit contributes independently to these differences, eg., the presence of residues on the complementary side of the agonist site can block entrance to agonists of a certain size (Mazzaferro *et al.*, 2014) or the presence of a potentiating  $\text{Zn}^{2+}$  site on the fifth subunit (Moroni *et al.*, 2008). In addition, as suggested by this study, the fifth subunit also appears to determine receptor function by modulating the activity of adjacent canonical agonist sites. The effect is asymmetrical, as judged by the asymmetrical function of the canonical agonist sites (this study) and by the distribution of the duration of the open channel times of  $(\alpha 4\beta 2)_2\alpha 4$  receptors.  $(\alpha 4\beta 2)_2\alpha 4$  receptors that are activated through canonical agonist sites exhibit openings with long mean duration, whereas receptor full activation exhibit relatively brief openings (Mazzaferro *et al.*, 2017). Thus, the agonist site on  $\alpha 4(+)/\alpha 4(-)$  appears to exert an allosteric effect on the canonical ABSs, either

by reducing their affinity for ACh or through the reduction of the ability of the channel to open in response to occupancy by agonist.

The modulatory effects of the fifth subunit could be driven by local conformational changes brought about by agonist occupation of  $\alpha 4(+)/\alpha 4(-)$ ; the conformational changes could be transmitted to the  $\alpha 4(+)/\beta 2(-)$  interfaces through specific intra- and inter-subunit pathways. One possible pathway is revealed through  $Zn^{2+}$  potentiation studies.  $Zn^{2+}$  enhances the ACh responses of the  $(\alpha 4\beta 2)_2\alpha 4$  receptor through a binding site located in loop C of the principal face of the  $\alpha 4(+)/\alpha 4(-)$  interface (Moroni *et al.*, 2008). Individual mutation of residues starting from loop C downward to  $\beta 2(+)/\alpha 4(-)$ -2 reduced potentiation by  $Zn^{2+}$ , suggesting that conformational changes initiated by binding of  $Zn^{2+}$  to its site on  $\alpha 4(+)/\alpha 4(-)$  (**Fig 3.6**) are transmitted across the fifth subunit to adjacent subunits.  $\beta 2W176$  and  $\alpha 4W88$ , on the  $\beta 2(+)/\alpha 4(-)$ -2 interface also affected  $Zn^{2+}$  potentiation, suggesting that the  $Zn^{2+}$  pathway may overlap or is the same downstream pathway modulating ABSs from the  $\alpha 4(+)/\alpha 4(-)$  interface. Communication between agonist sites has not been described so far but binding sites for modulatory compounds have been shown to modulate the responses of adjacent agonist sites through pathways comprising elements of the  $\alpha$  complementary subunit of the agonist sites (Short *et al.*, 2015). Thus, it may be that allosteric binding sites such as that for benzodiazepines in the  $GABA_A$  receptor evolved from interdependent agonist sites interactions.

In summary, the studies presented in this chapter confirm that canonical agonist sites and the agonist site on the  $\alpha 4(+)/\alpha 4(-)$  interface are functionally and structurally different. Significantly, the studies also demonstrate that the canonical sites function non-equivalently, even though they are structurally equivalent. Functional non-equivalency appears to be due to the presence of an  $\alpha 4$  subunit in the fifth position of the receptor. This subunit not only contributes to the signature  $\alpha 4(+)/\alpha 4(-)$  interface of the receptor but also creates different flanking environments for the canonical agonist sites, which are the structural basis underlying the differential function of the ABS site.

## **Chapter 4**

**The  $\beta 2(+)/\beta 2(-)$  subunit interface of  $(\alpha 4\beta 2)_2\beta 2$  receptors is a key element of an allosteric system that modulates maximal agonist responses**





## 4.1 Introduction

The fifth subunit in the  $(\alpha 4\beta 2)_2\alpha 4$  nAChR contributes to a third agonist site that both increases ion channel gating and modulates the function of agonist sites on  $\alpha 4(+)/\beta 2(+)$  interfaces (Mazzaferro *et al.*, 2011, 2014, 2017; this study). The previous Chapter identified residues in loop B of the (+) side of  $\beta 2$  and loop E residues on the (-) side of  $\alpha 4$  as residues contributing to intersubunit communication between the  $\alpha 4(+)/\alpha 4(-)$  and  $\alpha 4(+)/\beta 2(-)$  interfaces. Interestingly, one of the residues on  $\alpha 4(-)$ , T152, together with Q150 and H142, has been identified as critical in defining the differences in agonist sensitivity between the  $(\alpha 4\beta 2)_2\beta 2$  and  $(\alpha 4\beta 2)_2\alpha 4$  receptors (Harpsoe *et al.*, 2011; Lucero *et al.*, 2016). Significantly, T152 is equivalent to L146 on the (-) side of  $\beta 2$ , and this residue is part of a system in  $\beta 2(+)/\beta 2(-)$  that modulates the maximal ACh responses of  $(\alpha 4\beta 2)_2\beta 2$  nAChRs (New *et al.*, 2017). In agonist binding sites, E loop residues such as L146 and T152 affect agonist binding selectivity by contributing to create a physico-chemical landscape in the agonist binding pocket that either facilitates or decreases agonist binding (see, for example, Harpsøe *et al.*, 2011; Mazzaferro *et al.*, 2014). In non-agonist binding interfaces such as  $\beta 2(+)/\beta 2(-)$  or  $\beta 2(+)/\alpha 4(-)$  in  $\alpha 4\beta 2$  nAChRs, E loop residues appear to modulate the agonist responses in a stoichiometry-selective manner but through pathways that link to loop B on the complementary subunit of agonist sites on  $\alpha 4(+)/\beta 2(-)$  (New *et al.*, 2017; Chapter 3 of this study). Interestingly, whilst in the  $(\alpha 4\beta 2)_2\alpha 4$  receptor, residues in loops A and B of  $\beta 2(+)/\alpha 4(-)$  affect ACh potency, equivalent residues in  $\beta 2(+)/\beta 2(-)$  affect maximal agonist responses with no changes in agonist potency (Harpsoe *et al.*, 2011). Although macroscopic maximal currents results from a combination of channel gating, desensitisation and ion channel blockade, it is tempting to suggest that the effects of  $\beta 2(+)/\beta 2(-)$  are mediated by coupling to the gating machinery of the receptors.

To address this possibility, potential intersubunit interactions of the fifth subunit with residues on the (+) side of  $\beta 2(+)/\beta 2(-)$  were examined. By examination of the crystal structure of  $(\alpha 4\beta 2)_2\beta 2$  (PDB ID 5kxi), combined with site-specific mutagenesis, and electrophysiological assays, the aminoacid residues W176 and T177 on the (+) side of  $\alpha 4$ , and F144 on the (-) side of  $\beta 2(+)/\beta 2(-)$  were identified as being elements of the system that modulates maximal agonist responses in  $(\alpha 4\beta 2)_2\beta 2$  receptors by introducing cysteines in residues in the (-) side of  $\beta 2(+)/\beta 2(-)$ . By using a modification of the mutant cycle approach, it was established that W176, T177, L146 and F144 selectively couple to L9' in the ion

channel, suggesting that  $\beta 2(+)/\beta 2(-)$  modulates maximal agonist responses by modulating gating.  $\beta 2(+)/\alpha 4(-)$  interfaces, although important for intersubunit communication in  $(\alpha 4\beta 2)_2\alpha 4$  receptors, cannot modulate maximal agonist responses of this receptor type because the E loop of  $\alpha 4$  lacks the hydrophobicity of  $\beta 2$ . These findings add further weight to the growing body of evidence that suggest E loop residues play a critical role in receptor dynamics.

## 4.2 Results

### 4.2.1 Identification of residues in $\beta 2(+)/\beta 2(-)$ that may modulate agonist responses in $(\alpha 4\beta 2)_2\beta 2$ nAChRs

SCAM studies carried out by New and collaborators (2017) showed that L146 in loop E of the complementary side of the  $\beta 2(+)/\beta 2(-)$  interface of the  $(\alpha 4\beta 2)_2\beta 2$  nAChR functionally links to ABS 1 to modulate the maximal responses to ACh. To achieve the long-range type of communication that these effects suggest, intersubunit residues must be involved in functionally linking ABS 1 to  $\beta 2(+)/\beta 2(-)$ . To identify prospective residues that could link L146 on the (-) side of  $\beta 2(+)/\beta 2(-)$  to ABS 1, the recently published crystal structure of the  $(\alpha 4\beta 2)_2\beta 2$  nAChR (PDB ID 5kxi) (Morales-Pérez *et al.*, 2016) was visually examined for residues on the (+) side of  $\beta 2(+)/\beta 2(-)$  that could interact with L146, focusing particularly on residues that could establish hydrophobic interactions with hydrophobic L146. On this basis, two residues were identified: As mentioned in Chapter 3,  $\beta 2$ W176 on the (-) side of  $\beta 2$  is equivalent to  $\alpha 4$ W182 on loop B in the (+) side of  $\alpha 4$  (**Fig. 4.1A, B**), the tryptophan residue that plays a critical role stabilising the quaternary ammonium moiety of ACh throughout the nAChR family (Zhong *et al.*, 1998; Celie *et al.*, 2004; Xiu *et al.*, 2009; Morales-Pérez *et al.*, 2016). T177 is also an invariant residue in the nAChR receptor family (**Fig. 4.1 A, B**); it has been suggested that it helps to restrict mobility of the tryptophan residue in muscle nAChR agonist sites to promote efficient binding between ACh and the agonist site (Lee and Sine, 2004).

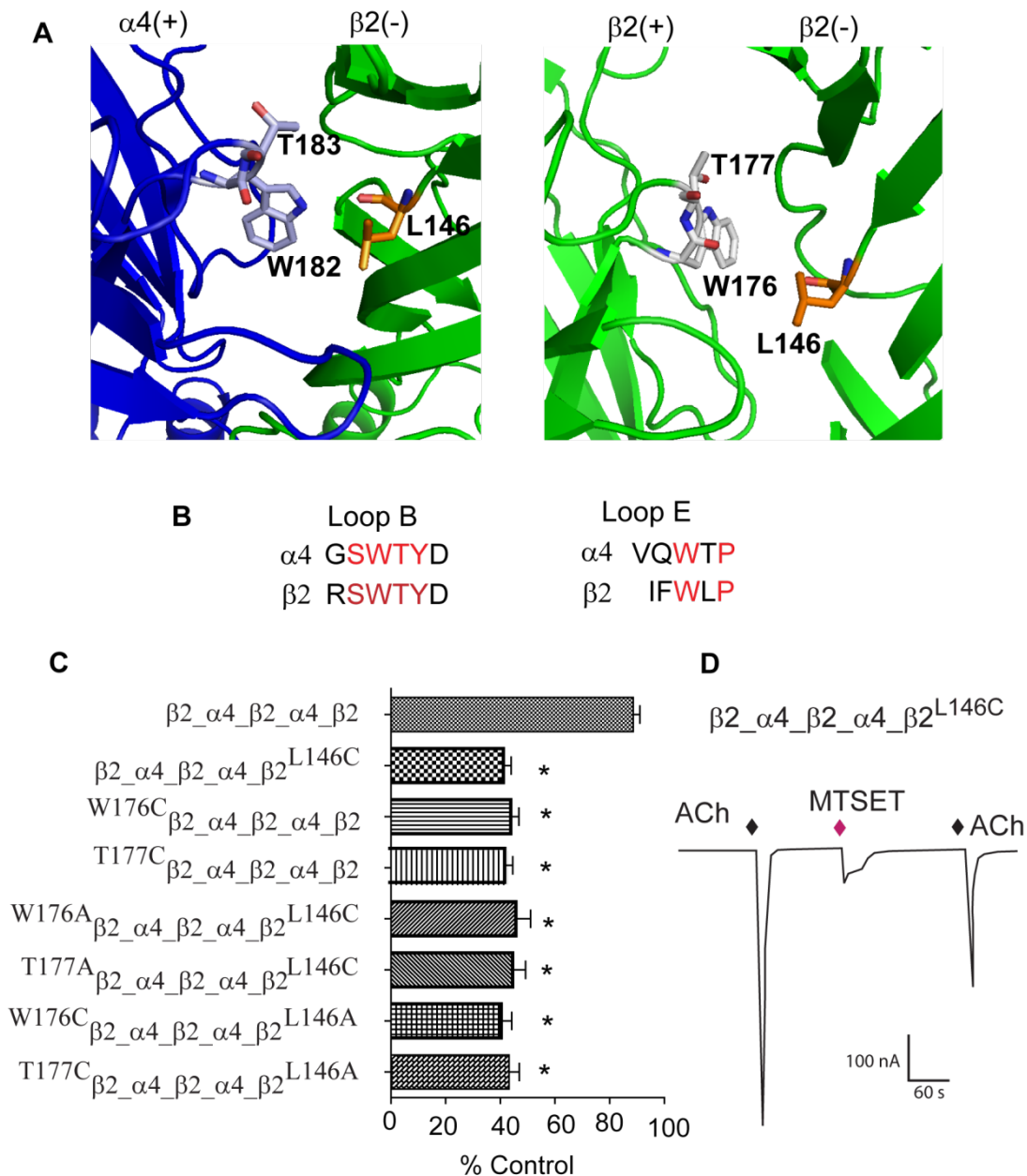


**Figure 4.1. Effects of maximal MTSET in wild type and cysteine substituted concatenated ( $\alpha 4\beta 2$ ) $_2\beta 2$  nAChRs.** **A)** Structure of the  $\alpha 4(+)/\beta 2(-)$  (left panel) and  $\beta 2(+)/\beta 2(-)$  (right panel) showing the position of W182, T183 and L146 in interface  $\alpha 4(+)/\beta 2(-)$  (right panel) and W175, T177 and L146 in  $\beta 2(+)/\beta 2(-)$  (right panel). **B)** Alignment showing conservation of B loop and E loop in  $\alpha 4$  and  $\beta 2$  subunits. **C)** Effects of maximal MTSET on ACh EC<sub>80</sub> responses in wild type and cysteine substituted concatenated ( $\alpha 4\beta 2$ ) $_2\beta 2$  nAChRs. 1 mM MTSET decreased significantly the responses to ACh EC<sub>80</sub> in all mutant receptors. The amplitude of the currents remaining after MTSET were calculated using the equation [(I<sub>after MTSET</sub>/ I<sub>initial</sub>)-1] x 100], as described in Chapter 2. Significant differences between the mutant receptors and control ( $\beta 2_{\alpha 4} \beta 2_{\alpha 4} \beta 2$ ) are shown by asterisk and were determined with one-way ANOVA (p<0.05) with Dunnett's post-test. The data shown represent n = 8 for each type of receptor tested. Data are summarised in **Table 4.3**. **D)** Representative traces of the responses elicited by maximal ACh before and after MTSET at  $\beta 2_{\alpha 4} \beta 2_{\alpha 4} \beta 2^{L146C}$  concatenated receptors expressed heterologously in *Xenopus* oocytes.

**Table 4.1. Concentration effects of ACh and TC2559 on concatenated ( $\alpha 4\beta 2$ )<sub>2</sub> $\beta 2$  nAChRs.** The concentration effects of ACh or TC2559 on oocytes expressing heterologously wild type or mutant concatenated ( $\alpha 4\beta 2$ )<sub>2</sub> $\beta 2$  nAChRs were determined using two-electrode voltage-clamp, as described in Chapter 2. The data points were used to generate concentration response curves from which EC<sub>50</sub> and maximal responses were estimated. EC<sub>50</sub> values represent the mean plus 95% confidence interval of n= 6-8 independent experiments. All other values represent the mean  $\pm$  SEM of n= 6-8 independent experiments. Statistical differences between wild type and mutant concatenated receptors were determined by one-way ANOVA with Dunnett's correction. Asterisks denote statistical difference; p < 0.05.

Receptor	ACh EC <sub>50</sub> $\pm$ SEM ( $\mu$ M)	TC2559 EC <sub>50</sub> $\pm$ SEM ( $\mu$ M)	TC2559 Relative Maximal Response $\pm$ SEM
$\beta 2_{\alpha 4}_{\beta 2}_{\alpha 4}_{\beta 2}$	6.59 (3.8-9.4)	4.0 (1.4-6.6)	4.03 $\pm$ 0.10
$\beta 2_{\alpha 4}_{\beta 2}_{\alpha 4}_{\beta 2}^{L146A}$	5.36 (3.01-7.71)	2.53 (2.19-2.81)	2.1 $\pm$ 0.03***
$\beta 2^{L146A}_{\alpha 4}_{\beta 2}_{\alpha 4}_{\beta 2}$	7.34 (5.19-9.49)	7.99* (6.15-9.83)	2.73 $\pm$ 0.21 ***
$\beta 2_{\alpha 4}_{\beta 2}^{L146A}_{\alpha 4}_{\beta 2}$	8.18 (3.06-13.3)	7.07* (6.11-8.03)	3.57 $\pm$ 0.18*
$\beta 2_{\alpha 4}_{\beta 2}_{\alpha 4}_{\beta 2}^{L146C}$	7.03 (5.16-8.89)	4.37 (2.69-6.04)	2.38 $\pm$ 0.09***
<sup>W176A</sup> $\beta 2_{\alpha 4}_{\beta 2}_{\alpha 4}_{\beta 2}^{L146C}$	6.31 (4.70-7.90)	3.90 (2.24-5.54)	2.60 $\pm$ 0.16***
<sup>T177A</sup> $\beta 2_{\alpha 4}_{\beta 2}_{\alpha 4}_{\beta 2}^{L146C}$	6.59 (5.49-7.82)	4.51 (2.98-6.04)	2.59 $\pm$ 0.063***
<sup>W176C</sup> $\beta 2_{\alpha 4}_{\beta 2}_{\alpha 4}_{\beta 2}$	6.98 (5.75-8.20)	4.16 (2.77-5.55)	2.68 $\pm$ 0.9***
<sup>T177C</sup> $\beta 2_{\alpha 4}_{\beta 2}_{\alpha 4}_{\beta 2}$	5.28 (2.95-7.61)	4.31 (2.64-5.97)	2.70 $\pm$ 0.10***
<sup>W176C</sup> $\beta 2_{\alpha 4}_{\beta 2}_{\alpha 4}_{\beta 2}^{L146A}$	6.24 (5.32-7.16)	4.92 (3.43-6.60)	2.45 $\pm$ 0.11***
<sup>T177C</sup> $\beta 2_{\alpha 4}_{\beta 2}_{\alpha 4}_{\beta 2}^{L146A}$	5.41 (4.4-6.4)	4.96 (3.84-6.08)	2.42 $\pm$ 0.12***
$\beta 2_{\alpha 4}_{\beta 2}^{W182A}_{\alpha 4}_{\beta 2}$	2.89** (0.19-5.58)	8.46*** (6.61-10.30)	2.28 $\pm$ 0.09***
	71.69*** (32-112)		
$\beta 2_{\alpha 4}_{\beta 2}^{W182A}_{\alpha 4}_{\beta 2}$	15*** (11.7-18.3)	10.53*** (5.36-15.7)	2.48 $\pm$ 0.16***
<sup>W176C</sup> $\beta 2_{\alpha 4}_{\beta 2}^{W182A}_{\alpha 4}_{\beta 2}$	38.26*** (15.06-61.43)	18.23*** (4-33)	2.10 $\pm$ 0.19

<sup>W176C</sup> $\beta_2$ _ $\alpha_4$ _ $\beta_2$ _ <sup>W182A</sup> $\alpha_4$ _ $\beta_2$	19.63*** (14.02-25.24)	12.10*** (5.28-18.92)	2.42±0.6
$\beta_2$ _ $\alpha_4$ _ $\beta_2$ _ $\alpha_4$ <sup>T152A</sup> _ $\beta_2$	5.76 (4.54-6.99)	4.59 (2.69-6.49)	4.28 ± 0.38
$\beta_2$ _ $\alpha_4$ <sup>T152A</sup> _ $\beta_2$ _ $\alpha_4$ _ $\beta_2$	6.51 (4.58-8.43)	5.32 (3.54-7.10)	3.92 ± 0.14
$\beta_2$ _ $\alpha_4$ _ $\beta_2$ _ $\alpha_4$ _ $\beta_2$ <sup>F144A</sup>	6.67 (5.48-7.65)	3.68 (2.8-4.8)	2.59±0.12***
$\beta_2$ _ $\alpha_4$ _ $\beta_2$ _ $\alpha_4$ <sup>Q150A</sup> _ $\beta_2$	6.23 (4.54-8.01)	4.72 (2.29-7.14)	4.05± 0.17
$\beta_2$ _ $\alpha_4$ <sup>Q150A</sup> _ $\beta_2$ _ $\alpha_4$ _ $\beta_2$	6.97 (4.83-9.11)	5.04 (2.46-7.55)	4.27± 0.15
$\beta_2$ _ $\alpha_4$ <sup>H142A</sup> _ $\beta_2$ _ $\alpha_4$ _ $\beta_2$	6.21 (5.03-7.38)	4.65 (2.48-6.81)	4.05±0.19
$\beta_2$ _ $\alpha_4$ _ $\beta_2$ _ <sup>H142A</sup> $\alpha_4$ _ $\beta_2$	6.62 (5.54-7.69)	5.16 (1.47-8.8.6)	3.7±0.17
<sup>W176A</sup> $\beta_2$ _ $\alpha_4$ _ $\beta_2$ _ $\alpha_4$ _ $\beta_2$	7.10 (3.0-11.20)	3.97 (2.55-5.38)	2.63±0.092***
$\beta_2$ _ $\alpha_4$ _ <sup>W176A</sup> $\beta_2$ _ $\alpha_4$ _ $\beta_2$	5.91 (3.96-7.85)	4.74 (2.61-6.87)	4.02±0.27
$\beta_2$ _ $\alpha_4$ _ $\beta_2$ _ $\alpha_4$ _ <sup>W176A</sup> $\beta_2$	6.82 (5.74-7.89)	5.18 (3.05-7.32)	3.95±0.16
<sup>T177A</sup> $\beta_2$ _ $\alpha_4$ _ $\beta_2$ _ $\alpha_4$ _ $\beta_2$	5.34 (1.52-9.74)	4.24 (-0.76-11.81)	2.64±0.22***
$\beta_2$ _ $\alpha_4$ _ <sup>T177A</sup> $\beta_2$ _ $\alpha_4$ _ $\beta_2$	4.99 (3.70-6.29)	4.17 (2.29-6.74)	4.14±0.75
$\beta_2$ _ $\alpha_4$ _ $\beta_2$ _ $\alpha_4$ _ <sup>T177A</sup> $\beta_2$	5.52 (3.97-7.05)	5.18 (2.17-8.19)	4.33±0.41
<sup>Y178A</sup> $\beta_2$ _ $\alpha_4$ _ $\beta_2$ _ $\alpha_4$ _ $\beta_2$	5.51 (3.14-7.87)	3.03 (1.78-4.50)	4.06±0.54
$\beta_2$ _ $\alpha_4$ _ $\beta_2$ _ $\alpha_4$ _ $\beta_2$ <sup>N135A</sup>	5.76 (2.79-8.73)	6.54 (2.93-10.16)	4.65±0.58
$\beta_2$ _ $\alpha_4$ _ $\beta_2$ _ $\alpha_4$ _ $\beta_2$ <sup>S134A</sup>	2.96 (2.28-3.64)	8.41 (3.17-13.64)	4.62±0.0.55
$\beta_2$ _ $\alpha_4$ _ $\beta_2$ _ $\alpha_4$ _ $\beta_2$ <sup>V137A</sup>	5.76 (2.79-8.73)	4.88 (1.39-8.39)	3.87±0.10

To assess the significance of the prospective modulatory residues for functionally coupling to L146, the residues W176 and T177 were individually replaced by alanine and then introduced in the (+) side of the first subunit of mutant receptor  $\beta_2\_ \alpha_4\_ \beta_2^{L146C}$  to establish whether the presence of the loop B mutants in  $\beta_2(+)/\beta_2(-)$  altered the rate of reaction between the thiol reagent MTSET and L146C. If L146, W176 and T177 are part of an allosteric ensemble that modulates the function of agonist-bound ABS 1, W176A or T177A should alter the accessibility of L146C to MTSET, which would change the rate of MTSET reaction in the presence and/or absence of agonist. As shown in **Table 4.1**, the ACh sensitivity of the single or double mutant receptors was comparable to wild type, indicating that none of the mutations, individually or simultaneously, altered the overall function of the concatenated  $(\alpha_4\beta_2)_2\beta_2$  receptor. W176A and T177A were accessible to MTSET, as judged by the significant reduction in the amplitude of the ACh responses following exposure to saturating MTSET (**Fig. 4.1C; Table 4.2**). In comparison to  $\beta_2\_ \alpha_4\_ \beta_2^{L146C}$ , the reduction was slightly greater for  $^{W176A}\beta_2\_ \alpha_4\_ \beta_2^{L146C}$  and  $^{T177A}\beta_2\_ \alpha_4\_ \beta_2^{L146C}$ , indicating that replacements of these residues by alanine affect the local physico-chemical environment around L146. To examine further whether W176A and T177A reduce accessibility of L146C to MTSET, the rates of MTSET reaction with the double substituted receptors were measured in the presence or absence of ACh. If W176 and T177 are part of the system that links ABS 1 and  $\beta_2(+)/\beta_2(-)$ , the rate of reaction between MTSET and L146C in the presence of ACh should be significantly slower than the control  $\beta_2\_ \alpha_4\_ \beta_2^{L146C}$ . As shown in **Fig. 4.2** (kinetic parameters shown in **Table 4.3**), the rate of modification of L146C by MTSET in  $^{W176A}\beta_2\_ \alpha_4\_ \beta_2^{L146C}$  or  $^{T177A}\beta_2\_ \alpha_4\_ \beta_2^{L146C}$  was slower, compared to control  $\beta_2\_ \alpha_4\_ \beta_2^{L146C}$ . Importantly, in the presence of ACh, MTSET was no longer able to modify L146C accessibility, unlike the equivalent reaction for control  $\beta_2\_ \alpha_4\_ \beta_2^{L146C}$  (**Fig. 4.2, Table 4.3**).

**Table 4.2. Effects of MTSET on the ACh responses of wild type and cysteine substituted concatenated ( $\alpha 4\beta 2$ ) $_2\beta 2$  nAChRs.** Wild type and cysteine substituted concatenated ( $\alpha 4\beta 2$ ) $_2\beta 2$  nAChRs were exposed to a saturating concentration of MTSET (1 mM) after the responses to 1mM ACh were stabilised (less than 5% differences in the amplitude of the responses of ACh applied every 5 min). The percentage of remaining activation by 1 mM ACh after MTSET treatment was defined as ( $I_{\text{afterMTSET}}/I_{\text{initial}}$ ) x 100. Data are the mean  $\pm$  SEM of 8 experiments. Significant differences between mutant and wild type receptors ( $p < 0.05$ ) (noted by \*) were estimated using One-way ANOVA with Dunnett's post-test.

Receptor	EC <sub>50</sub> ( $\mu$ M)	nHill	Remaining I <sub>ACh</sub> After MTSET (%)
$\beta 2_{\alpha 4}_{\beta 2_{\alpha 4}_{\beta 2}}$	6.53 $\pm$ 1.3	1	89 $\pm$ 10
$\beta 2_{\alpha 4}_{\beta 2_{\alpha 4}_{\beta 2}^{L146C}}$	3.68 $\pm$ 0.76	0.93 $\pm$ 0.12	42 $\pm$ 3*
<sup>W176C</sup> $\beta 2_{\alpha 4}_{\beta 2_{\alpha 4}_{\beta 2}}$	6.8 $\pm$ 0.43	1.18 $\pm$ 0.06	43 $\pm$ 3*
<sup>T177C</sup> $\beta 2_{\alpha 4}_{\beta 2_{\alpha 4}_{\beta 2}}$	4.87 $\pm$ 0.9	1.1 $\pm$ 0.09	45 $\pm$ 4*
<sup>W176A</sup> $\beta 2_{\alpha 4}_{\beta 2_{\alpha 4}_{\beta 2}^{L146C}}$	5.48 $\pm$ 0.71	0.78 $\pm$ 0.04	57 $\pm$ 4*
<sup>T177A</sup> $\beta 2_{\alpha 4}_{\beta 2_{\alpha 4}_{\beta 2}^{L146C}}$	6.53 $\pm$ 0.5	1.01 $\pm$ 0.1	55 $\pm$ 2*
<sup>W176C</sup> $\beta 2_{\alpha 4}_{\beta 2_{\alpha 4}_{\beta 2}^{L146A}}$	6.43 $\pm$ 1.3	0.98 $\pm$ 0.1	56 $\pm$ 4*
<sup>T177C</sup> $\beta 2_{\alpha 4}_{\beta 2_{\alpha 4}_{\beta 2}^{L146A}}$	7.2 $\pm$ 2.1	1.1 $\pm$ 0.2	52 $\pm$ 5*

**Table 4.3. Second order rate constants for MTSET-modification of residues within the  $\beta 2(+)/\beta 2(-)$  interface of concatenated ( $\alpha 4\beta 2$ ) $_2\beta 2$  nAChRs.** Second order rate constants ( $k_2$ ) represent the mean  $\pm$  SEM of  $n = 5$  independent experiments. The rate of reactions was determined in resting (minus ACh) or in the presence of ACh. For each mutant, the significance level applies to comparison between the resting (-ACh) and (+ACh). The significance levels were estimated using unpaired Student's t tests. \*, denotes significance at  $p < 0.05$ .

Receptor	$k_2$ - ACh ( $M^{-1}s^{-1}$ )	$k_2$ + ACh ( $M^{-1}s^{-1}$ )
$\beta 2_{\alpha 4}_{\beta 2_{\alpha 4}_{\beta 2}^{L146C}}$	2082 $\pm$ 250	613 $\pm$ 102*
<sup>W176A</sup> $\beta 2_{\alpha 4}_{\beta 2_{\alpha 4}_{\beta 2}^{L146C}}$	1666 $\pm$ 302	1123 $\pm$ 129
<sup>W176C</sup> $\beta 2_{\alpha 4}_{\beta 2_{\alpha 4}_{\beta 2}}$	2118 $\pm$ 146	450 $\pm$ 128*
<sup>W176C</sup> $\beta 2_{\alpha 4}_{\beta 2_{\alpha 4}_{\beta 2}^{L146A}}$	1123 $\pm$ 350	1034 $\pm$ 205
<sup>W176C</sup> $\beta 2_{\alpha 4}_{\beta 2_{\alpha 4}_{\beta 2}^{W182A}}$	389 $\pm$ 105	354 $\pm$ 101
<sup>W176C</sup> $\beta 2_{\alpha 4}_{\beta 2_{\alpha 4}_{\beta 2}^{W182A}}$	2200 $\pm$ 160	499 $\pm$ 97*
<sup>W176C</sup> $\beta 2_{\alpha 4}_{\beta 2_{\alpha 4}_{\beta 2}^{W182A}}$	2110 $\pm$ 303	593 $\pm$ 117*
<sup>T177A</sup> $\beta 2_{\alpha 4}_{\beta 2_{\alpha 4}_{\beta 2}^{L146C}}$	1078 $\pm$ 156	988 $\pm$ 130
<sup>T177C</sup> $\beta 2_{\alpha 4}_{\beta 2_{\alpha 4}_{\beta 2}}$	1995 $\pm$ 350	453 $\pm$ 187*
<sup>T177C</sup> $\beta 2_{\alpha 4}_{\beta 2_{\alpha 4}_{\beta 2}^{L146A}}$	1248 $\pm$ 187	1081 $\pm$ 200



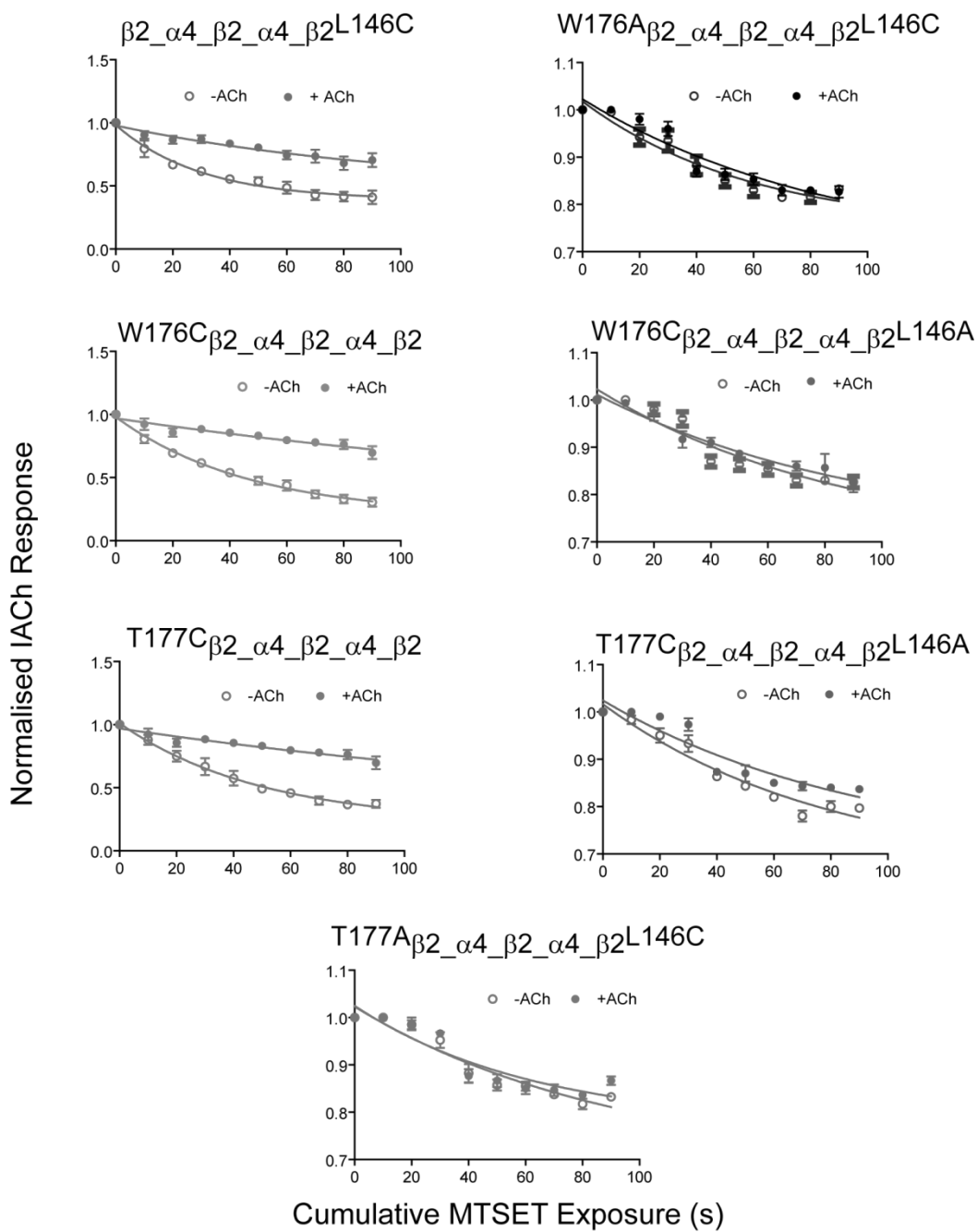


**Figure 4.2. Effect of ACh on the rate of MTSET modification of substituted concatenated  $(\alpha 4\beta 2)_2\beta 2$  nAChRs.** Prior to the rate reactions, the ACh responses were stabilised. Rates were measured in the absence or presence of ACh. Data were normalised and fit to a single phase exponential decay, as described in Chapter 2. Second order rate constants for MTSET modification of L146C are summarised in **Table 4.4**.

Thus far, the findings show that accessibility of L146C to MTSET in  $\beta 2(+)/\beta 2(-)$  is significantly impaired by alanine replacement of W176 or T177 on the (+) side of  $\beta 2(+)/\beta 2(-)$ . This suggests that these residues are elements of a system capable of modulating the maximal agonist responses of  $(\alpha 4\beta 2)_2\beta 2$  through long-range coupling to ABS 1. Demonstrating that impairment of ABS 1 disrupts the reaction of MTSET with W176C or T177C would strengthen the conclusion that these residues may be part, together with L146, of an allosteric pathway functionally linking  $\beta 2(+)/\beta 2(-)$  to ABS 1. To test this possibility, the rate of MTSET reaction with  $^{W176C}\beta 2_{-}^{W182A}\alpha 4_{-}\beta 2_{-}\alpha 4_{-}\beta 2$  was measured in the absence or presence of ACh. Introducing W182A in ABS 1 impairs the ability of ABS 1 to bind ACh, leading to a severe decrease in ACh  $EC_{50}$  and maximal responses (New *et al.*, 2017). Thus, if ABS 1 is functionally coupled to this residue, detrimental structural changes in ABS 1 should affect the accessibility of the cysteine substituted residues to MTSET. Introduction of W182A individually into ABS 1 of the agonist sites of wild type or  $^{W176C}\beta 2_{-}\alpha 4_{-}\beta 2_{-}\alpha 4_{-}\beta 2$  drastically reduced the potency of ACh (**Table 4.1**), in accord with the central role of W182 in agonist binding (Xiu *et al.*, 2009) and with previously published data (New *et al.*, 2017). As shown in **Figure 4.3 (A)**, the rate of reaction of  $^{W176C}\beta 2_{-}^{W182A}\alpha 4_{-}\beta 2_{-}\alpha 4_{-}\beta 2$  was significantly slowed down, compared to control ( $^{W176C}\beta 2_{-}\alpha 4_{-}\beta 2_{-}\alpha 4_{-}\beta 2$ ). Furthermore, in the presence of ACh, the rate of MTSET reaction did not change (**Fig. 4.3**), suggesting that impairment of ABS 1 ablates the effect of agonist-bound ABS 1 on the accessibility to W176C to MTSET. This effect is selective because MTSET reactions with  $^{W176C}\beta 2_{-}\alpha 4_{-}\beta 2_{-}^{W182A}\alpha 4_{-}\beta 2$  did not abolish the effect of ACh on the rate of MTSET reaction (**Fig 4.3 B**). Similar findings were reported by New and collaborators (2017) for the reaction of MTSET with  $\beta 2_{-}^{W182A}\alpha 4_{-}\beta 2_{-}\alpha 4_{-}\beta 2^{L146C}$  or  $\beta 2_{-}\alpha 4_{-}\beta 2_{-}^{W182A}\alpha 4_{-}\beta 2^{L146C}$ , supporting the view of the present study that loop B and loop E residues in  $\beta 2(+)/\beta 2(-)$  are functionally linked to ABS 1.

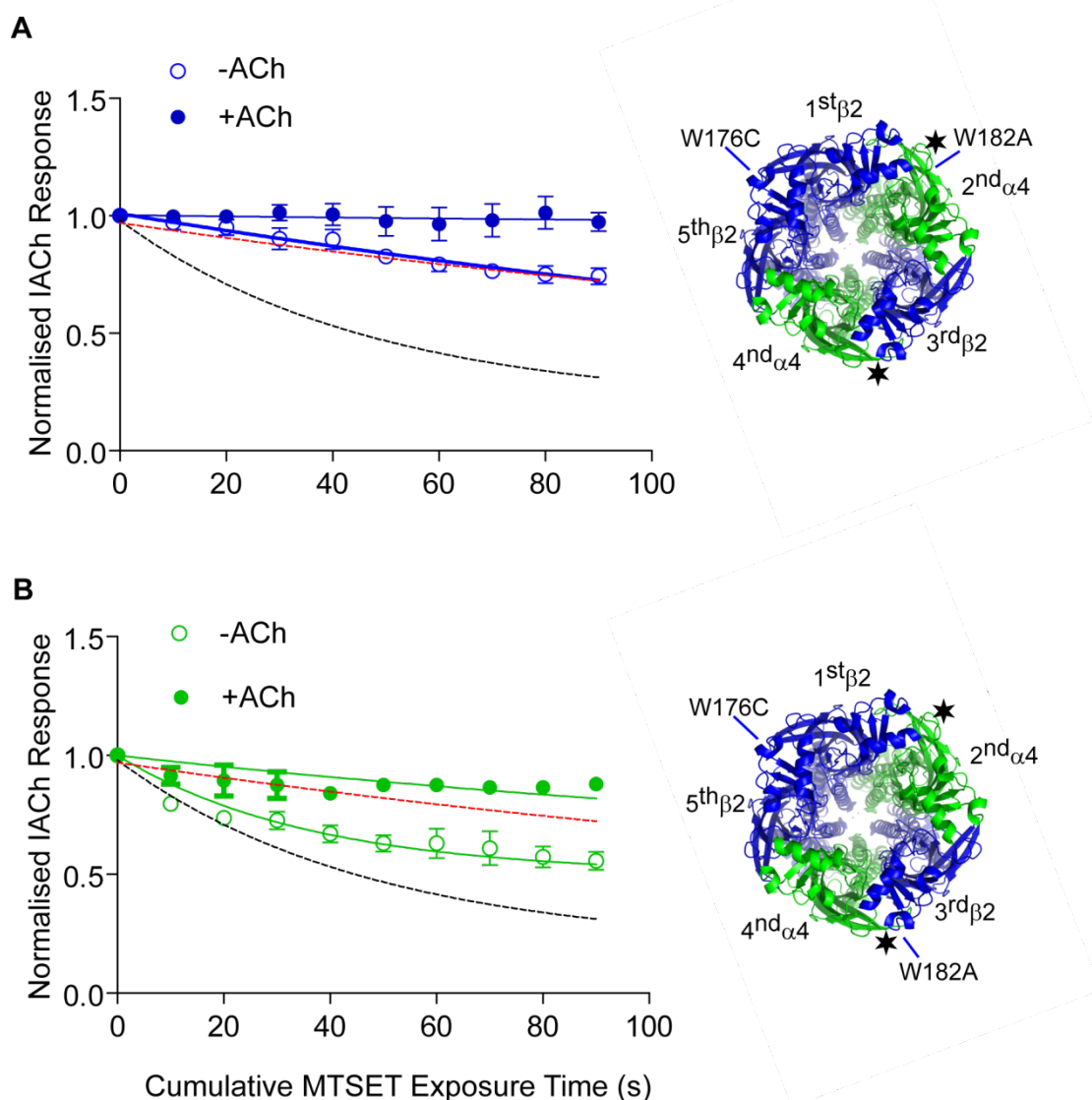


**Figure 4.3 Effect of impaired agonist binding sites on the rates of MTSET reaction with  $^{W176C}\beta2_{\alpha4}\beta2_{\alpha4}\beta2$ .** The rate of MTSET modification of  $^{W176C}\beta2_{\alpha4}\beta2_{\alpha4}\beta2$  in the absence or presence of ACh was altered when the W182A mutation was incorporated in the  $\alpha4(+)/\beta2(-)$  agonist sites to form  $^{W176C}\beta2_{W182A}\alpha4_{\beta2}\alpha4_{\beta2}$ . **A)** or  $^{W176C}\beta2_{\alpha4}\beta2_{W182A}\alpha4_{\beta2}$  **B)** receptors. Data fit to a single phase exponential decay, as described in Chapter 2. Second order rate constants are shown in **Table 4.4**. The cartoons in the right side show the mutated agonist site (W182A) in relation to W176C. The dotted lines show the rate of MTSET reactions with  $^{W176C}\beta2_{\alpha4}\beta2_{\alpha4}\beta2$  in the presence and absence of ACh.

## 4.2.2 The allosteric unit in $\beta 2(+)/\beta 2(-)$ is coupled to gating

The observation that mutant receptors  $\beta 2\_ \alpha 4\_ \beta 2\_ \alpha 4\_ \beta 2^{L146C}, W176C\beta 2\_ \alpha 4\_ \beta 2$  and  $T177C\beta 2\_ \alpha 4\_ \beta 2\_ \alpha 4\_ \beta 2$  did not affect ACh potency but decreased maximal ACh responses following modification by MTSET suggested these residues may modulate gating. Since the channel is approximately 50Å away from W176, T177 or L146 in  $\beta 2(+)/\beta 2(-)$ , the relationship between these residues and the channel gate would constitute long-range coupling, as it is for residues in agonist binding sites and the ion channel in all pLGICs. Macroscopic maximal agonist responses are composites of gating, agonist-induced channel blockade and desensitisation (Colquhoun, 1998); however, Dennis Dougherty and his team developed a simple strategy, derived from mutant cycle analysis, for identifying gating pathway residues using macroscopic measurements alone the elucidating long-range functional coupling of allosteric receptors (ELFCAR) (Gleitsman *et al.*, 2009; Shanata *et al.*, 2012). Based on this strategy, potential coupling between the ion channel and the residues of  $\beta 2(+)/\beta 2(-)$  established to affect ACh maximal responses was tested by determining ACh  $EC_{50}$  in concatemers containing the L9'T reporter mutation in the ion channel of the first  $\beta 2$  subunit of  $\beta 2\_ \alpha 4\_ \beta 2\_ \alpha 4\_ \beta 2$  in the absence or presence of L146A, W176A or T177A. As mentioned in Chapter 1, L9' (in the TM2 numbering of Miller, 1989), is the 9<sup>th</sup> residue downstream from the proximal end of TM2 (**Fig. 1.5 B**). L9' is highly conserved in the nAChR family, it lies approximately in the middle of the sequence of the ion channel (M2) (**Fig. 1.5 B, Fig 4.4 A**). L9' likely provides a gate to the channel, which would be kept closed by the hydrophobic interaction between the L9' residues of all receptor subunits in the receptor ensemble (Unwin, 1993, 2005, 2012). The effect of swapping L9' with a more hydrophilic amino acid such as threonine is consistent across the nAChR family, leading to an increase in agonist efficacy and a corresponding decrease in the  $EC_{50}$  in the mutated receptor (Revah *et al.*, 1991; Labarca *et al.*, 1995; Filatov and White, 1995; Moroni *et al.*, 2006). Thus, if L9'T is co-introduced with a residue that only increases binding affinity and, therefore, the  $EC_{50}$  will be shifted multiplicative to the left because the two residues act independently. In contrast, if the residues are functionally coupled, the simultaneous mutations will lead to a multiplicative effect, producing a coupling factor ( $\Omega$ ) that deviates significantly from 1. Long-range coupling between two residues is considered to occur when  $\Omega$  is higher than 2 (Gleitsman *et al.*, 2009).

To validate this approach, long-range coupling between the L9'T in the channel and Y126A in ABS 1 was examined (**Fig. 4.4 A**). Y126 is a loop A (+ side of  $\alpha 4$ ) residue that contributes

to both agonist binding and gating in nAChRs (Akk *et al.*, 2001). As shown in **Table 4.4**, Y126A decreased ACh potency, compared to wild type, whilst L9'T increased potency, leading to a coupling factor ( $\Omega$ ) equal to 3 (**Fig. 4.4 B**). Thus, when Y126A in ABS 1 and L9'T are in tandem, the gating pathway is disrupted. This finding is consistent with the role of Y126 in agonist binding and gating (Akk *et al.*, 2001), thus validating the ELFCAR approach to examine coupling of the  $\beta 2(+)/\beta 2(-)$  allosteric unit to gating. **Table 4.4** summarises the  $EC_{50}$  values estimated by single and double mutant concatemers. L9'T produced a leftward shift in the ACh response curve compared to wild type. This shift was reversed in a nonmultiplicative manner when W176A, T177A or L146A in  $\beta 2(+)/\beta 2(-)$  and L9'T were in tandem, producing  $\Omega$  values higher than 2.

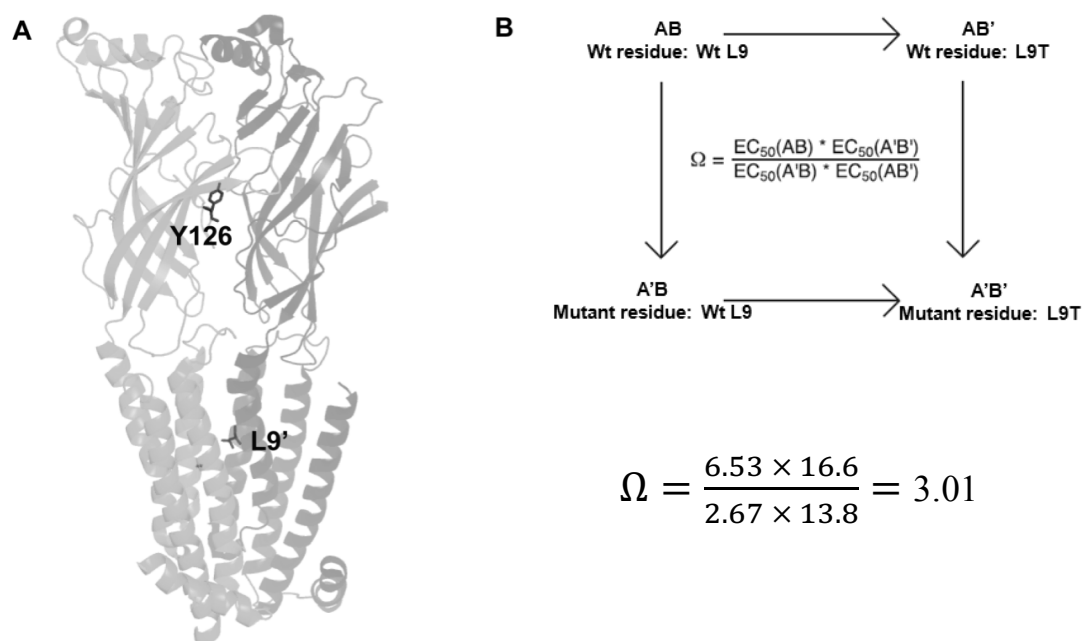


**Figure 4.4 The elucidating long-range functional coupling of allosteric receptors (ELFCAR).** **A)** Lateral side view, showing the residue Y126 at the ECD and the residue L9' at the TMD domains of the receptor. **B)** Diagram for the ELFCAR analysis. The coupling parameter,  $\Omega$ , is calculated for Y126 residue.

**Table 4.4 ELFCAR analysis of E loop and L9' in concatenated  $(\alpha 4\beta 2)_2\beta 2$  nAChRs.**  $EC_{50}$  for ACh with and without  $\beta 2L'9T$  in the first subunit of  $(\alpha 4\beta 2)_2\beta 2$  receptors were determined as reported in Chapter 2. The coupling parameter ( $\Omega$ ) was calculated as described in Chapter 2. Residues were considered coupled to L9'T if the value of  $\Omega$  was higher than 2 (Gleitsman *et al.*, 2009). Significant coupling is seen because both the  $\beta 2L'9T$  mutation and residues in the ECD of the  $\beta 2(+)/\beta 2(-)$  interface disrupt the gating pathway. Data shown represent the mean  $\pm$  SEM of  $n = 5$  independent experiments. Statistical differences were determined using ANOVA tests (\*,  $p < 0.05$ ).

Target mutation	ACh $EC_{50} - L9'T$ ( $\mu M$ )	ACh $EC_{50} + L9'T$ ( $\mu M$ )	$\Omega$
$\beta 2_{\alpha 4} \beta 2_{\alpha 4} \beta 2$	$6.53 \pm 1.3$	$2.67 \pm 0.06^*$	1
$\beta 2_{\alpha 4} \beta 2_{\alpha 4} \beta 2^{L146A}$	$5.24 \pm 0.12$	$5.78 \pm 0.04$	2.7
$\beta 2_{\alpha 4} \beta 2_{\alpha 4} \beta 2^{F144A}$	$5.45 \pm 0.11$	$8.28 \pm 0.10$	3.7
$^{W176A}\beta 2_{\alpha 4} \beta 2_{\alpha 4} \beta 2$	$5.02 \pm 0.12$	$5.4 \pm 0.11$	2.4
$^{T177A}\beta 2_{\alpha 4} \beta 2_{\alpha 4} \beta 2$	$3.46 \pm 0.23$	$4.2 \pm 1.16$	2.9
$^{Y178A}\beta 2_{\alpha 4} \beta 2_{\alpha 4} \beta 2$	$7.30 \pm 0.13$	$2.78 \pm 0.18$	0.9
$\beta 2_{Y126A} \alpha 4_{\beta 2} \alpha 4_{\beta 2}$	$13.8 \pm 0.10^*$	$16.6 \pm 0.04^*$	3.01

### 4.2.3 F144 from loop E also contributes to the modulatory ensemble in $\beta 2(+)/\beta 2(-)$

To identify other residues that could be part of the modulatory ensemble in  $\beta 2(+)/\beta 2(-)$ , the crystal structure of the  $(\alpha 4\beta 2)_2\beta 2$  receptor was further examined, focusing on residues structurally close to W176, T177 and L146 in  $\beta 2(+)/\beta 2(-)$ . This strategy highlighted residues Y178 in the (+) side of  $\beta 2(+)/\beta 2(-)$  and S134, N135, V137 and F144 in the (-) side of  $\beta 2(+)/\beta 2(-)$  (**Fig. 4.5**). These residues were individually mutated to alanine and then incorporated into the relevant side (- or +) of  $\beta 2(+)/\beta 2(-)$  in concatenated  $\beta 2\_ \alpha 4\_ \beta 2\_ \alpha 4\_ \beta 2$  nAChRs. To assess the significance of the prospective modulatory residues for maximal agonist responses, the functional consequence of the alanine substitutions were determined for the agonist TC2559, compared to ACh. This strategy was chosen to avoid the prolonged recording times that SCAM-based experiments require. Because TC2559 has higher efficacy than the full agonist ACh (Moroni *et al.*, 2006; Zwart *et al.*, 2006; Carbone *et al.*, 2009), changes in the maximal responses of TC2559 brought about by residue replacement should be detected by normalising the responses of TC2559 to  $EC_{100}$  ACh responses. To validate this approach, the maximal responses of concatemers  $T177^A\beta 2\_ \alpha 4\_ \beta 2\_ \alpha 4\_ \beta 2$ ,  $W176^A\beta 2\_ \alpha 4\_ \beta 2\_ \alpha 4\_ \beta 2$  and  $\beta 2\_ \alpha 4\_ \beta 2\_ \alpha 4\_ \beta 2^{L146A}$  to TC2559 were estimated from TC2559 CRCs. As expected, maximal TC2559 responses on these mutant concatemers were significantly reduced by approximately 50% ( $p < 0.05$ , ANOVA) without changes in the potency of TC2559 or ACh (**Fig. 4.5 B; Table 4.1**). Thus, if alanine replacement of the selected residues induces decrease in TC2559 with no changes in  $EC_{50}$ , the residues could be elements of the modulatory ensemble in  $\beta 2(+)/\beta 2(-)$ . As shown in **Table 4.1**, neither S134A, N135A, V137A nor Y178A decreased TC2559 maximal responses. In contrast, F144A reduced maximal TC2559 by approximately 50%, without changes in TC2559  $EC_{50}$ . Critically, ELFCAR analysis of F144A and L9'T produced a  $\Omega$  value of 3.7, strongly supporting long-range coupling between F144A and L9'T (**Table 4.4**). Of relevance, Y178A, which did not affect the potency or the maximal responses of TC2559, was not coupled to L9'T because ELFCAR analysis produced a  $\Omega$  value lower than 2 (**Table 4.4**).

Taken together, the results of the mutagenesis/functional assay studies suggests that interfacing residues W176, T177, L146 and F144 are functionally linked to ABS-1. To test whether these residues are involved in stabilising the interfaces, the crystal structure data for the  $(\alpha 4\beta 2)_2\beta 2$  was examined using the PISA software available from PDBe

([http://www.ebi.ac.uk/msd-srv/prot\\_int/cgi-bin/piserver](http://www.ebi.ac.uk/msd-srv/prot_int/cgi-bin/piserver)). As shown in **Table 4.5**, neither T177, L146 nor F144 are engaged in hydrogen bonding or salt-bridges, but they are solvent accessible and located at the interface. W176 appears to hydrogen bond with R106; however, alanine substitution of R106 had no effect on ACh sensitivity or TC2559 maximal responses (not shown). These suggests that the effects of the substituted alanine residues on the maximal agonist responses were due to a loss of function effect rather than to a general structural change in the receptor.

**Table 4.5. PISA analysis of the crystal structure (PDB ID 5kxi) data for the  $\beta 2/\beta 2$  interface of the  $(\alpha 4\beta 2)_2\beta 2$  isoform.** PISA software available from PDBe ([http://www.ebi.ac.uk/msd-srv/prot\\_int/cgi-bin/piserver](http://www.ebi.ac.uk/msd-srv/prot_int/cgi-bin/piserver)).

#### Hidrophobic interactions between interfacing residues

##		5 <sup>th</sup> $\beta 2$	_Dist. [A]		1 <sup>st</sup> $\beta 2$
1	C:THR	27 [ OG1 ]	3.40	B:THR	51 [ O ]
2	C:THR	27 [ OG1 ]	2.45	B:ALA	50 [ O ]
3	C:THR	27 [ OG1 ]	3.54	B:TYR	91 [ OH ]
4	C:ASP	28 [ N ]	3.76	B:TYR	91 [ OH ]
5	C:GLN	67 [ NE2 ]	3.64	B:ASN	123 [ O ]
6	C:ASN	81 [ ND2 ]	3.64	B:TYR	128 [ OH ]
7	C:ARG	107 [ NE ]	3.83	B:THR	178 [ O ]
8	C:SER	134 [ OG ]	3.83	B:TRP	177 [ O ]
9	C:LEU	236 [ N ]	3.44	B:SER	292 [ OG ]
10	C:PHE	237 [ N ]	3.26	B:SER	292 [ OG ]
11	C:TYR	370 [ OH ]	3.85	B:THR	328 [ O ]
12	C:THR	27 [ O ]	3.63	B:ARG	92 [ NH2 ]
13	C:GLU	31 [ OE2 ]	3.19	B:ARG	92 [ NH1 ]
14	C:GLU	31 [ OE2 ]	3.40	B:ASN	44 [ N ]
15	C:ASN	135 [ OD1 ]	2.97	B:THR	178 [ OG1 ]
16	C:LYS	234 [ O ]	2.48	B:SER	292 [ OG ]
17	C:TYR	258 [ O ]	3.01	B:ASN	321 [ ND2 ]
18	C:GLU	265 [ OE1 ]	3.45	B:THR	268 [ OG1 ]

#### Salt bridges between interfacing residues

##		5 <sup>th</sup> $\beta 2$	_Dist. [A]		1 <sup>st</sup> $\beta 2$
1	C:GLU	31 [ OE1 ]	3.52	B:ARG	92 [ NH1 ]



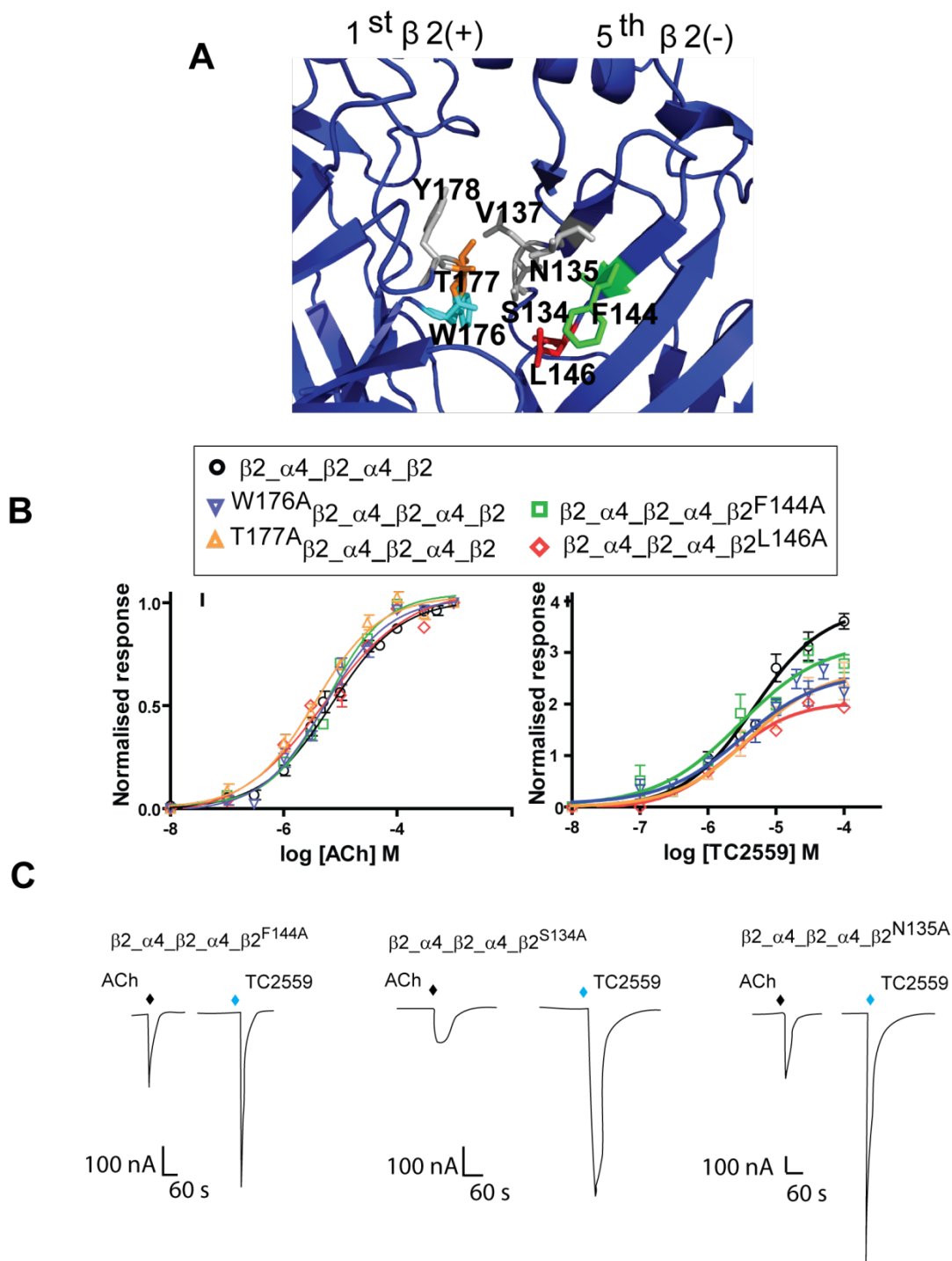


**Figure 4.5. Alanine Substitution of Conserved Residues in  $\beta_2$  (+)/ $\beta_2$  (-) interfaces.** **A)** Representation of the residues L146 and F144 of the 5<sup>th</sup> subunit (E-loop) and W176A, T177A, Y178A of the 1<sup>st</sup> subunit which points towards the  $\beta_2$ (+)/ $\beta_2$ (-) interface in  $(\alpha_4\beta_2)_2\beta_2$  nAChRs (Pymol). **B)** On the left, currents activated by ACh in wild-type  $(\alpha_4\beta_2)_2\beta_2$  and mutants nAChRs expressed heterologously in *Xenopus* oocytes. Error bars indicate SEM. On the right, currents activated by TC2559 normalised to maximal ACh response (100  $\mu$ M) in wild-type  $(\alpha_4\beta_2)_2\beta_2$  and mutants nAChRs. Error bars indicate SEM. **C)** Representative traces of the responses elicited by maximal ACh and TC2559 at  $\beta_2\_ \alpha_4\_ \beta_2\_ \alpha_4\_ \beta_2$  F144A,  $\beta_2\_ \alpha_4\_ \beta_2\_ \alpha_4\_ \beta_2$  S134A and  $\beta_2\_ \alpha_4\_ \beta_2\_ \alpha_4\_ \beta_2$  N135A concatenated receptors expressed heterologously in *Xenopus* oocytes.

#### 4.2.4 $\beta 2(+)/\alpha 4(-)$ interfaces do not affect TC2559 responses in $\alpha 4\beta 2$ nAChRs

Although the (+) side of  $\beta 2(+)/\alpha 4(-)$  interfaces is structural identical to the (+) side of  $\beta 2(+)/\beta 2(-)$ , the (-) side in  $\beta 2(+)/\alpha 4(-)$  is not. Residues in the (-) side differ significantly between  $\beta 2$  and  $\alpha 4$ : E loop in  $\alpha 4$  is more hydrophilic due to H142, Q150 and T152 (**Fig. 4.6**). In such environment, interactions between  $\beta 2$ W176,  $\beta 2$ T177,  $\alpha 4$ Q150 and  $\alpha 4$ T152 seem energetically unlikely, which suggests that  $\beta 2(+)/\alpha 4(-)$  interfaces may not modulate maximal agonist responses in  $\alpha 4\beta 2$  nAChRs. To test this view, the agonist effects of TC2559 were tested on mutant  $\beta 2(+)/\alpha 4(-)$  interfaces in concatenated  $(\alpha 4\beta 2)_2\beta 2$  and  $(\alpha 4\beta 2)_2\alpha 4$  receptors. Neither  $\beta 2$ W176A nor  $\beta 2$ T177A introduced in individual  $\beta 2(+)/\alpha 4(-)$  interfaces affected the TC2559 responses of concatenated  $(\alpha 4\beta 2)_2\beta 2$  (**Table 4.1**) or  $(\alpha 4\beta 2)_2\alpha 4$  (**Table 4.5**) receptors. Similarly, neither Q150A nor T152A affected TC2559 responses in  $(\alpha 4\beta 2)_2\alpha 4$  receptors.

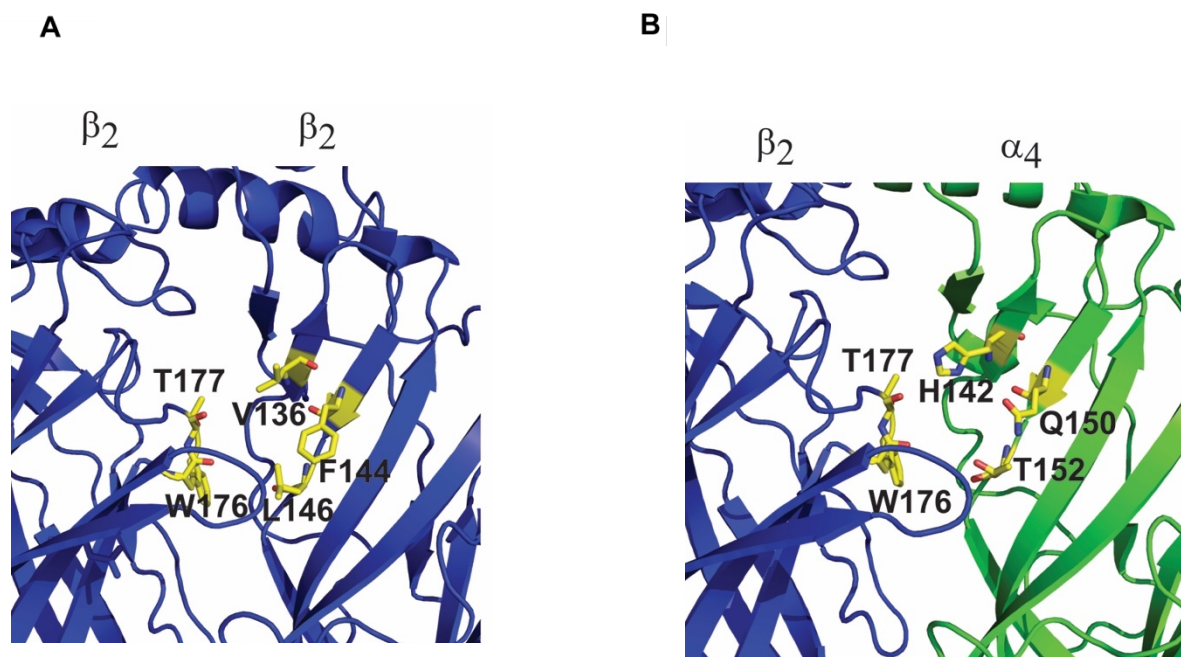


**Figure 4.6 Structure of the  $\beta 2(+)/\beta 2(-)$  and  $\beta 2(+)/\alpha 4(-)$  in  $\alpha 4\beta 2$  nAChRs. A) Conserved residues at  $\beta 2(+)/\beta 2(-)$  subunit interfaces in  $\alpha 4\beta 2$  nAChRs B) Conserved residues at  $\beta 2(+)/\alpha 4(-)$  subunit interfaces of  $\alpha 4\beta 2$  nAChRs. Images were generated using PYMOL and the X-ray structure of the  $(\alpha 4\beta 2)_2\beta 2$  nAChR. PDB ID 5kxi. (Morales-Pérez *et al.*, 2016).**

**Table 4.6. Effects of ACh and TC2559 on concatenated ( $\alpha 4\beta 2$ ) $_2\alpha 4$  nAChRs.** EC<sub>50</sub> for ACh and TC2559 were estimated from CRC data obtained as described in Chapter 2. The responses to TC2559 were normalised to ACh EC<sub>100</sub> (1 mM). The data represent the mean  $\pm$  SEM of n = 5 independent experiments, unless otherwise noted. CRCs were fitted to monophasic and biphasic Hill equations, as described in the Materials and Methods Chapter. The best fit was determined by F-tests; the simpler one-component model was preferred unless the extra sum-of-squares F test had a value of p less than 0.05, noted by +. Statistical analysis was carried out by Anova with post-hoc Dunnet's test; differences between data for control and mutant receptors were considered significant if p < 0.05 (noted by \*; n=6).

Receptor	ACh EC <sub>50</sub> $\pm$ SEM ( $\mu$ M)	TC2559 EC <sub>50</sub> $\pm$ SEM ( $\mu$ M)	TC2559 I/I <sub>AChmax</sub> $\pm$ SEM
$\beta 2_{\alpha 4}_{\beta 2_{\alpha 4}_{\alpha 4}}$	15 $\pm$ 3 294 $\pm$ 105 +	6.47 $\pm$ 1.20	0.21 $\pm$ 0.02
<sup>W176A</sup> $\beta 2_{\alpha 4}_{\beta 2_{\alpha 4}_{\alpha 4}}$	213 $\pm$ 68*	3.96 $\pm$ 1	0.31 $\pm$ 0.25
$\beta 2_{\alpha 4}_{\sup{W176A}\beta 2_{\alpha 4}_{\alpha 4}}$	268.9 $\pm$ 78*	3.31 $\pm$ 0.80	0.15 $\pm$ 0.008
<sup>T177A</sup> $\beta 2_{\alpha 4}_{\beta 2_{\alpha 4}_{\alpha 4}}$	107 $\pm$ 16*	3.7 $\pm$ 1.15	0.13 $\pm$ 0.04
$\beta 2_{\alpha 4}_{\sup{T177A}\beta 2_{\alpha 4}_{\alpha 4}}$	94.9 $\pm$ 30*	ND	0.14 $\pm$ 0.02
<sup>Y120A</sup> $\beta 2_{\alpha 4}_{\beta 2_{\alpha 4}_{\alpha 4}}$	207 $\pm$ 60*	3.7 $\pm$ 1.10	0.24 $\pm$ 0.13
$\beta 2_{\alpha 4}_{\sup{Y120A}\beta 2_{\alpha 4}_{\alpha 4}}$	142.4 $\pm$ 56 *	ND	0.15 $\pm$ 0.01
$\beta 2_{\alpha 4}_{\beta 2_{\alpha 4}_{\alpha 4}}^{\sup{Q150A}}$	62.39 $\pm$ 11*	4.41 $\pm$ 1.06	0.14 $\pm$ 0.009
$\beta 2_{\alpha 4}_{\beta 2_{\alpha 4}_{\alpha 4}}^{\sup{T152A}}$	80.2 $\pm$ 15*	4.03 $\pm$ 1.11	0.21 $\pm$ 0.02
$\beta 2_{\alpha 4}_{\beta 2_{\alpha 4}_{\alpha 4}}^{\sup{Q150F}}$	84.2 $\pm$ 10*	4.96 $\pm$ 0.81	0.30 $\pm$ 0.02
$\beta 2_{\alpha 4}_{\beta 2_{\alpha 4}_{\alpha 4}}^{\sup{T152L}}$	50 $\pm$ 6.8*	2.10 $\pm$ 0.66	0.51 $\pm$ 0.05 *
$\beta 2_{\alpha 4}_{\beta 2_{\alpha 4}_{\alpha 4}}^{\sup{Q150F, T152L}}$	47.3 $\pm$ 1.41*	3.15 $\pm$ 0.17	1.1 $\pm$ 0.09 *

#### 4.2.5. The modulatory unit $\beta$ 2W176- $\beta$ 2F144- $\beta$ 2L146 is transferable

To further test the subunit dependency of the effects of the modulatory residues in  $\beta$ 2(+)/ $\beta$ 2(-), the E loop of the  $\alpha$ 4 subunit in  $\beta$ 2(+)/ $\alpha$ 4(-)-1 in  $(\alpha$ 4 $\beta$ 2)<sub>2</sub> $\alpha$ 4 receptors was made  $\beta$ 2-like by introducing sequentially Q150F and T152L in  $\beta$ 2(+)/ $\alpha$ 4(-)-1.  $\alpha$ 4Q150 is equivalent to  $\beta$ 2F144 and  $\alpha$ 4T152 is equivalent to  $\beta$ L146 (**Fig. 4.6**). If interactions between W176, T177A, L146 and F144 are sufficient and necessary to modulate agonist responses, the maximal TC2559 responses of  $\beta$ 2\_ $\alpha$ 4\_ $\beta$ 2\_ $\alpha$ 4\_  $\alpha$ 4<sup>Q150F</sup>,  $\beta$ 2\_ $\alpha$ 4\_ $\beta$ 2\_ $\alpha$ 4\_  $\alpha$ 4<sup>T152L</sup> or  $\beta$ 2\_ $\alpha$ 4\_ $\beta$ 2\_ $\alpha$ 4\_  $\alpha$ 4<sup>Q150F,T152L</sup> should increase, compared to wild type. As shown in **Fig. 4.7** (data summarised in **Table 4.5**), the maximal responses of TC2559 on  $\beta$ 2\_ $\alpha$ 4\_ $\beta$ 2\_ $\alpha$ 4\_  $\alpha$ 4<sup>T152L</sup> increased by 30% ( $p < 0.05$ ;  $n = 5$ ) but, although the responses of  $\beta$ 2\_ $\alpha$ 4\_ $\beta$ 2\_ $\alpha$ 4\_  $\alpha$ 4<sup>Q150F</sup> increased (approx. 9%), the increase was not statistically significant. However, when Q150F and T152L were introduced simultaneously, the maximal responses to TC2559 increased by 86% ( $p < 0.05$ ;  $n = 5$ ) (**Fig. 4.7, Table 4.5**). These effects were not accompanied by changes in the potency of TC2559, although, like any of the other mutations introduced in the  $\beta$ 2(+)/ $\alpha$ 4(-) interfaces of the  $(\alpha$ 4 $\beta$ 2)<sub>2</sub> $\alpha$ 4 receptor, they did abolish the biphasic nature of the ACh effects (**Table 4.5**).

To determine if the effects of Q150F and T152L affected the maximal responses of other agonists that selectively bind ABS 1 and ABS 2, the maximal responses of Saz-A were determined. Saz A is a poorly efficacious agonist on  $(\alpha$ 4 $\beta$ 2)<sub>2</sub> $\alpha$ 4 receptors but a full agonist on  $(\alpha$ 4 $\beta$ 2)<sub>2</sub> $\beta$ 2 receptors (Zwart *et al.*, 2006; Carbone *et al.*, 2009); like TC2559, Saz A only binds the agonist sites on  $\alpha$ 4(+)/ $\beta$ 2(-) interfaces (Mazzaferro *et al.*, 2014). As shown in **Table 4.6**, the maximal responses of Saz-A increased respectively by 9% and 6% on  $\beta$ 2\_ $\alpha$ 4\_ $\beta$ 2\_ $\alpha$ 4\_  $\alpha$ 4<sup>Q150F</sup> and  $\beta$ 2\_ $\alpha$ 4\_ $\beta$ 2\_ $\alpha$ 4\_  $\alpha$ 4<sup>T152L</sup> receptors, compared to wild type, but the increases were not significant. However, when both Q150F and T152L were present, Saz A maximal responses increased significantly by 53% (**Table 4.6**).

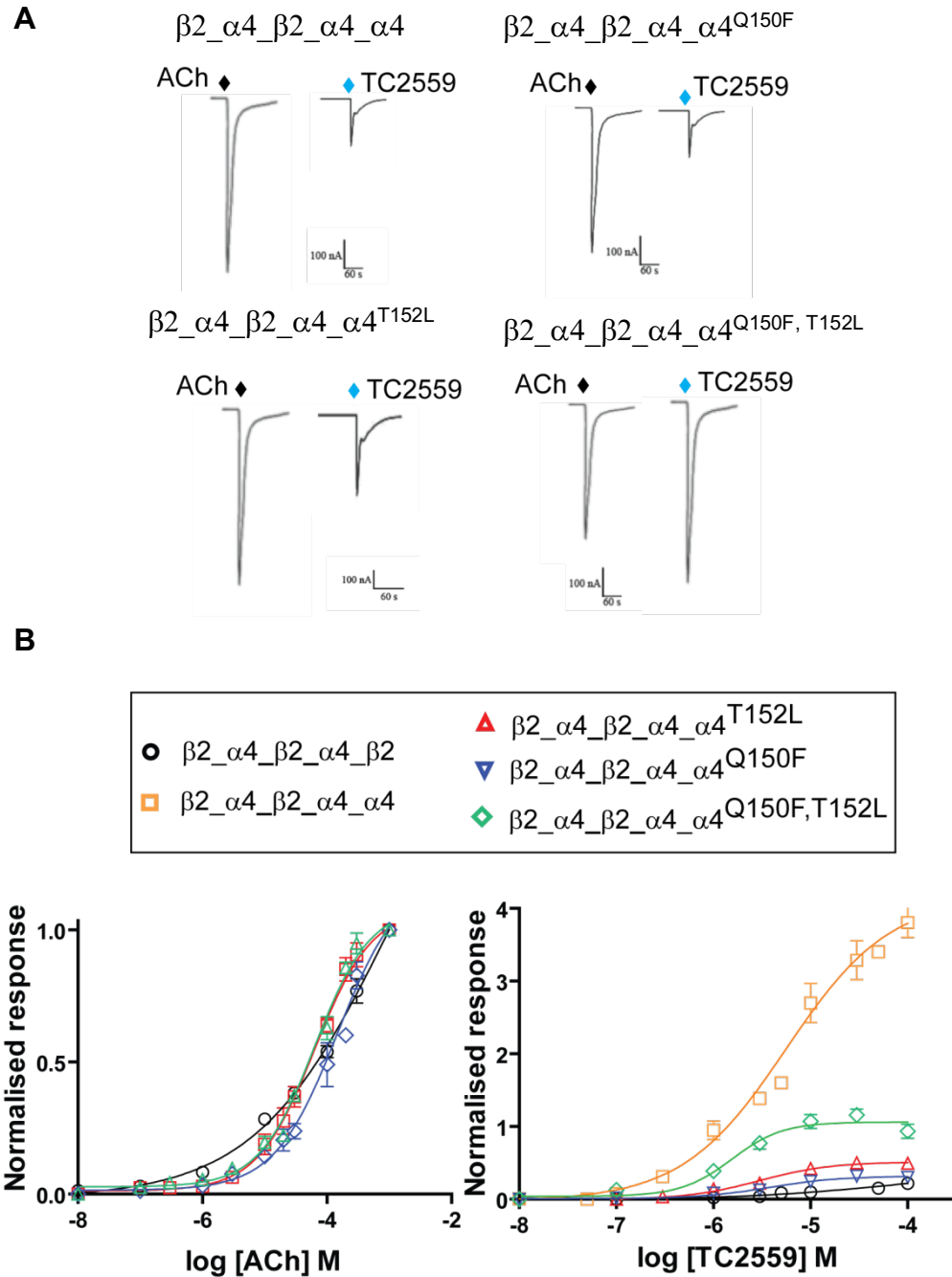


**Figure 4.7. Effect on the ACh and TC2559 sensitivity of concatenated  $\alpha_4\beta_2$  nAChRs.**

**A)** Representative traces of the responses elicited by maximal ACh and TC2559 at  $\beta_2\_ \alpha_4\_ \beta_2\_ \alpha_4\_ \alpha_4$ ,  $\beta_2\_ \alpha_4\_ \beta_2\_ \alpha_4\_ \alpha_4^{Q150F}$ ,  $\beta_2\_ \alpha_4\_ \beta_2\_ \alpha_4\_ \alpha_4^{T152L}$  and  $\beta_2\_ \alpha_4\_ \beta_2\_ \alpha_4\_ \alpha_4^{Q150F, T152L}$  concatenated receptors expressed heterologously in *Xenopus* oocytes. **B)** Currents activated by ACh and TC2559 in WT  $\alpha_4\beta_2$  and mutants nAChR expressed heterologously in *Xenopus* oocytes. Error bars indicate SEM.

**Table 4.7. Maximal effect of Saz-A responses of concatenated ( $\alpha_4\beta_2$ ) $_2\alpha_4$  receptors.** The responses of Saz-A were normalised to ACh EC<sub>100</sub> (1mM). CRCs were not constructed because the amplitude of the Saz-A responses was too low to construct reliable CRCs. The values represent the mean  $\pm$ SEM of 10 independent experiments. Statistical differences were determined using ANOVA tests (\*,  $p < 0.05$ ).

Saz A I/I <sub>AChmax</sub>			
$\beta_2_{\alpha_4}\beta_2_{\alpha_4}_{\alpha_4}$	$\beta_2_{\alpha_4}\beta_2_{\alpha_4}_{\alpha_4}^{Q150F}$	$\beta_2_{\alpha_4}\beta_2_{\alpha_4}_{\alpha_4}^{T152L}$	$\beta_2_{\alpha_4}\beta_2_{\alpha_4}_{\alpha_4}^{Q150F, T152L}$
0.08 $\pm$ 0.01	0.17 $\pm$ 0.03	0.14 $\pm$ 0.01	0.61 $\pm$ 0.102*

### 4.3 Discussion

It has been previously reported that L146 on the (-) side of the  $\beta 2(+)/\beta 2(-)$  interface of  $(\alpha 4\beta 2)_2\beta 2$  nAChRs is an element of an allosteric system linking ABS 1 to  $\beta 2(+)/\beta 2(-)$  to modulate maximal agonist responses (New *et al.*, 2017). This study identified three additional residues that are part of this system: W176 and T177 on the (+) side of the  $\beta 2(+)/\beta 2(-)$  interface and F144, which is structurally close to L146 on the (-) side. These residues reside in close spatial proximity and their replacement by alanine or cysteine decreases the maximal response of TC2559. Importantly, examination of the subunit interface using PISA ([http://www.ebi.ac.uk/msd-srv/prot\\_int/cgi-bin/piserver](http://www.ebi.ac.uk/msd-srv/prot_int/cgi-bin/piserver)) showed that these residues are interfacing and solvent accessible (**Table 4.5**). Experiments using MTSET demonstrated that MTSET labelling in the presence of agonist was significantly slower than in resting receptors; however, when the receptors contained simultaneously an alanine and a cysteine substitution, the rate of MTSET reaction in the presence of agonist was no different from that of resting receptors, indicative of functional coupling between the alanine and cysteine residues. Significantly, when ABS 1 was impaired by mutagenesis, the rates of modification of the cysteine substituted residues in  $\beta 2(+)/\beta 2(-)$  was significantly slower in the presence of agonist than in resting receptors.

The second order rate constant for modification of cysteine substituted  $\beta 2(+)/\beta 2(-)$  residues is significantly lower in the presence of ACh, suggesting that receptor activation by ACh induces a conformational movement near the substituted residues that reduces the accessibility of the substituted cysteines to MTSET labelling. The results are therefore consistent with the idea that the conformational change at the  $\beta 2(+)/\beta 2(-)$  interface is associated with global rearrangements during channel activation rather than as a consequence of agonist binding. Agonists produce a conformational change that protects the cysteine substituted  $\beta 2(+)/\beta 2(-)$  residues from MTSET modification. In contrast, the competitive inhibitor DH $\beta$ E has no effect on MTSET labelling because as an inhibitor it is unable to trigger such a rearrangement (New *et al.*, 2017).

The results suggest that the structural changes induced by receptor activation on the  $\beta 2(+)/\beta 2(-)$  interface extend over considerable distance. In support of the above view, this study also describes, for the first time, coupling of the  $\beta 2(+)/\beta 2(-)$  allosteric residues to gating. ELFCAR analysis showed that W176, T177, F144 and L146 in the  $\beta 2(+)/\beta 2(-)$

interface produced a  $\Omega$  value for coupling to  $\beta 2L9'T$  higher than 2, indicating functional interdependence of these residues. This establishes a long-range coupling between the ECD of  $\beta 2(+)/\beta 2(-)$  and the ion channel. The coupling region comprises four structures from the ligand binding domain ( $\beta 1-\beta 2$ ,  $\beta 8-\beta 9$ ,  $\beta 10$ , and Cys-loop) and two structures from the channel domain (pre-M1 and M2-M3). Numerous studies demonstrate that these regions, individually and in combination, contribute to transduction of agonist binding to channel gating (Kash *et al.*, 2003; Spitzmaul *et al.*, 2004; Xiu *et al.*, 2005; Lee *et al.*, 2009). Interestingly, work on  $\alpha 7$  nAChRs has shown that the non-consecutive arrangement of binding sites in the Cys-loop receptors allows bound agonist sites to transmit the agonist-induced structural perturbation to all five coupling regions in the pentamer (Rayes *et al.*, 2009). Significantly though, agonist sites contribute interdependently and asymmetrically to open channel stability (Rayes *et al.*, 2009). This scenario is consistent with the asymmetrical nature of the links between  $\beta 2(+)/\beta 2(-)$  and ABS 1; whilst impairment of agonist binding in ABS 1 severely affected MTSET-labelling of cysteine substituted  $\beta 2(+)/\beta 2(-)$ , impairment to ABS 2 did not.  $\beta 2(+)/\beta 2(-)$  does not appear to couple to the binding site because mutagenesis of W176, T177, L146 or F144 did not alter agonist potency. Thus, structurally, allosteric coupling between ABS 1 and  $\beta 2(+)/\beta 2(-)$  could occur at the level of the coupling domain and/or the channel itself. In support of this possibility, it has been reported that in the GABA<sub>A</sub>  $\alpha 1\beta 2\gamma 2s$  receptor bound agonist sites induce conformational changes to residues in M2 and the M2-M3 linker ( $\gamma 2s$  T281, I282 and S291 and,  $\alpha 1$  V279) (Boileau and Czajkowski, 1999).

The findings of this study add further weight to the increasing body of evidence supporting a major role for E loop in agonist-binding (Harpsoe *et al.*, 2011; Dash *et al.*, 2014) and non-agonist binding subunit interfaces in defining the functional properties of nAChRs (Mazzaferro *et al.*, 2014; Lucero *et al.*, 2016; Jin *et al.*, 2017). The effects of E loop in non-agonist binding interfaces are likely driven by interactions with residues on the opposing subunit interface. Thus, E loop residues such as L146 are part of a functional unit. This functional unit is transferable producing gain or loss of function when swapped from one subunit to another. Thus, by simply transferring the relevant  $\beta 2$  E loop residues (F144 and L146) to the (-) side of  $\beta 2(+)/\alpha 4$  interfaces in  $(\alpha 4\beta 2)_2\alpha 4$  nAChR, the macroscopy efficacy of agonist TC2559 and Saz-A increases markedly. These agonists are poorly efficacious on  $(\alpha 4\beta 2)_2\alpha 4$  nAChR but they behave as superagonist (TC2559) or full agonist on  $(\alpha 4\beta 2)_2\beta 2$  receptors (Moroni *et al.*, 2006; Zwart *et al.*, 2006; 2008; Carbone *et al.*, 2009). Similarly, by transferring  $\alpha 4$  E loop residues to the (-) side of  $\beta 2(+)/\beta 2(-)$ , the modulatory effect of



$\beta 2(+)/\beta 2(-)$  on maximal agonist responses is ablated. E loop functions are transferable in non-agonist binding interfaces in the  $\alpha 4\beta 2$  nAChR because regardless of whether the E loop is from  $\alpha 4$  or  $\beta 2$ , the (+) side of the interface with which loop E residues appear to interact is provided by  $\beta 2$ .

The E loop residues that affect  $\alpha 4\beta 2$  function occupy equivalent positions in the  $\alpha 4$  and  $\beta 2$  subunits, but because of the signature subunit interfaces that distinguish the  $(\alpha 4\beta 2)_2\beta 2$  nAChR from the  $(\alpha 4\beta 2)_2\alpha 4$  nAChR, the effect of loop E on the receptor function is receptor stoichiometry-dependent. Thus, in the  $(\alpha 4\beta 2)_2\alpha 4$  receptor, three E loop residues (T152, Q150 and H142) differentiate the (-) side of the agonist site on the  $\alpha 4(+)/\alpha 4(-)$  from that of agonist sites on  $\alpha 4(+)/\beta 2(-)$  interfaces (Harpsøe *et al.*, 2011; Mazzaferro *et al.*, 2014; Lucero *et al.*, 2016) resulting in two types of structurally and functionally different agonist sites, which creates a complex activation dynamics governed by functional interdependence between the two types of agonist sites. In  $(\alpha 4\beta 2)_2\beta 2$  receptors, it is  $\beta 2L146$  and  $\beta 2F144$  E loop residues that underlie a selective ABS 1- $\beta 2(+)/\beta 2(-)$  allosteric coupling. The receptor isoforms have in common  $\beta 2(+)/\alpha 4(-)$  interfaces, but even these interfaces, which are structurally equivalent influence receptor function in a receptor type-selective manner, likely reflecting differences in the landscape created by the flanking subunits. Thus, as for the function of the agonist sites of  $(\alpha 4\beta 2)_2\alpha 4$  what defines the functional effects of non-agonist binding interfaces in the alternate  $\alpha 4\beta 2$  nAChR is the physico-chemical nature of the E loop residues.

In summary, the present chapter has identified three more residues that contribute to the allosteric system linking ABS 1 and  $\beta 2(+)/\beta 2(-)$ . Significantly, so far, all residues identified couple to L9. This suggests that the functional entity ABS 1-  $\beta 2(+)/\beta 2(-)$  modulates agonist maximal responses by modulating the gating machinery. Single channel studies, accompanied by mutagenesis studies of the gating domain should clarify this issue.



## **Chapter 5**

### **Final discussion**



During the last 18 years there has been a tremendous leap forward in our understanding of the molecular mechanisms that drive receptor activation and modulation by ligands and, the structures and conformational transitions that underpin these events. A critical event that triggered this leap was the resolution of the crystal structure of the AChBP, a homologue of the ECD of nAChRs (Brejc *et al.*, 2001). This, together with high resolution cryo-electronmicroscopic images of the full structure of the *Torpedo* nAChR (Unwin, 2005) paved the way for a decade or so of breakthrough studies that sustain such changes of receptor function paradigms as the molecular mechanisms that define agonist efficacy (Lape *et al.*, 2009; Mukhtasimova *et al.*, 2009) and the global mechanisms of gating that involves a large reorganisation of the whole receptor mediated by two distinct conformational transitions; a global twisting and a radial expansion.

The focus of research in the pLGICs has largely been on the mechanisms and conformational transitions that result in activation. The resolution of the crystal structures of prokaryotic (Hilf and Dutzler, 2008, 2009; Bocquet *et al.*, 2009; Sauguet *et al.*, 2014) and eukaryotic pLGICs in resting, open and desensitised states (Hibbs and Gouaux, 2011; Nury *et al.*, 2010; Callimet *et al.*, 2013; Miller and Aricescu, 2014; 5-HT<sub>3</sub>; Hassaine *et al.*, 2014; Althoff *et al.*, 2014; Morales-Pérez *et al.*, 2016), cryo-electronmicroscopic images (Unwin, 2005; Unwin and Fujiyosi, 2012; Du *et al.*, 2015), molecular dynamics analysis of the gating of pLGICs (Nury *et al.*, 2010; Calimet *et al.*, 2013) as well as studies of the microscopic kinetics of these ion channels (Purohit *et al.*, 2007) and single channel studies (Lape *et al.*, 2009; Mukhtasimova *et al.*, 2009) have given notable insights on how pLGICs transit energetically and structurally from the resting (unbound close) to the open (bound) and then desensitised (close bound) states. The emerging picture of gating is that of a progressive stepwise isomerisation or conformational wave that starts from the agonist-bound agonist site in the ECD, propagates to the coupling regions in the interface between the ECD and TMD via a rigid rearrangement of the  $\beta$ -sandwiches in the ECD and moves down to M2 and then M3 and M4 to open the gate of M2. Similar molecular and structural mechanisms appear to mediate positive and negative allosteric modulation of pLGICs, albeit from different binding sites (Hibbs and Gouaux, 2011; Callimet *et al.*, 2013; Althoff *et al.*, 2014; Miller *et al.*, 2017; Lavery *et al.*, 2017).

The conformational transitions triggered by agonist binding are transduced into gating by a coupling pathway that runs along the long axis of the protein consisting of a series of loops in

the (+) side of the agonist site:  $\beta 1$ - $\beta 2$  loop, the Cys loop and M2-M3 linker at the ECD/TMD interface (Lee and Sine 2005; Jha *et al.*, 2007; Lee *et al.*, 2009; Althoff *et al.*, 2014; Sauguet *et al.*, 2014). Additionally, mutagenesis-functional studies (Sine *et al.*, 2002) and cryo-electron microscopy images of the *Torpedo* (muscle) nAChR (Unwin and Fujiyoshi, 2012), together with electrophysiological studies of ligand-induced conformational transitions in the GABA<sub>A</sub> receptor (Eaton *et al.*, 2012), suggest that interfaces lying adjacent to agonist sites may also play a role in receptor activation. More recent studies, including this thesis, have highlighted the E loop of non-agonist binding interfaces as an important player in receptor function (Mazzaferro *et al.*, 2011; 2014; Lucero *et al.*, 2016; New *et al.*, 2017; this study).

The studies presented here were inspired by and, extend the studies of tethered  $\alpha 4\beta 2$  nAChRs that suggest the functional importance of the fifth subunit in defining the signature functional properties of the alternate forms of the  $\alpha 4\beta 2$  nAChR. As mentioned in Chapter 1, these receptors comprise a cassette made of two non-consecutive  $\alpha 4(+)/\beta 2(-)$  interfaces, each containing a classical  $\alpha(+)/\beta(-)$  agonist site, and a fifth subunit. In the  $(\alpha 4\beta 2)_2\alpha 4$  receptor isoform, the fifth subunit is an  $\alpha 4$  subunit, which due to the conservation of the aromatic residues that line the classical agonist sites forms a third agonist site in this receptor type. Unlike  $\alpha 4$ , one of the tyrosine residues that flank the all-important loop C, is not conserved in  $\beta 2$ . Consequently,  $\beta 2$  cannot provide the mandatory (+) side of an operational agonist site. However, as shown by New *et al* (2017) and this study the fifth subunit in  $(\alpha 4\beta 2)_2\beta 2$  receptor forms the  $\beta 2(+)/\beta 2(-)$  interface that acts essentially as an allosteric device to modulate receptor activation.

The muscle nAChR contains two agonist sites, which when bound to agonists are sufficient to trigger full activation of the receptors. Being the prototype of the Cys loop receptors, it was widely believed that the full activation of all Cys loop receptors is mediated by two agonist sites. However, studies by Lucia Sivilotti and her team in University College London suggested for the first time that the kinetics of activation of heteromeric  $\alpha 1\beta$  glycine receptors could only be explained by postulating a third agonist site (Burzomato *et al.*, 2004). Subsequently, Rayes *et al.* (2009) addressed the question of the organisation of the agonist site using a chimeric receptor made of the ECD of the  $\alpha 7$  nAChR and the TMD and C-terminus of the 5HT3A receptor, and found that maximal open duration is achieved by agonist occupation of three non-consecutive agonist sites. This mirrors the activation of the  $(\alpha 4\beta 2)_2\alpha 4$  receptor. Pioneering work by Harpsøe *et al.* (2011) and Mazzaferro *et al.* (2011)

showed that occupation of the two agonist sites was sufficient to trigger gating but occupation of the three agonist sites increased the maximal agonist responses of the receptor. As for the  $\alpha 7/5HT3A$  chimera, the agonist sites in the  $(\alpha 4\beta 2)_2\alpha 4$  appeared to work asymmetrically and interdependently (Mazzaferro *et al.*, 2011; 2014). The key issue that needs to be answered for this receptor is what are the molecular and structural mechanisms that underpin the “asymmetrical and interdependently” activity of this receptor type. Mazzaferro *et al.* (2017) examined the microscopic function of the  $(\alpha 4\beta 2)_2\alpha 4$  nAChR and found that agonist occupation of the agonist binding pocket of the  $\alpha 4(+)/\alpha 4(-)$  interface dramatically altered the mean duration time of channel openings in a non-multiplicative manner, which suggest that the additional site not only contributes to gating but also modulates the function of the agonist sites on the  $\alpha 4(+)/\beta 2(-)$  sites.

The question that this study addressed was how the  $\alpha 4(+)/\alpha 4(-)$  agonist site may modulate the adjacent agonist sites in the  $(\alpha 4\beta 2)_2\alpha 4$  nAChR. Since the  $\alpha 4(+)/\alpha 4(-)$  interface is separated from the  $\alpha 4(+)/\beta 2$  interfaces, the obvious receptor regions to search for prospective sites that may functionally link the agonist sites were the  $\beta 2(+)/\alpha 4(-)$  interfaces, and within these interfaces loop E residues projecting towards the cavity between  $\beta 2(+)$  and  $\alpha 4(-)$  were residues that could be pivotal for intersubunit communication in the  $(\alpha 4\beta 2)_2\alpha 4$  nAChR. The E loop in the  $\alpha 4(+)/\alpha 4(-)$  agonist site was already known to be important in the function of the  $(\alpha 4\beta 2)_2\alpha 4$  nAChR (Harpsoe *et al.*, 2011; Mazzaferro *et al.*, 2014; Lucero *et al.*, 2016) but its role in the  $\beta 2(+)/\alpha 4(-)$  interfaces has not been examined in detail up until this thesis. The studies described in Chapter 3 present strong functional evidence that loop E in  $\beta 2(+)/\alpha 4(-)$  interfaces in the  $(\alpha 4\beta 2)_2\alpha 4$  nAChR is an element of a system that enables agonist sites to function interdependently and asymmetrically. Mutagenesis of E loop residue T152 in the fifth subunit has a marked effect on ACh responses as well as  $Zn^{2+}$  potentiation. How could loop E of the fifth subunit affect adjacent agonist sites? The loop could be part of a modulatory binding site housed on the  $\beta 2(+)/\alpha 4(-)$  interfaces. In accord with this possibility, alanine replacement on W176 and Y120 on the (+) side of the  $\beta 2(+)/\alpha 4(-)$  interface anticlockwise to  $\alpha 4(+)/\alpha 4(-)$  transformed the biphasic ACh CRC into a monophasic curve, which suggest that alanine replacements on these sites affect the physico-chemical landscape of agonist binding residues to an extent that the sites either bind the agonists with different affinities or that the coupling-binding transduction pathways transmit the gating signal differently to M2. Alternatively, it may be that the agonist site at  $\alpha 4(+)/\beta 2(-)$  interfaces affects the orientation and/or conformation of the fifth subunit and that this impacts the gating

of the ion channel. Electron micrographs of the *Torpedo* nAChR suggests that agonist bound agonist sites push the fifth subunit outwardly, which leads to channel gating (Unwin and Fuyijoshi, 2012; Unwin, 2013). It is not known whether displacement of the fifth subunit in agonist bound *Torpedo* nAChR is driven by inter-subunit interactions or by simply physical displacement of fifth subunit brought about by motions of adjacent agonist-bound subunit interfaces.

Chapter 4 explored intersubunit communication and its effects on agonist site function in the  $(\alpha 4\beta 2)_2\beta 2$  receptor. A key advantage of using this receptor isoform, compared to the  $(\alpha 4\beta 2)_2\alpha 4$  receptors, is that  $(\alpha 4\beta 2)_2\beta 2$  contain only two agonist sites and these are located on the  $\alpha 4(+)/\beta 2(-)$  interfaces. Thus, one can explore the asymmetric function of these agonist sites without the complex functional influence of an additional agonist site. The key finding of the studies presented in Chapter 4 is that the previously reported modulatory link between ABS 1 and the  $\beta 2(+)/\beta 2(-)$  interface (New *et al.*, 2017) is underpinned by interactions between residues in loop E on the (-) side of  $\beta 2(+)/\beta 2(-)$  and conserved residues in loop B in the (+) side of  $\beta 2(+)/\beta 2(-)$ . From the data, it seems that the modulatory effects is exerted at the coupling regions or the channel itself, although this possibility should be examined using single channel approaches.

The studies of Chapter 3 and 4 that highlight the fifth subunit as an element of an intersubunit system that conferring asymmetry to the agonist sites on  $\alpha 4(+)/\beta 2(-)$  are in accord with the interpretation of the most recent cryo-electronmicroscopic structures of *Torpedo* nAChRs by Unwin and Fujiiyoshi (2012). These authors propose that both bound-agonist sites asymmetrically push the auxiliary subunit ( $\beta 1$ ) to gate the channel. Thus, it is the displacement of the fifth subunit that ultimately opens the gate. Agonists gate receptors with distinct efficacy (i.e., full, partial or super-agonism). Gating efficacy in the Cys loop LGICs is thought to be determined by closed states preceding gating (Lape *et al.*, 2009; Mukhtasimova *et al.*, 2009). The structures that underlie the transition to these closed states themselves are not known but it is tempting to suggest that they will likely be partly involved in agonist site-non-binding interface interactions.

Finally, the modulatory effects of the fifth subunit on the function of the  $\alpha 4\beta 2$  agonist sites in the alternate  $\alpha 4\beta 2$  receptor resemble the effects of the benzodiazepine binding interface and adjacent agonist site in the GABA<sub>A</sub> receptor. In the case of the GABA<sub>A</sub> receptor binding of a ligand to the benzodiazepine site triggers motions that are transmitted to the gating region and



from there back to the adjacent agonist sites (see, for example, Boileau and Czajkowski, 1999). Thus, ECD based allosteric binding sites may have evolved from sites that initially emerge as pathways to communicate agonist sites. It will be interesting to examine the evolution of those pathways. Insights into this evolution may unmask novel sites in the  $\alpha 4\beta 2$  nAChR for the development of stoichiometry-selective  $\alpha 4\beta 2$  drugs.



## **Acknowledgments**

I wish to express my deep gratitude and thanks to my supervisor Professor Isabel Bermudez for the continuous support and motivation. My PhD has been an amazing experience and I thank Isabel Bermudez, not only for the tremendous academic support, but also for giving me so many wonderful opportunities. I would like to thank also Dr. Andrew Jones as my second supervisor for his advice during my project.

I wish to thank my labmates in Oxford Brookes University: Simone Mazzaferro for his guidance at the beginning of this research project and for transmitting me his passion for the nicotinic receptors; Teresa Minguez for her time in the lab and in the interesting conferences that we were lucky to attend; Jennina Taylor-Wells, Karina New, Constanza Alcaino, Anish Senan and Joseph Hawkins for helping me in this adventure.

I thank Nigel Groome PhD grant for give me the opportunity to develop my project at Oxford Brookes University.

I thank my colleagues from the Autonomous University of Madrid: Antonio Lázaro, Miguel Martínez and Omar Kourani for their help and inspiration during my undergraduate studies.

Thank you Suzanne O'Donnell and Claire O'Donnell for always believing in me.

I want to thank my brother Pablo and my friends Gabriela Smith and Dan Drew for support me during my research and my time in Oxford.

Later but not the least, I would like to thank my family and Óscar Luengo for their unconditional support and encouragement throughout my studies and my life.



## Bibliography

Ables JL, Görlich A, Antolin-Fontes B, Wang C, Lipford SM, Riad MH, Ren J, Hu f, Luo M, Kenny PJ, Heintz N and Ibañez-Tallon I (2017). Retrograde inhibition by a specific subset of interpeduncular  $\alpha 5$  nicotinic neurons regulates nicotine preference. *Proc. Natl. Acad. Sci. U.S.A.*, 114 (49) 13012-13017

Absalom NL, Quek G, Lewis TM, Qudah T, von Arenstorff I, Ambrus JI, Harpsøe K, Karim N, Balle T, McLeod MD, Chebib M (2013). Covalent Trapping of Methyllycaconitine at the alpha 4-alpha 4 Interface of the alpha 4 beta 2 Nicotinic Acetylcholine Receptor antagonist binding site and mode of receptor inhibition revealed. *J Biol Chem*, 288(37): 26521-32.

Ahring PK, Liao VWY, Balle T (2018). Concatenated nicotinic acetylcholine receptors: A gift or a curse? *J Gen Physiol*, 150 (3): 453-473

Akk G, Bracamontes J and Steinbach JH (2001). Pregnenolone sulfate block of GABA<sub>A</sub> receptors: mechanism and involvement of a residue in the M2 region of the  $\alpha$  subunit. *J Physiol*, 532(Pt 3), 673–684

Albuquerque EX, Pereira EF, Alkondon M, Rogers, SW (2009). Mammalian Nicotinic Acetylcholine Receptors: From Structure to Function. *Physiol Rev*, 89(1), 73–120

Alcaino C, Musgaard M, Minguez T, Mazzaferro S, Faundez M, Iturriaga-Vasquez P, Biggin PC, Bermudez I (2016). Role of the Cys Loop and Transmembrane Domain in the Allosteric Modulation of  $\alpha 4\beta 2$  Nicotinic Acetylcholine Receptors. *J Biol Chem*, 13; 292(2):551-562

Alcaino C, Musgaard M, Minguez T, Mazzaferro S, Faundez M, Iturriaga-Vasquez P, Biggin PC, Bermudez I (2017). Role of the cys loop and transmembrane domain in the allosteric modulation of  $\alpha 4\beta 2$  nicotinic acetylcholine receptors. *J Biol Chem*, 292(2): 551-562

Althoff T, Hibbs RE, Banerjee S, Gouaux E (2014). X-ray structures of GluCl in apo states reveal a gating mechanism of Cys-loop receptors. *Nature*, 512:333–337

Andreasen JT, Olsen GM, Wiborg O, Redrobe JP (2009). Antidepressant-like effects of nicotinic acetylcholine receptor antagonists, but not agonists, in the mouse forced swim and mouse tail suspension tests. *J Psychopharmacol*, 23(7):797-804

Arias HR (1998). Binding sites for exogenous and endogenous non-competitive inhibitors of the nicotinic acetylcholine receptor. *Biochim Biophys Acta*, 1376(2):173-220

Barron SC, McLaughlin JT, See JA, Richards VL, Rosenberg, RL (2009). An allosteric modulator of  $\alpha 7$  nicotinic receptors, N-(5-Chloro-2,4-dimethoxyphenyl)-N'-(5-methyl-3-isoxazolyl)-urea (PNU-120596), causes conformational changes in the extracellular ligand binding domain similar to those caused by acetylcholine. *Mol Pharmacol*, 76(2), 253–263

Baumann SW, Baur R and Sigel E (2003). Individual properties of the two functional agonist sites in GABA<sub>A</sub> receptors. *J Neurosci*, 23, 11158e11166

- Benallegue N, Mazzaferro S, Alcaino, Bermudez I (2013). The additional acetylcholine binding site at the  $\alpha 4 (+)/\beta 2 (-)$  interface of the  $(\alpha 4\beta 2)_2$   $\alpha 4$  nicotinic acetylcholine receptor contributes to desensitisation. *Br. J. Pharmacol*, 170: 304-316
- Benowitz NL (1996). Pharmacology of nicotine: addiction and therapeutics. *Annu Rev Pharmacol Toxicol*. 36:597-613
- Benwell EM, Balfour D, Anderson J (1988). Evidence That Tobacco Smoking Increases the Density of  $(-)-[3H]$  Nicotine Binding Sites in Human Brain. *J Neurochem*, 50. 1243 – 1247
- Bertrand S, Weiland S, Berkovic SF, Steinlein OK, Bertrand D (1998). Properties of neuronal nicotinic acetylcholine receptor mutants from humans suffering from autosomal dominant nocturnal frontal lobe epilepsy. *Br J Pharmacol*. 125 (4):751-60
- Bertrand D, Elmslie F, Hughes E, Trounce J, Sander T, Bertrand S, Steinlein OK (2005). The CHRN2 mutation I312M is associated with epilepsy and distinct memory deficits. *Neurobiol Dis*, 20(3):799–804
- Billen B, Spurny R, Brams M, Van Elk R, Valera-Kummer S, Yakel JL, Voets T, Bertrand D, Smit AB and Ulens C (2012). Molecular actions of smoking cessation drugs at  $\alpha 4\beta 2$  nicotinic receptors defined in crystal structures of a homologous binding protein. *Proc. Natl. Acad. Sci. U.S.A.*, 109: 9173-9178
- Bocquet N, Nury H, Baaden M, Le Poupon C, Changeux JP, Delarue M, Corringer PJ (2009). X-ray structure of a pentameric ligand-gated ion channel in an apparently open conformation. *Nature*, 1; 457(7225)
- Boileau AJ, Czajkowski C (1999). Identification of transduction elements for benzodiazepine modulation of the GABA (A) receptor: three residues are required for allosteric coupling. *J Neurosci*, 1; 19(23):10213-20
- Bondarenko V, Mowrey D, Tillman T, Cui T, Liu LT, Xu Y, Tang P (2012). NMR Structures of the Transmembrane Domains of the  $\alpha 4\beta 2$  nAChR. *Biochim Biophys Acta*, 1818(5), 1261–1268
- Bondarenko V, Mowrey D, Liu LT, Xu Y, Tang P (2013). NMR resolved multiple anesthetic binding sites in the TM domains of the  $\alpha 4\beta 2$  nAChR. *Biochim Biophys Acta*, 1828(2), 398–404
- Bourne Y, Talley TT, Hansen SB, Taylor P, Machot P (2005). Crystal structure of a Cbtx-AChBP complex reveals essential interactions between snake alpha-neurotoxins and nicotinic receptors. *EMBO J*, 24, 1512–152
- Brams M, Pandya A, Kuzmin D, van Elk R, Krijnen L, Jerrel L, Yakel, Victor Tsetlin, August B. Smit, Chris Ulens (2011). A Structural and Mutagenic Blueprint for Molecular Recognition of Strychnine and d-Tubocurarine by Different Cys-Loop Receptors. *PLoS Biology*, 9(3), e1001034

Brannigan G, LeBard DN, Hénin J, Eckenhoff RG and Klein ML (2010). Multiple binding sites for the general anesthetic isoflurane identified in the nicotinic acetylcholine receptor transmembrane domain. *Proc. Natl. Acad. Sci. U.S.A.* 107(32), 14122–14127

Brašić JR, Cascella N, Kumar A, Zhou Y, Hilton J, Raymont V, Crabb A, Guevara MR, Horti AG, Wong DF (2012). Positron emission tomography experience with 2-[<sup>18</sup>F] fluoro-3-(2 (s)-azetidinyloxy) pyridine (2-[<sup>18</sup>F] fa) in the living human brain of smokers with paranoid schizophrenia. *Synapse*, 66(4):352–368

Breese CR, Marks MJ, Logel J, Adams CE, Sullivan B, Collins AC, Leonard S (1997). Effect of smoking history on [<sup>3</sup>H] nicotine binding in human postmortem brain. *J Pharmacol Exp Ther*, 282:7–13

Brejč K, Van Dijk WJ, Klaassen RV, Schuurmans M, Van Der Oost J, Smit AB, Sixma TK (2001). Crystal structure of an ACh-binding protein reveals the ligand-binding domain of nicotinic receptors. *Nature*, 411(6835):269-76

Breslau N (1995). Psychiatric comorbidity of smoking and nicotine dependence. *Behav Genet* ,25(2):95-101

Burford NT, Watson J, Bertekap R, Alt A (2011). Strategies for the identification of allosteric modulators of G-protein-coupled receptors. *Biochem Pharmacol*, 15; 81(6):691-702

Burzomato V, Beato M., Groot-Kormelink PJ, Colquhoun D and Sivilotti LG (2004). Single-channel behavior of heteromeric  $\alpha 1\beta$  glycine receptors: an attempt to detect a conformational change before the channel opens. *J. Neurosci.* 24:10924–10940

Calimet N, Simoes M, Changeux JP, Karplus M, Taly A, Cecchini M (2013) A gating mechanism of pentameric ligand-gated ion channels. *Proc Natl Acad Sci*, 110(42): E3987–E3996

Carbone AL, Moroni M, Groot-Kormelink PJ, Bermudez I (2009). Pentameric concatenated ( $\alpha 4$ )<sub>2</sub>( $\beta 2$ )<sub>3</sub> and ( $\alpha 4$ )<sub>3</sub>( $\beta 2$ )<sub>2</sub> nicotinic acetylcholine receptors: subunit arrangement determines functional expression. *Br J Pharmacol*, 156:970-81

Cecchini M and Changeux JP (2014). The nicotinic acetylcholine receptor and its prokaryotic homologues: Structure, conformational transitions & allosteric modulation. *Neuropharmacology*, 96(Pt B):137-49

Celie PH, Van Rossum-Fikkert SE, Van Dijk WJ, Brejč K, Smit AB, Sixma TK (2004). Nicotine and carbamylcholine binding to nicotinic acetylcholine receptors as studied in AChBP crystal structures. *Neuron*, 41 (6), 907–14

Celie PH, Klaassen RV, van Rossum-Fikkert SE, van Elk R, van Nierop P, Smit AB, Sixma TK (2005). Crystal structure of acetylcholine-binding protein from *Bulinus truncatus* reveals the conserved structural scaffold and sites of variation in nicotinic acetylcholine receptors. *J Biol Chem*, 280:26457–66

Centers for Disease Control and Prevention (CDC) (2008). Smoking-attributable mortality, years of potential life lost, and productivity losses. *MMWR Morb Mortal Wkly Rep*, 14; 57(45):1226-8

Coe JW, Brooks PR, Vetelino MG, Wirtz MC, Arnold EP, Huang J, Sands SB, Davis TI, Lebel LA, Fox CB, Shrikhande A, Heym JH, Schaeffer E, Rollema H, Lu Y, Mansbach RS, Chambers LK, Rovetti CC, Schulz DW, Tingley FD, O'Neill BT (2005). Varenicline: an alpha4beta2 nicotinic receptor partial agonist for smoking cessation. *J Medl Chem*, 48 (10), 3474–7

Colombo SF, Mazzo F, Pistillo F and Gotti C (2013). Biogenesis, trafficking and up-regulation of nicotinic ACh receptors. *Biochem Pharmacol*, 15;86(8):1063-73

Colquhoun D (1998). Binding, gating, affinity and efficacy: The interpretation of structure-activity relationships for agonists and of the effects of mutating receptors. *Br J Pharmacol*, 125, 923 - 947

Corrigal, WA., Coen KM., Adamson KL (1994). Self-administered nicotine activates the mesolimbic dopamine system through the ventral tegmental area. *Brain research*, 653(1-2), 278-284

Corringer PJ, Le Novere, N, Changeux JP (2000). Nicotinic receptors at the amino acid level. *Ann Rev Pharmacol. Toxicol*, 40, 431–458

Corringer PJ, Poitevin F, Prevost MS, Sauguet L, Delarue M, Changeux JP (2012). Structure and pharmacology of pentameric receptor channels: from bacteria to brain. *Structure*, 6; 20(6):941-56

Curtis MJ, Bond RA, Spina D, Ahluwalia A, Alexander SP, Giembycz M, Gilchrist A, Hoyer D, Insel PA, Izzo AA, Lawrence AJ, MacEwan DJ, Moon LD, Wonnacott S, Weston AH, McGrath, JC (2015). Experimental design and analysis and their reporting: new guidance for publication in BJP. *Br J Pharmacol*, 172(14), 3461–3471

Chang Y and Weiss DS (1999). Channel opening locks agonist onto the GABAC receptor. *Nat Neurosci*, 2(3):219-25

Changeux JP, Kasai M, Lee CY (1970). Use of a snake venom toxin to characterize the cholinergic receptor protein. *Proc Natl Acad Sci U S A*, 67:1241–1247

Changeux JP, Eldelstein SJ (1998). Allosteric receptors after 30 years. *Neuron*, 21(5):959-80

D' Incamps BL and Ascher P (2014). High affinity and low affinity heteromeric nicotinic acetylcholine receptors at central synapses. *J Physiol*, 592(Pt 19), 4131–4136

Daly JW, Garraffo HM, Spande TF, Decker MW, Sullivan JP, Williams M (2000). Alkaloids from frog skin: the discovery of epibatidine and the potential for developing novel non-opioid analgesics. *Nat Prod Rep*, 17(2):131-5

Dani, JA (2001) Overview of nicotinic receptors and their roles in the central nervous system. *Biol. Psychiatry*, 49 (3), 166-174



- Dash B, Li MD, Lukas RJ (2014). Roles for N-terminal extracellular domains of nicotinic acetylcholine receptor (nAChR)  $\beta 3$  Subunits in enhanced functional expression of mouse  $\alpha 6\beta 2\beta 3$ - and  $\alpha 6\beta 4\beta 3$ -nAChRs. *J Biol Chem*, 289(41), 28338–28351
- de Leon J, Diaz FJ (2005). A meta-analysis of worldwide studies demonstrates an association between schizophrenia and tobacco smoking behaviors. *Schizophrenia Research*, 76 (2–3):135–157
- Dehaene S and Changeaux JP (1991). The Wisconsin Card Sorting Test: theoretical analysis and modeling in a neuronal network. *Cereb Cortex*, 1(1):62-79
- Dickinson JA, Kew JN, Wonnacott S (2008). Presynaptic alpha 7- and beta 2-containing nicotinic acetylcholine receptors modulate excitatory amino acid release from rat prefrontal cortex nerve terminals via distinct cellular mechanisms. *Mol. Pharmacol*, 74, 348–359
- Doggreli SA and Evans S (2003). Treatment of dementia with neurotransmission modulation. *Expert Opin Investig Drugs*, 12(10):1633-54.
- Du J, Lug W, Wu S, Cheng Y, Gouaux E (2015). Glycine receptor mechanism elucidated by electron cryo-microscopy. *Nature*, 526(7572):224-9
- Eaton MM, Lim YB, Bracamontes J, Steinbach JH, Akk G (2012). Agonist-specific conformational changes in the  $\alpha 1$ - $\gamma 2$  subunit interface of the GABA<sub>A</sub> receptor. *Mol Pharmacol*, 82: 255-63
- Echeverria V, Zeitlin R, Burgess S, Patel S, Barman A, Thakur G, Mamcarz M, Wang L, Sattelle DB, Kirschner DA, Mori T, Leblanc RM, Prabhakar R, Arendash GW (2011). Cotinine reduces amyloid-beta aggregation and improves memory in Alzheimer's disease mice. *J Alzheimer's Dis JAD*, 24:817–835
- Eggert M, Winterer G, Wanischek M, Hoda J-C, Bertrand D, Steinlein O (2015). The nicotinic acetylcholine receptor alpha 4 subunit contains a functionally relevant SNP Haplotype. *BMC Genet*, 16:46
- Exley R, Clements MA, Hartung H, McIntosh JM, Cragg SJ (2008). Alpha 6-containing nicotinic acetylcholine receptors dominate the nicotine control of dopamine neurotransmission in nucleus accumbens. *Neuropsychopharmacology*, 33, 2158–2166
- Faiman GA and Horovitz A (1996). On the choice of reference mutant states in the application of the double-mutant cycle method. *Protein Eng*, 9 (1996), pp. 315-316
- Filatov GN, White MM (1995). The role of conserved leucines in the M2 domain of the acetylcholine receptor in channel gating. *Mol. Pharmacol*, 48:379–384
- Fiore MC, Bailey WC, Cohen SJ (2000). Rockville (MD): US Department of Health and Human Services, Public Health Service; 2000. Treating tobacco use and dependence. *Clinical practice guideline*

Fox-Loe AM, Moonschi FH, Richards CI (2017). Organelle-specific single-molecule imaging of  $\alpha 4\beta 2$  nicotinic receptors reveals the effect of nicotine on receptor assembly and cell-surface trafficking. *J Biol Chem*, 292(51):21159-21169

Fucile S (2004).  $Ca^{2+}$  permeability of nicotinic acetylcholine receptors. *Cell Calcium*, 35(1):1-8.

Galindo-Charles L, Hernandez-Lopez S, Galarraga E, Tapia D, Bargas J, Garduño J, Frías, C, Drucker-Colin R, Mihailescu S (2008). Serotonergic dorsal raphe neurons possess functional postsynaptic nicotinic acetylcholine receptors. *Synapse*, 62(8):601-15

Gao M, Jin Y, Yang K, Zhang D, Lukas RJ, Wu J (2010). Mechanisms involved in systemic nicotine-induced glutamatergic synaptic plasticity on dopamine neurons in the ventral tegmental area. *J Neurosci*, 30(41), 13814–13825

Garduno J, Galindo-Charles L, Jiménez-Rodríguez J, Galarraga E, Tapia D, Mihailescu S, Hernandez-Lopez S (2012). Presynaptic  $\alpha 4\beta 2$  nicotinic acetylcholine receptors increase glutamate release and serotonin neuron excitability in the dorsal raphe nucleus. *J Neurosci*, 24; 32(43):15148-57

Gergalova G, Lykhmus O, Kalashnyk O, Koval L, Chernyshov V, Kryukova E, Tsetlin V, Komisarenko S, Skok M (2012) Mitochondria Express  $\alpha 7$  Nicotinic Acetylcholine Receptors to Regulate  $Ca^{2+}$  Accumulation and Cytochrome c Release: Study on Isolated Mitochondria. *PLoS ONE*, 7(2): e31361

Giacobini E and Michel JP (1998). Treatment of Alzheimer's disease. New developments. *Ann Med Interne*, 149(4):231-7

Glassman AH, Helzer JE, Covey LS, Cottler LB, Stetner F, Tipp JE, Johnson J. (1990) Smoking, Smoking Cessation, and Major Depression. *JAMA*, 264(12):1546–1549

Gleitsman KR, Shanata JAP, Frazier, SJ, Lester HA, Dougherty DA (2009). Long-Range Coupling in an Allosteric Receptor Revealed by Mutant Cycle Analysis. *Biophys J*, 96(8), 3168–3178

Gotti C, Moretti M, Clementi F, Riganti L, McIntosh JM, Collins AC, Marks MJ, Whiteaker P (2005). Expression of nigrostriatal  $\alpha 6$ -Containing nicotinic acetylcholine receptors is selectively reduced, but not eliminated, by  $\beta 3$  subunit gene deletion. *Mol Pharmacol*, 67 (6) 2007-2015

Gotti C, Zoli M, Clementi F (2006). Brain nicotinic acetylcholine receptors: native subtypes and their relevance. *Trends Pharmacol. Sci*, 27(9):482–491

Gotti C, Moretti M, Meinerz NM, Clementi F, Gaimarri A, Collins A and Marks M (2008). Partial Deletion of the Nicotinic Cholinergic Receptor  $\alpha 4$  or  $\beta 2$  Subunit Genes Changes the Acetylcholine Sensitivity of Receptor-Mediated  $86Rb^{+}$  Efflux in Cortex and Thalamus and Alters Relative Expression of  $\alpha 4$  and  $\beta 2$  Subunits. *Mol Pharmacol*, 73 (6) 1796-180

Gotti C, Clementi F, Fornari A, Gaimarri A, Guiducci S, Manfredi I, Moretti M, Pedrazzi P, Pucci L, Zoli M (2009). Structural and functional diversity of native brain neuronal nicotinic receptors. *Biochem Pharmacol*, 78(7): 703-11

Groot-Kormelink PJ., Broadbent S, Boorman JP, Sivilotti LG (2004). Incomplete Incorporation of Tandem Subunits in Recombinant Neuronal Nicotinic Receptors. *J Gen Physiol*, 123(6), 697–708

Grutzendler J and Morris JC (2001). Cholinesterase inhibitors for Alzheimer's disease. *Drugs*, 61(1):41-52

Guan ZZ, Zhang X, Ravid R, Nordberg A (2000). Decreased protein levels of nicotinic receptor subunits in the hippocampus and temporal cortex of patients with Alzheimer's disease. *J Neurochem*, 74(1):237-43

Haddad F, Sawalha M, Khawaja Y, Najjar A and Karaman R (2017). Dopamine and Levodopa prodrugs for treatment of Parkinson's disease. *Molecules*, 25; 23 (1)

Hansen SB, Sulzenbacher G, Huxford T, Marchot P, Taylor P, Bourne Y (2005). Structures of Aplysia AChBP complexes with nicotinic agonists and antagonists reveal distinctive binding interfaces and conformations. *EMBO Journal*, 24: 3635–3646

Harpsøe K, Ahring PK, Christensen JK, Jensen ML, Peters D, Balle T (2011). Unravelling the high- and low-sensitivity agonist responses of nicotinic acetylcholine receptors. *J Neurosci*, 31: 10759–10766

Harvey RJ, Thomas P, James CH, Wilderspin A and Smart TG (1999). Identification of an inhibitory Zn<sup>2+</sup> binding site on the human glycine receptor  $\alpha 1$  subunit. *J Physiol*, 520 (Pt 1), 53–64

Hassaine G, Deluz C, Grasso L, Wyss R, Tol MB, Hovius R, Graff A, Stahlberg H, Tomizaki T, Desmyter A, Moreay C, Li XD, Poitevin F, Vogel H, Nury H (2014). X-ray structure of the mouse serotonin 5-HT<sub>3</sub> receptor. *Nature*, 21; 512(7514):276-81

Henault CM, Sun J, Therien JP, da Costa C, Carswell CL, Labriola JM, Juranka PF, Baenziger JE (2015). The role of the M4 lipid-sensor in the folding, trafficking and allosteric modulation of nicotinic acetylcholine receptors. *Neuropharmacol*, 96 (Pt B):157-68

Henderson BJ, Pavlovicz RE, Allen JD, González-Cestari TF, Orac CM, Bonnell AB, Zhu MX, Boyd RT, Li C, Bergmeier SC, McKay DB (2010). Negative allosteric modulators that target human  $\alpha 4\beta 2$  neuronal nicotinic receptors. *J Pharmacol Exp Ther*, 334(3), 761–774

Henderson BJ, González-Cestari TF, Yi B, Pavlovicz RE, Boyd RT, Li Chenglong, Bergmeier SC, McKay DB (2012). Defining the putative inhibitory site for a selective negative allosteric modulator of human  $\alpha 4\beta 2$  neuronal nicotinic receptors. *ACS Chem Neurosci*, 3(9), 682–692

Hendrickson LM, Guildford MJ and Tapper AR (2013). Neuronal nicotinic acetylcholine receptors: common molecular substrates of nicotine and alcohol Dependence. *Front Psychiatry*, 4: 29

Hernan MA, Zhang SM, Rueda de Castro AM, Colditz GA, Speizer FE, Ascherio A (2001). Cigarette smoking and the incidence of Parkinson's disease in two prospective studies. *Ann Neurol*, 50(6):780-6

Hibbs RE, Sulzenbacher G, Shi J, Talley TT, Conrod S, Kem WR, Taylor P, Marchot P and Bourne Y (2009). Structural determinants for interaction of partial agonists with acetylcholine binding protein and neuronal  $\alpha 7$  nicotinic acetylcholine receptor. *EMBO J*, 28(19), 3040–3051

Hibbs RE and Gouaux E. (2011). Principles of activation and permeation in an anion-selective Cys-loop receptor. *Nature*, 474(7349), 54–60

Hidalgo P and MacKinnon R (1995) Revealing the architecture of a  $K^+$  channel pore through mutant cycles with a peptide inhibitor. *Science*, 14; 268(5208):307-10

Hilf RJ and Dutzler R (2008). X-ray structure of a prokaryotic pentameric ligand-gated ion channel. *Nature*, 20; 452(7185):375-9

Hilf RJ and Dutzler R (2009). A prokaryotic perspective on pentameric ligand-gated ion channel structure. *Curr Opin Struct Biol*, 19(4):418-24

Holden JH and Czajkowski C (2002). Different residues in the GABA(A) receptor alpha 1T60-alpha 1K70 region mediate GABA and SR-95531 actions. *J Biol Chem*, 24; 277(21):18785-92

Huang X, Chen H, Michelsen K, Schneider S, Shaffer PL (2015). Crystal structure of human glycine receptor alpha3 bound to antagonist strychnine. *Nature*, 8; 526(7572):277-80

Imoto K, Methfessel C, Sakmann B, Mishina M, Mori Y, Konno T, Fukuda K, Kurasaki M, Bujo H, Fujita Y, Numa S (1986). Location of a delta-subunit region determining ion transport through the acetylcholine receptor channel. *Nature*, 324:670–674

Imoto K, Busch C, Sakmann B, Mishina M, Konno T, Nakai J, Bujo H, Mori Y, Fukuda K, Numa S (1988). Rings of negatively charged amino acids determine the acetylcholine receptor channel conductance. *Nature*, 335, 645–648

Indurthi DC, Lewis TM, Ahring PK, Balle T, Chebib M, Absalom NL (2016). Ligand Binding at the  $\alpha 4$ - $\alpha 4$  Agonist-Binding Site of the  $\alpha 4\beta 2$  nAChR Triggers Receptor Activation through a Pre-Activated Conformational State. *PLoS ONE*, 11(8): e0161154

IUPHAR Database (2014). Nicotinic acetylcholine receptors: Introduction. International Union of Basic and Clinical Pharmacology

Jackson KJ, Marks MJ, Vann RE, Chen X, Gamage TF, Warner JA, Damaj MI (2010). Role of  $\alpha 5$  nicotinic acetylcholine receptors in pharmacological and behavioral effects of nicotine in mice. *J. Pharmacol. Exp. Ther*, 334(1), 137–146

Jain A, Kuryatov A, Wang J, Kamenecka TM, Lindstrom J (2016). Unorthodox Acetylcholine Binding Sites Formed by  $\alpha 5$  and  $\beta 3$  Accessory Subunits in  $\alpha 4\beta 2^*$  Nicotinic Acetylcholine Receptors. *J Biol Chem*, 291 (45): 23452-23463

Janowsky DS, el-Yousef MK, Davis JM, Sekerke HJ (1972). A cholinergic-adrenergic hypothesis of mania and depression. *Lancet*, 23; 2(7778):632-5

Jeanclous EM, Lin L, Treuil MW, Rao J, DeCoster MA, Anand R (2001). The chaperone protein 14-3-3beta interacts with the nicotinic acetylcholine receptor alpha 4 subunit. Evidence for a dynamic role in subunit stabilization. *J Biol Chem*, 27;276(30):28281-90

Jensen AA, Frølund B, Liljefors T, Krosgaard-Larsen P (2005). Neuronal nicotinic acetylcholine receptors: structural revelations, target identifications, and therapeutic inspirations. *J Med Chem*, 28; 48(15):4705-45

Jha A, Cadugan DJ, Purohit P, Auerbach A (2007). Acetylcholine Receptor Gating at Extracellular Transmembrane Domain Interface: the Cys-Loop and M2–M3 Linker. *J Gen Physiol*, 130(6), 547–558

Jin Z, Khan P, Shin Y, Wang J, Lin L, Cameron MD, Lindstrom JM, Kenny PJ, Kamenecka TM (2014). Synthesis and activity of substituted heteroaromatics as positive allosteric modulators for  $\alpha 4\beta 2\alpha 5$  nicotinic acetylcholine receptors. *Bioorg Med Chem Lett*, 24(2), 674–678

Jin Z, Lin H, Srinivasan S, Nwachukwu JC, Bruno N, Griffin PR, Nettles KW, Kamenecka TM (2017). Synthesis of novel steroidal agonists, partial agonists, and antagonists for the glucocorticoid receptor. *Bioorg Med Chem Lett*, 15; 27(2):347-353

Karlin A and Akabas MH (1998). Substituted-cysteine accessibility method. *Methods Enzymol*, 293:123-45

Kash TL, Jenkins A, Kelley JC, Trudell JR, Harrison NL (2003). Coupling of agonist binding to channel gating in the GABAA receptor. *Nature*, 421:272–275

Kedmi M, Beaudet AL, Orr-Urtreger A (2004). Mice lacking neuronal nicotinic acetylcholine receptor beta4-subunit and mice lacking both alpha5- and beta4-subunits are highly resistant to nicotine-induced seizures. *Physiol Genomics*, 13;17(2):221-9

Kim JS, Padnya A, Weltzin M, Edmonds BW, Schulte MK, Glennon RA. (2007). Synthesis of desformylflustrabromine and its evaluation as an  $\alpha 4\beta 2$  and  $\alpha 7$  nACh receptor modulator. *Bioorg Med Chem Lett*, 17:4855–4860

Kuryatov A, Luo J, Cooper J, Lindstrom J (2005). Nicotine acts as a pharmacological chaperone to up-regulate human alpha4beta2 acetylcholine receptors. *Mol Pharmacol*, 68:1839–1851

Kuryatov A, Berrettini W and Lindstrom J (2011). Acetylcholine receptor (AChR)  $\alpha 5$  subunit variant associated with risk for nicotine dependence and lung cancer reduces ( $\alpha 4\beta 2$ ) $2\alpha 5$  AChR function. *Mol Pharmacol*, 79(1), 119–125

Labarca C, Nowak MW, Zhang H, Tang L, Deshpande P, Lester HA (1995). Channel gating governed symmetrically by conserved leucine residues in the M2 domain of nicotinic receptors. *Nature*, 376:514–516

Labarca C, Schwarz J, Deshpande P, Schwarz S, Nowak MW, Fonck C, Nashmi R, Kofuji P, Dang H, Shi W, Fidan M, Khakh B, Chen Z, Bowers B, Boulter J, Wehner J, Lester HA (2001). Point mutant mice with hypersensitive  $\alpha 4$  nicotinic receptors show dopaminergic deficits and increased anxiety. *Proc Natl Acad Sci U S A*, 98(5), 2786–2791

Lambert JJ, Peters JA, Hales TG, Dempster J (1989). The properties of 5-HT<sub>3</sub> receptors in clonal cell lines studied by patch clamp techniques. *Br. J. Pharmacol*, 97:27–40

Langley JN (1905). On the reaction of cells and of nerve-endings to certain poisons, chiefly as regards the reaction of striated muscle to nicotine and to curari. *J. Physiol*, 33 (4-5), 374-413

Lape R, Krashia P, Colquhoun D, Sivilotti LG (2009). Agonist and blocking actions of choline and tetramethylammonium on human muscle acetylcholine receptors. *J Physiol*, 1;587 (Pt 21):5045-72

Laverty D, Thomas P, Field M, Andersen OJ, Gold MG, Biggin PC, Gielen M and Smart TG (2017). Crystal structures of a GABAA-receptor chimera reveal new endogenous neurosteroid-binding sites. *Nat Struct Mol Biol*, 24(11):977-985

Laviolette SR and Van der Kooy D (2004). The neurobiology of nicotine addiction: bridging the gap from molecules to behaviour. *Nat Rev Neurosci*, 5(1):55-65

Le Novere N, Corringer PJ, Changeux JP (2002). The diversity of subunit composition in nAChRs: evolutionary origins, physiologic and pharmacologic consequences. *J Neurobiol*, 53(4):447-56

Lee WY and Sine S (2004). Invariant aspartic acid residue in muscle nicotinic receptor contributes selectively to the kinetics of agonist binding. *J. Gen. Physiol*, 124:555-567

Lee WY and Sine SM (2005). Principal pathway coupling agonist binding to channel gating in nicotinic receptors. *Nature*, 438, 243–247

Lee WY, Free C, Sine SM (2009). Binding to gating transduction in nicotinic receptors: Cys-loop energetically couples to pre-M1 and M2-M3 regions. *J Neurosci*, 29(10), 3189–3199

Lee CH, Zhu C, Malysz J, Campbell T, Shaughnessy T, Honore P, Polakowski J, Gopalakrishnan (2011).  $\alpha 4\beta 2$  neuronal nicotinic receptor positive allosteric modulation: an approach for improving the therapeutic index of  $\alpha 4\beta 2$  nAChR agonists in pain. *Biochem Pharmacol*, 82:959–966

Léna C and Changeux JP (1999). The role of beta 2-subunit-containing nicotinic acetylcholine receptors in the brain explored with a mutant mouse. *Ann N Y Acad Sci*, 30; 868:611-6

Lepeta K, Lourenco MV, Schweitzer BC, Martino Adami PV., Banerjee P, Catuara-Solarz S, Seidenbecher C (2016). Synaptopathies: synaptic dysfunction in neurological disorders – A review from students to students. *Journal of Neurochemistry*, 138(6), 785–805

Lester HA, Dibas MI, Dahan DS, Leite JF and Dougherty DA (2004) Cys-loop receptors: new twists and turns. *Trends neurosci*, 27 (6), 329–36

Levin ED and Simon BB (1998). Nicotinic acetylcholine involvement in cognitive function in animals. *Psychopharmacology*, 138(3-4):217-30

Lindstrom J, Anand R, Gerzanich V, Penq X, Wang D, Wells G (1996). Structure and function of neuronal nicotinic acetylcholine receptors. *Prog Brain Res*. 109:125–137

Liu Q, Huang Y, Xue F, Simard A, DeChon J, Li G, Zhang J, Lucero L, Wang M, Sierks M, Hu G, Chang Y, Lukas RJ, Wu J (2009). A novel nicotinic acetylcholine receptor subtype in basal forebrain cholinergic neurons with high sensitivity to amyloid peptides. *J Neurosci*, 29:918–929

Lu JYD, Su P, Barber JEM, Nash JE, Le AD, Liu F, Wong AHC (2017). The neuroprotective effect of nicotine in Parkinson's disease models is associated with inhibiting PARP-1 and caspase-3 cleavage. *PeerJ*, 5:e3933

Lucero LM, Weltzin MM, Eaton JB, Cooper JF, Lindstrom JM, Lukas RJ, Whiteaker P (2016). Differential  $\alpha 4(+)/(-)\beta 2$  Agonist-binding Site Contributions to  $\alpha 4\beta 2$  Nicotinic Acetylcholine Receptor Function within and between Isoforms. *J Biol Chem*, 291(5): 2444–59

Lysek N, Rachor E, Lindel T (2002). Isolation and structure elucidation of deformylflustrabromine from the North Sea bryozoan *Flustra foliacea*. *Nature*, 57(11-12):1056-61

Mansvelder HD and MCGEhee DS (2002). Cellular and synaptic mechanisms of nicotine addiction. *J. Neurobiol*, 53(4):606-17

Mantione E, Micheloni S, Alcaino C, New K, Mazzaferro S, Bermudez I (2012). Allosteric modulators of  $\alpha 4\beta 2$  nicotinic acetylcholine receptors: a new direction for antidepressant drug discovery. *Future Med Chem*, 4(17):2217-30

Marchi M and Crilli M (2010). Presynaptic nicotinic receptors modulating neurotransmitter release in the central nervous system: functional interactions with other coexisting receptors. *Prog Neurobiol*, 92(2):105-11

Markett S, Montag C, Reuter M (2011). The nicotinic acetylcholine receptor gene *CHRNA4* is associated with negative emotionality. *Emotion*, 11(2):450-5

Marks MJ, Burch JB, Collins AC (1983). Effects of chronic nicotine infusion on tolerance development and nicotinic receptors. *J Pharmacol Exp Ther*, 226:817–25

Marks MJ, Whiteaker P, Calcaterra J, Stitzel JA, Bullock AE, Grady SR, Picciotto MR, Changeux JP and Collins AC (1999). Two pharmacologically distinct components of nicotinic receptor-mediated rubidium efflux in mouse brain require the beta2 subunit. *J Pharmacol Exp Ther*, 289:1090–103

- Marks MJ, Meinerz NM, Brown RWB, Collins AC (2010).  $86\text{Rb}^+$  Efflux Mediated by  $\alpha 4\beta 2^*$ -Nicotinic Acetylcholine Receptors with High and Low Sensitivity to Stimulation by Acetylcholine Display Similar Agonist-Induced Desensitization. *Biochem Pharmacol*, 80(8), 1238–1251
- Martin NE, Malik S, Calimet N, Changeux J-P, Cecchini M (2017). Un-gating and allosteric modulation of a pentameric ligand-gated ion channel captured by molecular dynamics. *PLoS Comput Biol*, 13(10): e1005784.
- Maskos U, Molles BE, Pons S, Besson M, Guiard BP, Guilloux JP, Evrard A, Cazala P, Cormier A, Mameli-Engvall M, Dufour N, Cloez-Tayarani I, Bemelmans AP, Mallet J, Gardier AM, David V, Faure P, Granon S, Changeux JP (2005). Nicotine reinforcement and cognition restored by targeted expression of nicotinic receptors. *Nature*, 436: 103-107
- Mayeux R. (2003). Epidemiology of neurodegeneration. *Annu Rev Neurosci*, 26:81–104
- Mazzaferro S, Benallegue N, Carbone AL, Gasparri F, Vijayan R, Biggin PC, Moroni M, Bermudez I (2011). Additional acetylcholine (ACh) binding site at  $\alpha 4/\alpha 4$  interface of  $(\alpha 4\beta 2)_2\alpha 4$  nicotinic receptor influences agonist sensitivity. *J. Biol. Chem*, 286: 31043–54
- Mazzaferro S, Gasparri F, New K, Alcaino C, Faundez M, Iturriaga Vasquez P, Vijayan R, Biggin PC, Bermudez I (2014). Non-equivalent Ligand Selectivity of Agonist Sites in  $(\alpha 4\beta 2)_2\alpha 4$  Nicotinic Acetylcholine Receptors. A key determinant of agonist efficacy. *J. Biol. Chem*, 289: 21795-21806
- Mazzaferro S, Bermudez I, Sine SN (2017).  $\alpha 4\beta 2$  nicotinic acetylcholine receptors: relationships between subunit stoichiometry and function at the single channel level. *J Biol Chem*, 292: 2729-40
- McLaughlin KA (2011). The Public Health Impact of Major Depression: A Call for Interdisciplinary Prevention Efforts. *Prev Sci*, 12(4), 361–371
- Mercado J and Czajkowski C (2006). Charged residues in the  $\alpha 1$  and  $\beta 2$  pre-M1 regions involved in GABAA receptor activation. *J Neurosci*, 26(7):2031-40
- Mercado J and Czajkowski C (2008).  $\gamma$ -Aminobutyric Acid (GABA) and Pentobarbital Induce Different Conformational Rearrangements in the GABAA Receptor  $\alpha 1$  and  $\beta 2$  Pre-M1 Regions. *J. Biol. Chem*, 283(22), 15250–15257
- Millar NS (2003). Assembly and subunit diversity of nicotinic acetylcholine receptors. *Biochem Soc Trans*, 31:869–74
- Miller C (1989). Genetic manipulation of ion channels: a new approach to structure and mechanism. *Neuron*, 2: 1195-1205
- Miller PS, Aricescu AR (2014). Crystal structure of a human GABAA receptor. *Nature*, 512: 270–275
- Miller PS, Scott S, Masiulis S, De Colibus L, Pardon E, Steyaert J, Aricescu AR (2017). Structural basis for GABAA receptor potentiation by neurosteroids. *Nat Struct Mol Biol*, 24(11):986-992



- Mineur YS and Picciotto MR (2010). Nicotine receptors and depression: revisiting and revising the cholinergic hypothesis. *Trends in Pharmacological Sciences*, 31(12), 580–586
- Miyazawa A, Fujiyoshi Y, Unwin N (2003) Structure and gating mechanism of the acetylcholine receptor pore. *Nature*, 423, 949–955.
- Moore TJ, Furberg CD, Glenmullen J, Maltzberger JT, Singh S (2011) Suicidal behavior and depression in smoking cessation treatments. *PLoS ONE*, 6(11): e27016
- Morales-Pérez CL, Noviello CM, Hibbs RE (2016). X-ray structure of the human  $\alpha 4\beta 2$  nicotinic receptor. *Nature*, 538: 411-15
- Moretti M, Zoli M, George AA, Lukas RJ, Pistillo F, Maskos U, Whiteaker P, Gotti, C (2014). The novel  $\alpha 7\beta 2$ -nicotinic acetylcholine receptor subtype is expressed in mouse and human basal forebrain: biochemical and pharmacological characterization. *Mol Pharmacol*, 86(3), 306–317
- Moroni M, Zwart R, Sher E, Cassels BK, Bermudez I (2006).  $\alpha 4\beta 2$  nicotinic receptors with high and low acetylcholine sensitivity: pharmacology, stoichiometry, and sensitivity to long-term exposure to nicotine. *Mol Pharmacol*, 70(2): 755-68
- Moroni M, Vijayan R, Carbone A, Zwart R, Biggin P, Bermudez I (2008). Non-agonist-Binding Subunit Interfaces Confer Distinct Functional Signatures to the Alternate Stoichiometries of the  $\alpha 4\beta 2$  nicotinic receptor: An  $\alpha 4$ - $\alpha 4$  interface is required for Zinc potentiation. *J Neurosci*, 28(27): 6884-6894
- Mukhtasimova N, Lee WY, Wang HL, Sine SM (2009). Detection and trapping of intermediate states priming nicotinic receptor channel opening. *Nature*, 459(7245), 451–454
- Mulle C, Lena Clement, Changeux JP (1992). Potentiation of nicotinic receptor response by external calcium in rat central neurons. *Neuron*, 8(5):937-45
- Nelson ME, Kuryatov A, Choi CH, Zhou Y and Lindstrom J (2003). Alternate stoichiometries of  $\alpha 4\beta 2$  nicotinic acetylcholine receptors. *Mol Pharmacol*, 63:332-41
- New K, Del Villar SG, Mazzaferro S, Alcaïno C and Bermudez I (2017). The fifth subunit of the  $(\alpha 4\beta 2)_2\beta 2$  nicotinic ACh receptor modulates maximal ACh responses. *Br J Pharmacol*. In Press
- Newell JG and Czajkowski C (2007). Cysteine Scanning Mutagenesis: Mapping Binding Sites of Ligand-Gated Ion Channels. In *Handbook of Neurochemistry and Molecular Neurobiology*, 439–454.
- Nury H, Poitevin F, Van Renterghem C, Changeux JP, Delarue M and Baaden M (2010). One-microsecond molecular dynamics simulation of channel gating in a nicotinic receptor homologue. *Proc. Natl. Acad. Sci. U.S.A.*, 107 (14) 6275-6280
- Nury H, Delarue M, Corringer PJ. (2011) X-ray structures of general anesthetics bound to their molecular targets. *Med Sci* 27(12):1056-7

Nys M, Kesters D, Ulens C (2013). Structural insights into Cys-loop receptor function and ligand recognition. *Biochem Pharmacol*, 86(8):1042-53

Pandya A, Yakel JL (2011). Allosteric modulator Desformylflustrabromine relieves the inhibition of  $\alpha 2\beta 2$  and  $\alpha 4\beta 2$  nicotinic acetylcholine receptors by beta-amyloid (1-42) peptide. *J Mol Neurosci*, 45:42-7

Pandya A and Yakel JL (2013). Effects of neuronal nicotinic acetylcholine receptor allosteric modulators in animal behavior studies. *Biochem Pharmacol*, 86(8), 1054-1062

Papke RL, Williams Dustin K, Horenstein AN and Stokes C (2011). The effective opening of nicotinic acetylcholine receptors with single agonist binding sites. *J Gen Physiol*, 37 (4), 369-84

Patel S, Grizzell JA, Holmes R, Zeitlin R, Solomon R, Sutton TL, Rohani A, Charry LC, Larkov A, Mori T and Echeverria V (2014). Cotinine halts the advance of Alzheimer's disease-like pathology and associated depressive-like behavior in Tg6799 mice. *Frontiers in Aging Neuroscience*, 6, 162

Pavlovicz RE, Henderson BJ, Bonnel AB, Boyd RT, McKay DB and Li C (2011). identification of a negative allosteric site on human  $\alpha 4\beta 2$  and  $\alpha 3\beta 4$  neuronal nicotinic acetylcholine receptors. *PLOS ONE*, 6(9), e24949

Perry DC, Dávila-García MI, Stockmeier CA, Kellar KJ (1999). Increased nicotinic receptors in brains from smokers: membrane binding and autoradiography studies. *J Pharmacol Exp Ther*, 289(3):1545-52

Picciotto MR, Caldarone BJ, King SL, Zachariou V (2000). Nicotinic receptors in the brain. Links between molecular biology and behavior. *Neuropsychopharmacology*.; 22:451-65

Picciotto MR, Caldarone BJ, Brunzell DH, Zachariou V, Stevens TR, King SL (2001). Neuronal nicotinic acetylcholine receptor subunit knockout mice: physiological and behavioral phenotypes and possible clinical implications. *Pharmacol Ther*. 92(2-3):89-108

Picciotto MR (2008) Galanin and addiction. *Cell Mol Life Sci*. 65(12):1872-9

Picciotto MR, Higley MJ, Mineur YS (2012). Acetylcholine as a neuromodulator: cholinergic signaling shapes nervous system function and behavior. *Neuron*, 76:116-29

Picciotto MR, Zoli M, Changeux JP (1999). Use of knock-out mice to determine the molecular basis for the actions of nicotine. *Nicotine Tob Res*, 1 Suppl 2: S121-5; discussion S139-40

Picciotto MR, Zoli M, Léna C, Bessis A, Lallemant Y, Le Novère N, Vicent P, Pich EM, Brûlet P, Changeux JP (1995). Abnormal avoidance learning in mice lacking functional high-affinity nicotine receptor in the brain. *Nature*, 2;374(6517):65-7

Picciotto MR, Zoli M, Rimondini R, Léna C, Marubio LM, Pich EM, Fuxe K, Changeux JP (1998). Acetylcholine receptors containing the beta2 subunit are involved in the reinforcing properties of nicotine. *Nature*, 8;391(6663):173-7

Quirk M and Wonnacott S (2011).  $\alpha 6\beta 2^*$  and  $\alpha 4\beta 2^*$  nicotinic acetylcholine receptors as drug targets for parkinson's disease. *Pharmacol Rev*, 63(4), 938–966

Rabenstein RL, Caldarone BJ, Picciotto MR (2006). The nicotinic antagonist mecamylamine has antidepressant-like effects in wild-type but not beta2- or alpha7 nicotinic acetylcholine receptor subunit knockout mice. *Psychopharmacology*, 189(3):395-401

Rayes D, De Rosa MJ, Sine SM and Bouzat C (2009). Number and locations of agonist binding sites required to activate homomeric cys-loop receptors. *J Neurosci*, 29(18), 6022–6032

Revah F, Bertrand D, Galzi JL, Devillers-Thiéry A, Mulle C, Hussy N, Bertrand S, Ballivet M, Changeux JP (1991). Mutations in the channel domain alter desensitization of a neuronal nicotinic receptor. *Nature*, 353(6347):846-9

Rode F, Munro G, Holst D, Nielsen EØ, Troelsen KB, Timmermann DB, Rønn LC, Grunet M (2012). Positive allosteric modulation of  $\alpha 4\beta 2$  nAChR agonist induced behaviour. *Brain Res*. 6; 1458:67-75

Rollema H, Guanowsky V, Mineur YS, Shrikhande A, Coe JW, Seymour PA and Picciotto MR (2009). Varenicline has antidepressant-like activity in the forced swim test and augments sertraline's effect. *Eur J Pharmacol*, 605(1-3), 114–116

Rosecrans JA (1979). Nicotine as a discriminative stimulus to behavior: its characterization and relevance to smoking behavior. *NIDA Res Monogr*, (23):58–69

Rucktooa P, Smit AB, Sixma TK (2009). Insight in nAChR subtype selectivity from AChBP crystal structures. *Biochem. Pharmacol*, 78, 777–787

Rucktooa P, Haseler CA, Van Elk R, Smit AB, Gallagher T, Sixma TK (2012). Structural characterization of binding mode of smoking cessation drugs to nicotinic acetylcholine receptors through study of ligand complexes with acetylcholine binding protein. *J Biol Chem*, 287: 23283–23293

Sacco KA, Bannon KL and George TP (2004). Nicotinic receptor mechanisms and cognition in normal states and neuropsychiatric disorders. *Psychopharmacology*, 18(4), 457–474

Saha S, Chant D, Welham J and McGrath J (2005). A systematic review of the prevalence of schizophrenia. *PLoS Medicine*, 2(5), e141

Sambrook J and Gething MJ (1989). Protein structure. Chaperones, paperones. *Nature*, 16; 342(6247):224-5

Sancar F and Czajkowski C (2011). Allosteric modulators induce distinct movements at the GABA-binding site of the GABA-A receptor. *Neuropharmacol*, 60:520-528

Sarter M and Bruno JP (1997). Trans-synaptic stimulation of cortical acetylcholine and enhancement of attentional functions: a rational approach for the development of cognition enhancers. *Behav Brain Res*, 83(1-2):7-14

Sauguet L, Shahsavari A, Poitevin F, Huon C, Menny A, Nemečková A, Haouz A, Changeux JP, Corringer PJ and Delarue M (2014). Crystal structures of a pentameric ligand-gated ion channel provide a mechanism for activation. *Proc. Natl. Acad. Sci. U.S.A.*, 111(3), 966–971

Scheffer IE, Bhatia KP, Lopes-Cendes I, Fish DR, Marsden CD, Andermann E, Andermann F, Desbiens R, Keene D, Cendes F (1995). Autosomal dominant nocturnal frontal lobe epilepsy. A distinctive clinical disorder. *Brain*, 118 (Pt 1):61-73

Schofield PR, Darlison MG, Fujita N, Burt DR, Stephenson FA, Rodrigues H, Rhee LM, Ramachandran J, Reale V, Glencorse TA (1987). Sequence and functional expression of the GABA A receptor shows a ligand-gated receptor super-family. *Nature*, 16-22,328(6127):221-7

Schwartz RD and Kellar KJ (1983). Nicotinic cholinergic receptor binding sites in the brain: regulation in vivo. *Science*, 8; 220(4593):214-6.

Seo S, Henry JT, Lewis AH, Wang, N and Levandoski MM (2009). The Positive Allosteric Modulator Morantel Binds at Non-canonical Subunit Interfaces of Neuronal Nicotinic Acetylcholine Receptors. *J Neurosci*, 29(27), 8734–8742.

Shahsavari A, Kastrup JS, Nielsen EØ, Kristensen JL, Gajhede M and Balle, T (2012). Crystal Structure of *Lymnaea stagnalis* AChBP Complexed with the Potent nAChR Antagonist DHβE Suggests a Unique Mode of Antagonism. *PLoS ONE*, 7(8), e40757

Shanata JAP, Frazier SJ, Lester HA and Dougherty DA (2012). Using Mutant Cycle Analysis to Elucidate Long-Range Functional Coupling in Allosteric Receptors. *Methods in Mol Biol*, 796, 97–113

Short CA, Cao AT, Wingfield MA, Doers ME, Jobe EM, Wang N, Levandoski NM (2015). Subunit interfaces contribute differently to activation and allosteric modulation of neuronal nicotinic acetylcholine receptors. *Neuropharmacology*, 91: 157-168

Sine SM (2002). The nicotinic receptor ligand binding domain. *J Neurobiol*, 53(4):431-46.

Sivilotti LG (2010). What single-channel analysis tells us of the activation mechanism of ligand-gated channels: the case of the glycine receptor. *J Physiol*, 588(Pt 1), 45–58.

Slater YE, Houlihan LM, Maskell PD, Exley R, Bermúdez I, Lukas RJ, Valdivia AC, Cassels BK (2003). Halogenated cytosine derivatives as agonist at human neuronal nicotinic acetylcholine receptor subtypes. *Neuropharmacology*, 44(4):503-15

Spitzmaul G, Corradi J, Bouzat C (2004). Mechanistic contributions of residues in the M1 transmembrane domain of the nicotinic receptor to channel gating. *Mol Membr Biol*, 21(1):39-50

Staley JK, Krishnan-Sarin S, Cosgrove KP, Jrantzler E, Frohlich E, Perry E, Dubin JA, Estok K, Brenner E, Baldwin RM, Tamagnan GD, Seibyl JP, Jatlow P, Picciotto MR, London ED, O'Malley S, Van Dyck CH (2006). Human tobacco smokers in early abstinence have higher levels of beta2\* nicotinic acetylcholine receptors than nonsmokers. *J Neurosci*, 26(34):8707-14

Steinlein OK, Mulley JC, Propping P, Wallace RH, Philips HA, Sutherland GR, Scheffer IE and Berkovic S (1995). A missense mutation in the neuronal nicotinic acetylcholine receptor alpha 4 subunit is associated with autosomal dominant nocturnal frontal lobe epilepsy. *Nat Genet*, 11:201–203

Taly A, Delarue M, Grutter T, Nilges M, Le Novère N, Corringer PJ and Changeux JP (2005). Normal mode analysis suggests a quaternary twist model for the nicotinic receptor gating mechanism. *Biophys. J*, 88(6), 3954–3965

Taly A, Corringer JP, Guedin D, Lestage P, Changeux JP (2009). Nicotinic receptors: allosteric transitions and therapeutic targets in the nervous system. *Nat Rev Drug Discovery*, 8:733-50

Taly A, Hénin J, Changeux JP and Cecchini M (2014). Allosteric regulation of pentameric ligand-gated ion channels: An emerging mechanistic perspective. *Channels*, 8(4), 350–360

Tapper AR, McKinney SL, Nashmi R, Schwarz J, Deshpande P, Labarca C, Whiteaker P, Marks MJ, Collins AC and Lester HA (2004). Nicotine activation of alpha4\* receptors: sufficient for reward, tolerance, and sensitization. *Science*, 306, 1029–103210

Terry AV, Buccafusco JJ, Bartoszyk GD (2005). Selective serotonin 5-HT2A receptor antagonist EMD 281014 improves delayed matching performance in young and aged rhesus monkeys. *Psychopharmacology*, 179:725–732

Thomsen MS, Zwart R, Ursu D, Jensen MM, Pinborg LH, Gilmour G, Wu J, Sher E and Mikkelsen JD (2015).  $\alpha 7$  and  $\beta 2$  Nicotinic acetylcholine receptor subunits form heteromeric receptor complexes that are expressed in the human cortex and display distinct pharmacological properties. *PLoS ONE*, 10(6), e0130572

Timmermann D, Sandager-Nielsen K, Dyhring T, Smith M, Jacobsen AM, Nielsen E, Grunnet M, Christensen JK, Peters D, Kohlhaas K, Olsen GM and Ahring P (2012). Augmentation of cognitive function by NS9283, a stoichiometry-dependent positive allosteric modulator of  $\alpha 2$ - and  $\alpha 4$ -containing nicotinic acetylcholine receptors. *Br. J. Pharmacol*, 167(1), 164–182

Turrini P, Casu MA, Wong TP, De Koninck Y, Ribeiro-da-Silva A, Cuello AC (2001). Cholinergic nerve terminals establish classical synapses in the rat cerebral cortex: synaptic pattern and age-related atrophy. *Neuroscience*, 105(2):277–285

Twyman RE, Rogers CJ, Macdonald RL (1989). Differential regulation of gamma-aminobutyric acid receptor channels by diazepam and phenobarbital. *Ann Neurol*, 25(3):213-20

- Unwin N (1993). Nicotinic acetylcholine receptor at 9 Å resolution. *J Mol Biol*, 20; 229(4):1101-24
- Unwin N (2005). Refined structure of the nicotinic acetylcholine receptor at 4Å resolution. *J Mol Biol*, 346(4):967-89
- Unwin N and Fujiyoshi Y (2012). Gating movement of acetylcholine receptor caught by plunge freezing. *J Mol Biol*, 422(5): 617–34
- Unwin N (2013). Nicotinic acetylcholine receptor and the structural basis of neuromuscular transmission: insights from Torpedo postsynaptic membranes. *Q Rev Biophys*, 46(4): 283-322
- Venkatachalan SP and Czajkowski C (2008). A conserved salt bridge critical for GABAA receptor function and loop C dynamics. *Proc. Natl. Acad. Sci. U.S.A.*, 105(36), 13604–13609
- Volkow ND (2009). Substance use disorders in schizophrenia: clinical implications of comorbidity. *Schizophr Bull.* 35(3):469–472
- Wang J, Kuryatov A, Sriram A, Jin Z, Kamenecka TM, Kenny PJ, Lindstrom J (2015). An Accessory Agonist Binding Site Promotes Activation of  $\alpha 4\beta 2^*$  Nicotinic Acetylcholine Receptors. *J Biol Chem* 290: 13907-13918
- Weltzin MM and Schulte MK (2010). Pharmacological characterization of the allosteric modulator desformylflustrabromine and its interaction with  $\alpha 4\beta 2$  neuronal nicotinic acetylcholine receptor orthosteric ligands. *J. Pharmacol. Exp. Ther.*, 334(3), 917–926
- Weltzin MM and Schulte MK (2015). Desformylflustrabromine Modulates  $\alpha 4\beta 2$  Neuronal Nicotinic Acetylcholine Receptor High- and Low-Sensitivity Isoforms at Allosteric Clefts Containing the  $\beta 2$  Subunit. *J Pharmacol Exp Ther.*, 354(2):184-94
- Wilkie GI, Hutson P, Sullivan JP, Wonnacott (1996). Pharmacological characterization of a nicotinic autoreceptor in rat hippocampal synaptosomes. *Neurochem Res*, 21(9):1141-8
- Wonnacott S, Irons J, Rapiet C, Thome B, Lunt GG (1989). Presynaptic modulation of transmitter release by nicotinic receptors. *Prog Brain Res.* 79:157-63
- Wonnacott S (1997). Presynaptic nicotinic ACh receptors. *Trends Neurosci.* 20(2):92-8
- Wooltorton JR, Pidoplichko VI, Broide RS, Dani JA (2003). Differential desensitization and distribution of nicotinic acetylcholine receptor subtypes in midbrain dopamine areas. *J Neurosci.* 23, 3176–3185
- Wu Z, Cheng H, Jiang Y, Melcher K and Xu HE (2015). Ion channels gated by acetylcholine and serotonin: structures, biology, and drug discovery. *Acta Pharmacol Sin.* 36(8), 895–907
- Xiu X, Hanek AP, Wang J, Lester HA, Dougherty DA (2005). A unified view of the role of electrostatic interactions in modulating the gating of Cys loop receptors. *J Biol Chem*, 280:41655–41666

Xiu X, Puskar NL, Shanata JA, Lester HA and Dougherty DA (2009). Nicotine binding to brain receptors requires a strong cation- interaction. *Nature*, 458, 534–537 34

Yakel JL (2013). Cholinergic receptors: functional role of nicotinic ACh receptors in brain circuits and disease. *Pflugers Arch, Eur J Physiol*, 465(4), 441–450

Zarotosky V, Sramek JJ, Cutler NR (2003). Galantamine hydrobromide: An agent for Alzheimer's disease. *Am J Health-Syst Pharm*, 60,446-452

Zhang H, Karlin A (1997). Identification of acetylcholine receptor channel-lining residues in the M1 segment of the beta-subunit. *Biochemistry*, 16;36(50):15856-64

Zhang J, Xiao YD, Jordan KG, Hammond PS, Van Dyke KM, Mazurov AA, Speake JD, Lippiello PM, James JW, Letchworth SR, Bencherif Merouane and Hauser TA (2012) Analgesic effects mediated by neuronal nicotinic acetylcholine receptor agonists: correlation with desensitization of  $\alpha 4\beta 2^*$  receptors. *Eur. J. Pharm. Sci*, 47 (5), 813–23

Zhong W, Gallivan JP, Zhang Y, Li L, Lester HA, Dougherty DA (1998). From ab initio quantum mechanics to molecular neurobiology: a cation-p binding site in the nicotinic receptor. *Proc. Natl. Acad. Sci. USA*. 95:12088–93

Zhou Y, Nelson ME, Kuryatov A, Choi C, Cooper J, Lindstrom J (2003). Human alpha4beta2 acetylcholine receptors formed from linked subunits. *J Neurosci*, 23:9004–9015

Zhu CZ, Chin CL, Rustay NR, Zhong C, Mikusa J, Chandran P, SAlyers A, Gomez E, Simler G, Lewis LG, Gauvin D, Baker S, Pai M, Tovcimak A, Brown K, Komater V, Fox GB, Decker MW, Jacobson PB, Gopalakrishnan M, Lee CH, Honore P (2011). Potentiation of analgesic efficacy but not side effects: co-administration of an  $\alpha 4\beta 2$  neuronal nicotinic acetylcholine receptor agonist and its positive allosteric modulator in experimental models of pain in rats. *Biochem Pharmacol*. 82(8):967-76

Zoli M, Pucci S, Vilella A, Gotti C (2017). Neuronal and extraneuronal nicotinic acetylcholine receptors. *Curr Neuropharmacol*, 20, 2, 92-98

Zwart R, Vijverberg HP (1998). Four pharmacologically distinct subtypes of  $\alpha 4\beta 2$  nicotinic acetylcholine receptor expressed in *Xenopus laevis* oocytes. *Mol Pharmacol*, 54:1124–1131

Zwart R, van Kleef RG, Gotti C, Smulders CJ, Vijverberg HP (2000). Competitive potentiation of acetylcholine effects on neuronal nicotinic receptors by acetylcholinesterase-inhibiting drugs. *J of Neurochem*. 75:2492-2500

Zwart R, Broad LM, Xi Q, Lee M, Moroni M, Bermudez I, and Sher E (2006). 5-I A-85380 and TC-2559 differentially activate heterologously expressed alpha4beta2 nicotinic receptors. *Eur J Pharmacol* 539:10–17

Zwart R, Carbone AL, Moroni M, Bermudez I, Mogg AJ, Folly EA, Broad LM, Williams AC, Zhang D, Ding C, Heinz BA, Sher E (2008) Sazetidine-A is a potent and selective agonist at native and recombinant alpha 4 beta 2 nicotinic acetylcholine receptors. *Mol Pharmacol*. 73(6):1838-4

